Technische Universität München

Department Chemie

Lehrstuhl für Biochemie

Bacillus anthracis purine riboswitches: functional characterization and screening for novel ligands

Marion Angelika Kirchner

Vollständiger Abdruck der von der Fakultät für Chemie der Technischen Universität München zur Erlangung des akademischen Grades eines Doktors der Naturwissenschaften (Dr. rer. nat) genehmigten Dissertation.

Vorsitzender:	Prof. Dr. Ville Kaila
Prüfer der Dissertation:	1. TUM Junior Fellow Dr. Sabine Schneider
	2. Prof. Dr. Stephan A. Sieber
	3. Prof. Dr. Kirsten Jung (LMU)

Die Dissertation wurde am 07.06.2017 bei der Technischen Universität München eingereicht und durch die Fakultät für Chemie am 24.08.2017 angenommen.

Meiner Familie

This thesis was realized at the Chair of Biochemistry at the Technische Universität München from January 2014 until April 2017.

Parts of this thesis have been published:

Kirchner M, Schneider S. Gene expression control by *Bacillus anthracis* purine riboswitches. RNA 2017; 23(5):762 – 769.

Kirchner M, Schorpp K, Hadian K, Schneider S. An *in vivo* high-throughput screening for riboswitch ligands using a reverse reporter gene system. Sci Rep 2017; 7:7732.

Publications not presented in this thesis:

Kirchner M, Schneider S. CRISPR-Cas: From the bacterial adaptive immune system to a versatile tool for genome engineering. Angew Chem Int Ed Engl 2015; 54:13508 – 14.

Kick L, Kirchner M, Schneider S. CRISPR-Cas9: From a bacterial immune system to genome-edited human cells in clinical trials. Bioengineered 2017; 8:280-6.

Abstract

Riboswitches are structured RNA elements that are able to regulate the expression of downstream genes in response to ligand binding. They are considered as good potential drug targets due to their absence in humans and high frequency in bacteria. Riboswitches commonly regulate genes encoding for metabolic enzymes and are able to respond to a variety of ligands as ions, amino acids or purines. Purine riboswitches share a common structural motif and comprise guanine-, adenine- and 2´-deoxyguanosine-responsive RNA elements.

The first part of this work focused on proposed guanine riboswitches from the pathogenic bacterium *Bacillus anthracis* and asked whether and how they are active. It was aimed to characterize them in terms of activity, sensitivity, ligand specificity and ligand binding. For this purpose, the riboswitches were studied *in silico* as well as *in vitro*. In addition, a novel *in vivo* reverse reporter gene system was established that is able to convert the negative response of OFF riboswitches to ligand binding into a positive output. The results demonstrate that five *B. anthracis* guanine riboswitches are active and inhibit transcription upon ligand binding. They considerably differ in their *in vivo* ligand response and in their ligand binding affinity. The obtained results are of importance in medicinal chemistry as well as in synthetic biology for the search for new drug targets and novel genetic tools.

The second part of the thesis highlights the development of an *in vivo* high-throughput screening to identify riboswitch activators. Therefore, the above-mentioned reverse reporter gene system was employed and optimized for high-throughput usage. Using the *B. anthracis xpt* riboswitch as a target, a library of 6.400 compounds was screened. One hit compound, gemcitabine, gave reproducible positive results in the follow-up hit validation. Additional counter assays and secondary assays indicated that gemcitabine indeed influences riboswitch activity *in vivo*, however, it possibly does not bind the riboswitch directly but acts through indirect effects. Nevertheless, these results support the functionality of the high-throughput procedure as well as the controls and recommend the screening for use in future experiments.

Zusammenfassung

Riboschalter sind strukturierte RNA-Elemente, die die Expression von nachgeschalteten Genen durch Ligandenbindung regulieren können. Sie werden aufgrund ihrer Abwesenheit im Menschen und ihrem häufigen Auftreten in Bakterien als gute potentielle Medikamentenziele angesehen. Riboschalter regulieren üblicherweise Gene, die für metabolische Enzyme kodieren, und sind in der Lage, auf eine Vielzahl von Liganden wie Ionen, Aminosäuren oder Purine zu reagieren. Die Gruppe der Purinriboschalter beinhaltet RNA-Elemente, die auf Guanin, Adenin oder 2´-Desoxyguanosin reagieren und ein gemeinsames Strukturmotiv besitzen.

Der erste Teil dieser Arbeit beschäftigt sich mit mutmaßlichen Guaninriboschaltern aus dem pathogenen Bakterium *Bacillus anthracis* und der Frage, ob und wie diese aktiv sind. Ihre Aktivität, Sensitivität, Ligandenspezifität und -bindung sollte untersucht werden. Dafür wurden die Riboschalter *in silico* und *in vitro* untersucht. Außerdem wurde ein neues reverses *in vivo* Reportergensystem etabliert, das die negative Antwort der OFF-Riboschalter auf die Ligandenbindung in ein positives Signal umwandeln kann. Die Ergebnisse zeigen, dass fünf *B. anthracis* Guaninriboschalter aktiv sind und bei Ligandenbindung die Transkription inhibieren. Sie unterscheiden sich deutlich in ihrer *in vivo* Ligandenantwort sowie in ihrer Ligandenaffinität. Die Ergebnisse sind sowohl in der medizinischen Chemie als auch in der synthetischen Biologie bei der Suche nach neuen Medikamentenzielen oder genetischen Werkzeugen von Bedeutung.

Der zweite Teil dieser Arbeit beschäftigt sich mit der Entwicklung eines Hochdurchsatzselektionsverfahrens zur Identifizierung von riboschalteraktivierenden Molekülen. Dafür wurde das oben erwähnte reverse *in vivo* Reportergensystem verwendet und für den Hochdurchsatz optimiert. Eine Bibliothek aus 6400 Substanzen wurde mit dem *xpt* Riboschalter aus *B. anthracis* als Zielstruktur getestet. In der darauffolgenden Treffervalidierung zeigte eine Verbindung, Gemcitabin, reproduzierbare positive Ergebnisse. Zusätzliche Gegen- und Zweitproben wiesen darauf hin, dass Gemcitabin zwar tatsächlich die Riboschalteraktivität *in vivo* beeinflusst, aber möglicherweise nicht den Riboschalter direkt bindet, sondern die beobachteten Effekte indirekt hervorruft. Trotzdem untermauern die Ergebnisse die Funktionalität des Hochdurchsatzverfahrens sowie

der Kontrollen und empfehlen dieses Screening für weitere zukünftige Verwendungen.

Table of Contents

1 Introduction

A few decades ago, RNA (ribonucleic acid) was primarily seen as intermediate in protein production from DNA (deoxyribonucleic acid) coding sequences according to the central dogma.[1] Little by little researchers realized that there are additional functions of RNA. The first regulatory RNA was discovered in bacteria in the late 1970s[2, 3] before the discovery of the first microRNA in 1993.[4] Since then a variety of non-coding regulatory RNAs have been identified, for example small interfering RNAs (siRNAs), piwi-interacting RNAs (piRNAs) or small nucleolar RNAs (snoRNAs). Small regulatory RNAs in bacteria (see [5] for a comprehensive review) include the recently discovered CRISPR (clustered regularly interspaced short palindromic repeat) RNAs as well as *cis*-acting RNAs called riboswitches.

1.1 Riboswitches

The term “riboswitch” was coined in 2002[6] and describes structured RNA elements usually located in 5´ untranslated regions of coding frames in bacteria and archaea (see [7, 8] for reviews). They consist of two parts called aptamer domain (the effector binding domain) and expression platform[9] that are connected by a switching sequence (Figure 1 A). Riboswitches are able to switch their conformation as a response to ligand binding. This ultimately leads to an altered expression of metabolic proteins or transporters whose functions are typically related to the riboswitch ligand.

In the following, various aspects of riboswitch activity and riboswitch research are presented.

1.1.1 Riboswitch classes

Riboswitches can be classified based on their nucleotide sequence, their ligands and the secondary structure of their aptamer domains. The aptamer domains of riboswitches are usually well-conserved,[10] which facilitates riboswitch identification. Aptamer domains utilize structures involving multi-helical junctions and pseudoknots for ligand binding.[10-12]

Numerous ligands are known so far: they range from small fluoride ions[13] to larger metabolites as *S*-adenosylmethionine[14] or thiamine pyrophosphate (TPP).[15, 16]

Several conserved, riboswitch-like sequences called orphan riboswitches are still waiting for the identification of their ligands and regulatory functions (for a review see [17]).

In one organism, a variety of different riboswitch classes may be found. For example, in the gram-positive pathogen *Bacillus anthracis* (*B. anthracis*) a *glmS* riboswitch — a ribozyme responding to glucosamine-6-phosphate — and a tandem TPP riboswitch have been investigated so far.[18-20] In addition, six guanine riboswitches were identified in *B. anthracis* in 2007 based on sequence homologies.[21]

1.1.2 Response mechanisms utilized by riboswitches

The regulatory response of riboswitches is transmitted by expression platforms. They are usually not conserved and display a huge variety in sequence as well as in possible functions. Nevertheless they can be grouped by the type of output they give. Riboswitches can either inhibit (OFF genetic logic = OFF switch) or activate (ON switch) gene expression upon ligand binding.

Ligand binding to the riboswitch typically results in modulation of transcription or translation, but regulation of an intrinsic ribozyme activity,[22] mRNA decay,[23] an antisense mechanism[24] or alternative splicing in plants, fungi and algae[25-28] have also been observed. Some riboswitches also employ cooperative ligand binding by tandem aptamers.[29]

In Firmicutes as *B. anthracis* or *Staphylococcus aureus* (*S. aureus*) riboswitches mainly act through transcription attenuation (Figure 1 A) by formation of a terminator hairpin.[21] In contrast, riboswitches in proteobacteria usually influence translation by regulating the accessibility of ribosome binding sites (Figure 1 B).[21, 30] Additionally, there are some unusual regulatory mechanisms; for example the *glmS* ribozyme undergoes self-cleavage upon glucosamine-6-phosphate binding.[22, 31]

Generally, ligand affinities are measured using dissociation constants (K_D). K_D values are equilibrium constants and therefore true in a thermodynamic regime. Riboswitches following a thermodynamic regime reach equilibrium before the decision for gene repression or activation is made. For these riboswitches, K_D values give the ligand concentration necessary for 50% occupancy of the riboswitch

aptamer domains. One example for this type of riboswitches is the adenine-responsive *add* riboswitch from *Vibrio vulnificus*.[32]

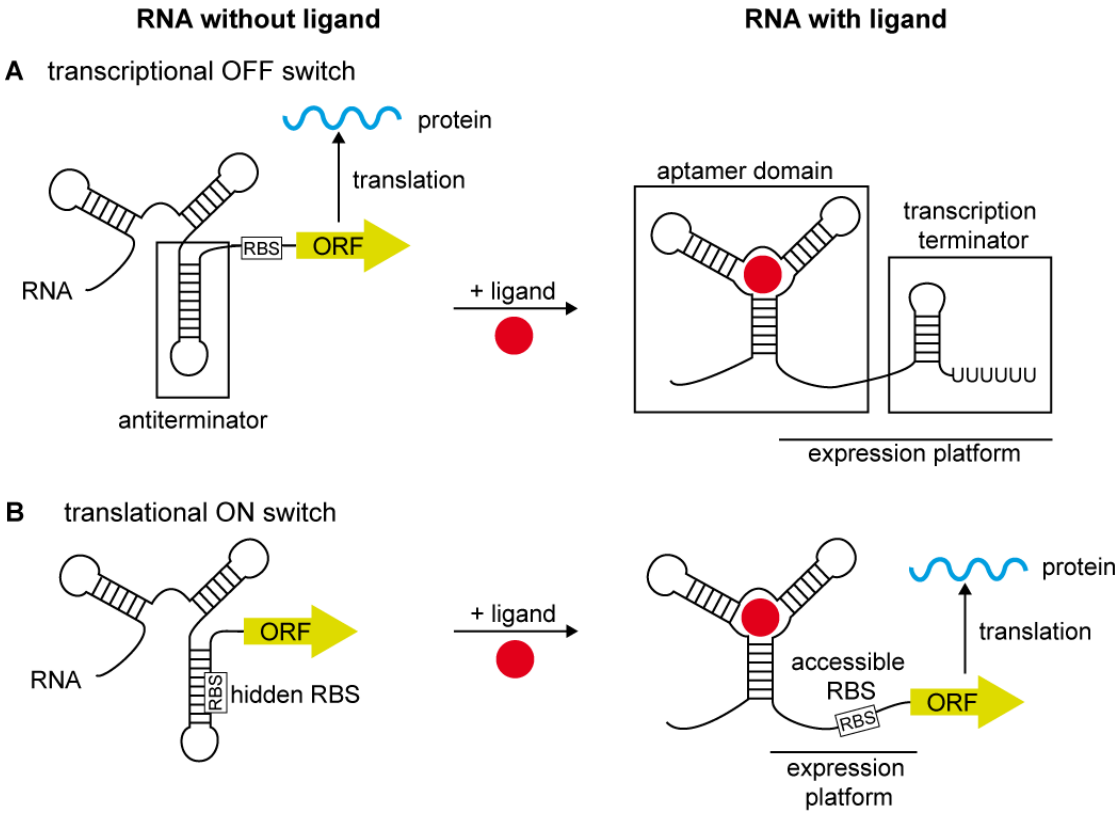

Figure 1. Two examples for riboswitch mechanisms.

(A) Scheme for a transcriptional OFF switch. Without ligand (left), an antiterminator is formed followed by an accessible ribosome binding site (RBS) and an open reading frame (ORF, green). Upon ligand (red) binding, an aptamer domain is formed followed by a transcription terminator.

(B) Scheme for a translational ON switch. Without ligand, the ribosome binding site is not accessible, thereby hindering ORF translation. The aptamer domain is formed upon ligand binding and the RBS is accessible leading to ORF translation (protein in blue). Color code and abbreviations as in A.

Other riboswitches, like the *ribD* FMN (flavin mononucleotide) riboswitch from *Bacillus subtilis* (*B. subtilis*) do not reach equilibrium und are kinetically driven instead.[33] Transcriptional riboswitches are likely to be kinetically driven because they have to fold and bind their ligand in the short time span after the release of the aptamer domain from the RNA polymerase exit channel (when ligand binding is theoretically possible) and before the RNA polymerase has passed the rho-independent terminator (when the decision point is reached).[34] This short time span is often not long enough for the riboswitch to reach equilibrium. Kinetically driven

riboswitches need a higher ligand concentration for the same response compared to a thermodynamically governed riboswitch with the same K_D value.

1.1.3 The model purine riboswitch: *xpt* from *B. subtilis*

The large class of purine riboswitches was discovered in 2003.[10] It is present in only a few taxonomic groups of bacteria[21] and comprises guanine-, adenine- and 2´-deoxyguanosine-sensing riboswitches[35] (Figure 2). The latter were recently suspected to also bind guanosine.[36]

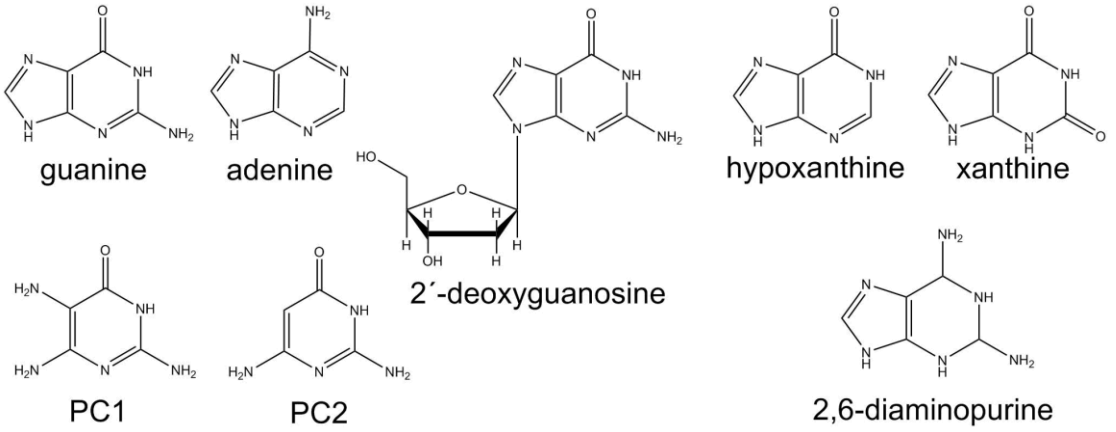

Figure 2: Chemical structures of natural and synthetic purine riboswitch regulators.

One of the best-investigated riboswitches is the *xpt* guanine riboswitch from *B. subtilis* that serves as a model for other purine riboswitches. It has been discovered in 2003[10] after findings that the *xpt-pbuX* expression is purine-repressible and the *xpt* leader mRNA (messenger RNA) contains a transcription terminator and an antiterminator (Figure 3 A).[37] It binds guanine tightly *in vitro* ($K_D \leq 5$ nM) but not adenine ($K_D > 300\,000$ nM).[10] Hypoxanthine and xanthine (both: $K_D \sim 50$ nM)[10] as well as some other purine or pyrimidine analogues as 2,5,6-triaminopyrimidin-4-one (PC1),[38] 2,6-diaminopyrimidin-4-one (PC2)[38] and 2,6-diaminopurine[39] do also bind to the *xpt* riboswitch. The effect of ligand binding to the riboswitch can be observed in *in vivo* reporter gene assays. For example, the β-galactosidase activity of a *B. subtilis xpt* riboswitch-*lacZ* fusion construct is reduced to 14.5% of the non-treated sample by addition of guanine.[10]

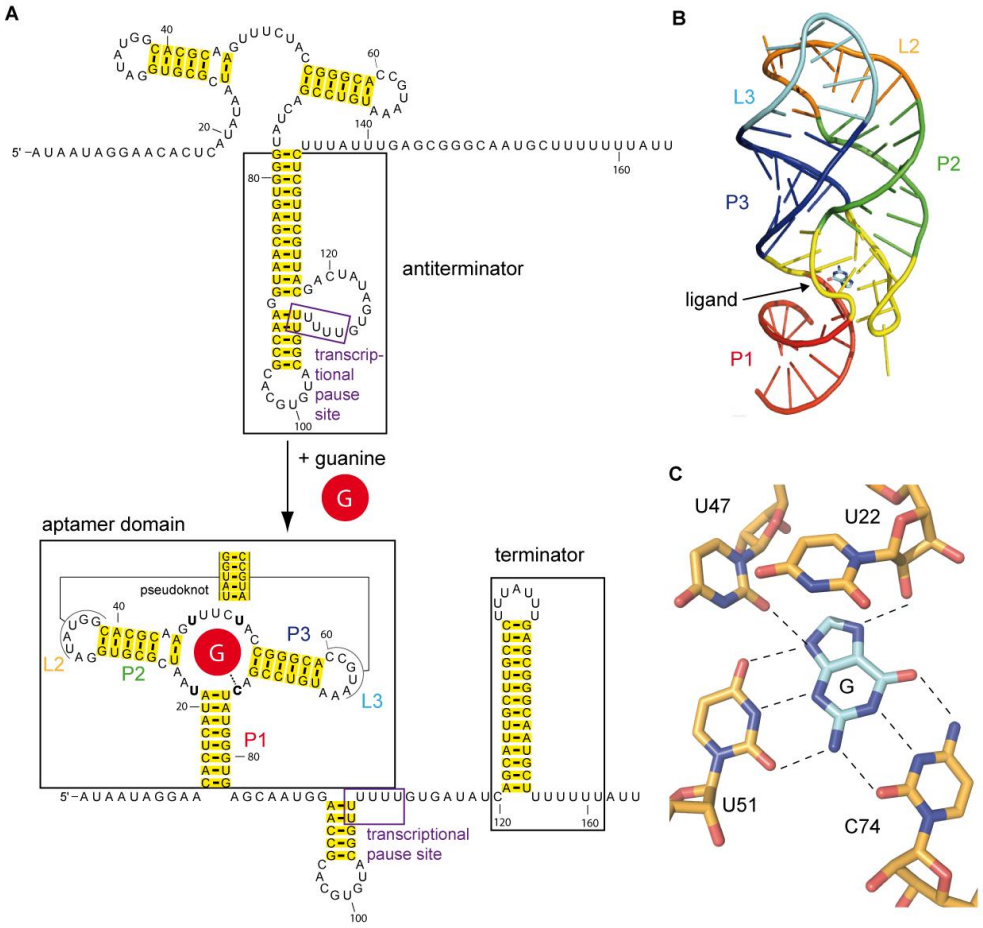

Figure 3. Structure of the *B. subtilis xpt* riboswitch.

(A) Scheme of the structure without (above) and with ligand (below). Base pairs are indicated by black lines and highlighted in yellow. The aptamer domain, the antiterminator, the terminator and the transcriptional pause site (violet) are boxed. The ligand guanine is represented by a red circle. The base numbers relative to the natural transcription start site are given.[10] In the bound structure, the pseudoknot, the helices P1 – P3, as well as the terminal loops L2 and L3 are indicated and bases with direct contacts to the ligand are written in bold. The Watson-Crick interaction between C74 and the ligand guanine is depicted by a dashed line.

(B) Structure of the *xpt* riboswitch (pdb code 1Y27).[11] The ligand guanine is represented by sticks and highlighted by an arrow; the riboswitch is shown as cartoon. The P1 helix is depicted in red, P2 in green, P3 in blue, L2 in orange and L3 in light blue. The junctions are shown in yellow.

(C) Close-up representation of the ligand guanine (G, light blue) and its hydrogen-bond interactions (dashed lines) with four riboswitch bases. Nitrogen atoms are shown in dark blue, oxygen atoms in red.

The aptamer domains of purine riboswitches are structurally conserved and consist of three-stem junctions where the loops L2 and L3 are able to form a pseudoknot through tertiary interactions (Figure 3 A).[10] The ligand is almost completely buried (Figure 3 B): the crystal structure of the *xpt* riboswitch aptamer domain in complex with hypoxanthine revealed that more than 97% of the ligand surface is solvent-

inaccessible.[12] The ligand-determining factor of guanine riboswitches is a cytosine at position 74 forming a Watson-Crick base pair with the ligand guanine. If C74 is changed to a uracil (C74U) the riboswitch is converted into an adenine-responsive riboswitch.[10, 40] The pyrimidine rings of U47 and U51, as well as the sugar ring of U22 form the guanine binding pocket in addition to C74 (Figure 3 C).[11, 12]

Purine riboswitches have a mainly pre-structured ligand-free state with a disordered central core.[41-43] A recent folding study[44] proposed that after beginning of transcription, helix 2 (P2) is folded first followed by P3. In a ligand-dependent step the junction between P2 and P3 (J2/3) is then closed and the kissing-loop interactions between L2 and L3 are established. Finally, the junctions P1 - P2 (J1/2) as well as P3 - P1 (J3/1) are formed before P1 folding. The folding of the *xpt B. subtilis* aptamer seems to be to a certain extent Mg^{2+}-dependent[45] and lasts less than one second *in vitro*.[44] Recent findings indicate that the transcription-terminating conformation is the only thermodynamically stable full-length *xpt* riboswitch RNA—independent of the presence of a ligand.[46] The ligand-dependent switch between the terminator and the metastable antiterminator is kinetically governed and requires a transcriptional pause site at a U-stretch 107 - 112 bases relative to the transcription start site (violet, Figure 3 A).[46]

1.1.4 Regulatory function in bacteria

Gene regulation by riboswitches is a common mechanism in bacteria influencing many different metabolic pathways. For example in *B. subtilis* about 2% of all genes are regulated by that means.[10] Usually, there is a connection between the ligand recognized by a riboswitch and the purposes of the genes regulated by the riboswitch. The largest number of purine pathway genes under the control of riboswitches was found in the family of the Bacillaceae.[47] These genes encode for proteins involved in purine salvage and *de novo* synthesis, as well as for permeases, transcription factors and transporters.[47]

In several pathogens such as *B. anthracis*,[48-50] *S. aureus*[51] or *Yersinia pestis*,[52] purine biosynthesis is crucial for virulence or growth in human blood. For example, in *S. aureus*, deletions of *guaA* (encoding for a guanosine monophosphate (GMP) synthase) or *guaB* (encoding for an inosine monophosphate (IMP) dehydrogenase) cause growth defects and avirulence.[53] In *B. subtilis*, the *guaB* gene as well as the

hprT gene (encoding for a hypoxanthine-guanine phosphoribosyltransferase) are essential.[54]

1.1.4.1 Guanine metabolism and its regulation in B. subtilis

Generally, there are two ways for the acquisition of purine building blocks: *de novo* synthesis and salvage pathways (Figure 4). The intermediates for purine and pyrimidine biosynthesis, uptake and nucleobase salvage are mainly preserved between prokaryotes, eukaryotes and archaea (reviewed in [55]). The *de novo* purine synthesis begins with the activation of ribose 5-phosphate to 5-phosphoribosyl-α-1-pyrophosphate (PRPP) and ultimately produces IMP, which is needed for adenosine triphosphate and GTP (guanosine triphosphate) biosynthesis.[56] The GTP precursor guanosine monophosphate (GMP) can either be produced from IMP, catalyzed by GuaB and GuaA, or from guanine through HprT.[57]

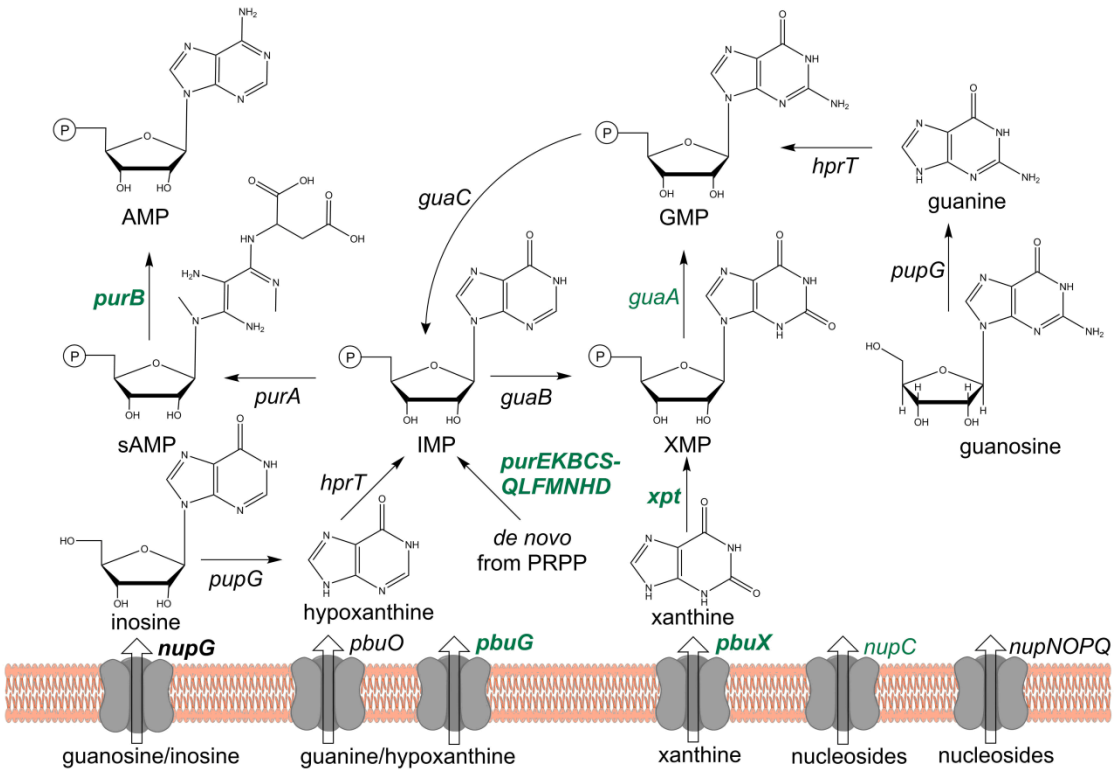

Figure 4. Scheme of the purine metabolism in *bacilli*.
Cell membrane is shown in brown and membrane transporters are depicted in grey. Genes regulated by guanine riboswitches in *B. subtilis* and/or *B. anthracis* are written in bold or green, respectively. Genes encoding for enzymes catalyzing the respective reactions are abbreviated according to MicrobesOnline. *purB*: adenylosuccinate lyase;[58] *guaC*: GMP reductase;[59] *guaA*: GMP synthase;[60] *hprT*: hypoxanthine-guanine phosphoribosyltransferase;[61] *purA*: adenylosuccinate synthase;[60] *guaB*: IMP dehydrogenase;[62] *pupG*: purine nucleoside phosphorylase;[63] *pbuG* and *pbuO*:

hypoxanthine-guanine permeases;[59] *pbuX*: xanthine permease;[37] *nup*C, *nupG* and *nupNOPQ*: nucleoside transporter;[37, 64, 65] *xpt*: xanthine phosphoribosyltransferase;[37]. AMP: adenosine monophosphate; sAMP: adenylosuccinate; GMP: guanosine monophosphate; IMP: inosine monophosphate; XMP: xanthosine monophosphate.

Nucleobase salvage is used by cells for the recycling of nucleic acids, but it is also a means to replace defective *de novo* synthesis. It is initiated from internal or external nucleotides, nucleosides and nucleobases. To import these molecules, the purine nucleoside transporter NupG, the guanosine transporter NupNOPQ, as well as the pyrimidine nucleoside transporter NupC, are used in *B. subtilis*.[65-67] Nucleobases can for example be shuttled into the cell via the xanthine permease PbuX or the hypoxanthine-guanine permeases PbuO and PbuG.[37, 59, 68] In general, the ability to utilize external nutrients does vary in bacteria.[57] However, in *B. subtilis* the pentose sugar and the purine bases can be used as carbon and nitrogen sources when preferred sources such as glucose and glutamine are absent[63, 69] (see [70, 71] for reviews).

The expression of genes involved in *B. subtilis* purine metabolism is orchestrated by two means: first, guanine-responsive riboswitches are present in front of the *B. subtilis* genes *xpt*, *pbuG*, *purE* (encoding for a phosphoribosyl carboxyaminoimidazole synthase) and *nupG*.[10] Second, the transcriptional repressor PurR downregulates genes like *pbuG* and the *xpt-pbuX* and *pur* operons in the absence of PRPP (Figure 5).[59, 72] As the PRPP pool is decreased by excess adenine in the growth medium, the transcription repressor PurR is activated in adenine-rich conditions.[73] Consequently, adenine starvation results in derepression of the PurR regulon.[73] Thus, a fine-tuned regulation of the genes is achieved, resulting in expression when PRPP is abundant and inhibition when sufficient amounts of guanine or adenine are present.

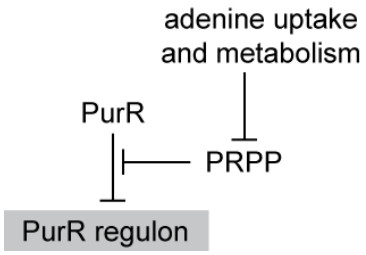

Figure 5: Regulation of the PurR regulon.
In adenine-rich growth medium, the PRPP pool is decreased. Thus, the transcriptional repressor PurR is active.

1.1.4.2 Guanine metabolism and its regulation in B. anthracis

The etiological agent of anthrax is the gram-positive bacterium *B. anthracis* (for additional information see [74, 75]) whose pathogenicity is largely dependent on two plasmids pXO1 and pXO2.[76, 77] Although *B. anthracis* primarily infects herbivores, humans are also susceptible.[75] Due to its infective and very resistant spores,[78] *B. anthracis* is a potential agent for bioterrorism and has already been used as such in the past.[79]

Anthrax infections can be acquired at the skin (cutaneous), through inhalation or through ingestion of the infective spores (gastrointestinal).[75] After inhalation, *B. anthracis* spores are taken up by macrophages and transported to the lymph nodes where bacterial replication takes place before the bacteria enter the blood stream.[80]

During inhalational infections, the tripartite anthrax toxin composed of protective antigen (PA), lethal factor (LF), and endema factor (EF) is expressed and secreted after *B. anthracis* germination. The first step of cellular infection involves PA binding to receptors on the host cell surface.[81, 82] Subsequently, PA is activated by proteolysis to form PA_{63},[83, 84] oligomerizes,[85, 86] binds LF and EF[87] and is internalized by clathrin-dependent endocytosis.[88] During this process, acidic pH causes the formation of membrane channels by a conformational change of PA_{63},[89] leading to the entry of EF and LF into the cytoplasm, either directly or through intraluminal vesicles.[90] EF is an adenylate cyclase[91] and LF is a metalloprotease cleaving MAP-kinase-kinases.[92] Both proteins thereby regulate a variety of cellular signaling pathways leading for example to disruption of cytokine secretion by dendritic cells[93] and the apoptosis of macrophages.[94] Anthrax infections can lead to meningitis or sepsis and finally to death.[75]

The guanine metabolism of *B. anthracis* is largely unknown. Even so, based on genome analysis it is supposed to be largely homologous to the metabolism of its phylogenetic relative and model organism *B. subtilis*.[49, 95, 96] *B. anthracis* is proposed to have six guanine riboswitches controlling the *pur* operon, the *xpt-pbuX* operon and genes presumably encoding for two transporters, a GMP synthase and a transcription regulator (Figure 4).[21] Although an early review states that the *B. anthracis* guanine riboswitches regulate only nine genes,[97] they probably control

up to 18 genes: the *B. anthracis pur* gene cluster has not been investigated closely and therefore it is not known whether the *purE* riboswitch controls one transcriptional unit comprising all genes or if there exist additional promoters and transcription terminators. However, there is no internal promoter known from the related organism *B. subtilis*[98] and the genes *purEKBCSQLFMNHD* are predicted to form an operon according to MicrobesOnline.[99, 100]

It is not quite clear to what extent *B. anthracis* pathogenesis and survival are dependent on guanine metabolism and guanine riboswitches. Inhibitors of PurE impair *B. anthracis* growth.[101] While *purA* and *purB* mutants are not able to infect mice, bacteria bearing mutations in genes involved in IMP production as well as *guaA* mutants are still infectious.[48] In contrast, *purE* but not *purK* mutations negatively affect *B. anthracis* virulence in mice.[50] This is supported by findings that *purH* deletions impair *B. anthracis* infection of guinea pigs but not of murine or rabbit models.[49] Thus, the pathogenicity of the mutants seems to be dependent on the model organism.

1.1.5 Methods to analyze riboswitches

After their identification, riboswitches need to be characterized in terms of activity, ligand sensitivity, mode of action, and structure. For this purpose, natural or synthetic riboswitches are tested in *in vivo* reporter gene experiments or *in vitro* assays.[102] One special means to analyze purine riboswitches *in vitro* is 2-aminopurine (2AP), a non-natural purine analog whose fluorescence is quenched by stacking interactions with adjacent bases upon binding.[103, 104] The non-natural adenine riboswitch ligand 2AP[11] thus can be used to monitor ligand binding *in vitro*.[105] Using a C74U mutation, guanine riboswitches can also be investigated with 2AP.[42, 106]

A frequently used *in vitro* method to determine changes in RNA structure as well as ligand affinity is the in-line probing assay.[107, 108] It utilizes the intrinsic instability of RNA due to intramolecular transesterification reactions to assess structural changes caused by ligand binding. The thereby-generated RNA cleavage patterns are visualized by polyacrylamide gel electrophoresis. Another common tool is called SHAPE (selective 2´-hydroxyl acylation and primer extension) that also relies on the structural changes of riboswitches caused by ligand binding. There, ligand binding

leads to altered accessibility of the ribose 2´ OH group that is monitored by its reactivity with chemical reagents such as *N*-methylisatoic anhydride.[109] The change in reactivity pattern is visualized by reverse transcription reactions that are stopped at the site of modification. Other methods to determine riboswitch-ligand binding involve equilibrium dialysis,[6, 16] gel-shift assays[110] or the cleavage of DNA-RNA duplexes by RNase H.[111]

The above-mentioned *in vitro* methods require radioactive labelling and sensitive devices (for example scintillation counter and equilibrium dialyzer). One radioactive-free method to determine relative dissociation constants (K_D´s) is by monitoring 3,5-difluoro-4-hydroxybenzylidene imidazolinone (DFHBI) binding of a spinach aptamer-riboswitch fusion (Figure 6). There, the P2 stem of the artificial DFHBI-binding spinach aptamer[112] (Figure 6 A) is fused to a riboswitch aptamer (Figure 6 B).[113, 114] Riboswitch ligand binding causes folding of the riboswitch aptamer domain that enables spinach aptamer folding. The subsequent formation of the fluorescent spinach-DFHBI complex can be monitored in fluorescence measurements.[112]

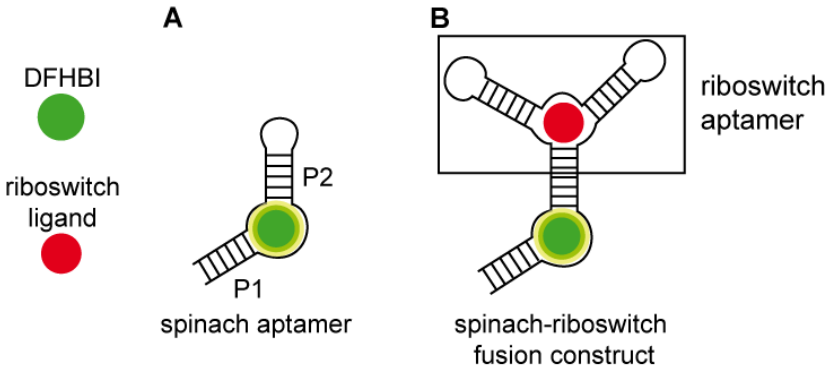

Figure 6: Schematic structure of the spinach aptamer (A) and the spinach-riboswitch fusion construct (B).
Upon spinach aptamer binding, DFHBI (green circle) causes fluorescence (light green). The riboswitch ligand is represented by a red circle.

1.1.6 Ways to utilize riboswitches…

1.1.6.1 … in synthetic biology

Riboswitch-containing genetic circuits can be utilized for a variety of applications ranging from intracellular adenosylcobalamine measurements[115] to medicinal chemistry. For instance, a drug-responsive ribozyme was used to regulate T-cell proliferation through cytokine expression.[116]

Due to their modular nature, riboswitches are well-suited as parts for genetic circuits in the field of synthetic biology. Another advantage is their ability to bind ligands with high selectivity. Their sensory domains (aptamers) and response domains (expression platforms) can be modified in many ways. Both parts can be mixed; however, a suitable linker domain has to be found.[117] To generate novel ligand-responsive elements, the ligand specificity of aptamer domains can be changed.[118] Additionally, novel aptamer domains binding natural or non-natural ligands can be engineered with SELEX (systematic evolution of ligands by exponential enrichment); for example the theophylline aptamer was identified using this method.[119-121] Expression platforms can be mimicked by formation of hairpins that enable or hinder the binding of the ribosome to a RBS in response to ligand binding.[122]

1.1.6.2 … in medicinal chemistry

So far there exist only a few RNA-targeting drugs as tetracycline[123] or fomivirsen[124] although RNA has several features that make it a good drug target (see [125] for a comprehensive review): RNA is composed of only four different building blocks and it is able to form helices or hairpins and also builds up small three-dimensional cavities, for example in riboswitches. RNA-ligand interactions can be mediated by base pairing, stacking or metal ion-mediated interactions.[126, 127]

Riboswitches are especially good potential drug targets due to their importance in bacteria and rare occurrence in eukaryotes.[97] To date no riboswitch is known in humans. Binding of a drug to a riboswitch can pretend the presence of a ligand while the cell is starving for the ligand molecule. Therefore, riboswitches in pathogenic bacteria that regulate genes essential for virulence or survival are interesting for drug development. Alternatively, it is possible that one riboswitch regulates several genes that are together essential for the organism.[97] Furthermore, ligands might target several riboswitches of the same class simultaneously. This combined effect could also negatively influence bacterial survival or virulence. Natural ligands can serve as lead structures to develop non-natural synthetic mimics for riboswitch ligands.

There are different ways to find synthetic riboswitch ligands: some groups designed and screened small libraries based on ligand similarity or docking.[38, 128-130] In a phenotypic screening targeting the *Escherichia coli* (*E. coli*) FMN riboswitch an

antibacterial compound was found that is structurally distinct from the native riboswitch ligand.[131] The *glmS* ribozyme was targeted in *in vitro* high-throughput assays utilizing its self-cleavage trait.[130, 132]

Since the beginning of the practical work for this thesis, the first two *in vivo* screenings using riboswitches as targets have been published. Both methods utilize riboswitch-β-galactosidase reporter constructs, which is less convenient and more time-consuming than a luciferase reporter (Section 1.2.4). First, a fluoride ON riboswitch was used to detect effectors of intracellular fluoride concentrations in a high-throughput screening.[133] Second, a low-throughput *in vivo* method was published to identify TPP riboswitch (OFF switch) activators with a direct reporter gene setup.[134] In a direct setup, OFF riboswitch hits cause a decrease in reporter activity (inhibition assay). Thus, a number of false-positive hits interfering with the reporter signal can be expected.[135] Therefore, a reverse setup, which leads to an activation assay, would be more convenient for OFF riboswitch screenings.

Some antibacterial compounds have already been found to act, at least partially, on riboswitches, e.g. L-aminoethylcysteine (a lysine analog)[136] or roseoflavin (a riboflavin analog).[137] The *guaA* riboswitch agonist PC1 was shown to inhibit *S. aureus* growth in a murine model[38] and to be active against bovine mastitis[138] although its activity does not seem to depend solely on the riboswitch.[53] Additionally, the compound 6-*N*-hydroxylaminopurine (G7) binds the *B. subtilis xpt* riboswitch and inhibits *B. subtilis* growth in minimal medium.[129]

When searching for synthetic riboswitch ligands, some general considerations concerning drug properties have to be kept in mind. Basically, drugs have to fulfill two major criteria to be active:[139] first, they should bind their target with high selectivity and affinity. Second, they should have favorable drug absorption, distribution and metabolism as well as excretion characteristics in the human body (pharmacokinetics). Orally taken drugs can be administered easily and are therefore generally favored although most of them need to pass the gastrointestinal tract and through the intestinal or gut wall.[139] Therefore, they should be able to pass cell membranes on the one hand but also be soluble in the gut to enhance absorption on the other hand. Consequently, they require not only chemical and enzymatic stability but also a balanced character between hydrophobicity and hydrophilicity. To judge

the probability of a hit compound to have suitable orally available drug properties Lipinski´s rule of five is used as a rule of thumb:[140] thereafter, a molecular weight of less than 500, at most 5 hydrogen bond donors and/or 10 hydrogen bond acceptors and a log P greater 5 (partition coefficient P = drug conc. in octanol/drug conc. in water) is required.

1.2 Parts of the reverse screening system

In this thesis, a reverse *in vivo* reporter gene setup to characterize riboswitches and to screen for novel riboswitch ligands should be developed. The genetic parts utilized for this purpose are presented in the following.

1.2.1 The chassis: *B. subtilis*

B. subtilis is a widely used, well-investigated gram-positive model organism. The soil-dwelling firmicute with low GC content grows aerobically and is able to form highly resistant endospores.[141] It is affirmed to be "generally recognized as safe" (GRAS) by the US Food and Drug administration (FDA).[142]

There exist many protocols for genetic modifications of *B. subtilis* ranging from the introduction of plasmids over deletions of part of the *B. subtilis* genome until genetic insertions into its genome.[143, 144] A well-established strategy for the introduction of synthetic reporter constructs is to stably integrate part of a plasmid into a pre-defined locus on the *B. subtilis* chromosome. The corresponding vectors (e.g. pXT[145] or $pSB_{BS}1C$[146]) usually contain a multiple cloning site flanked by two DNA sequences homologous to the target integration site in the *B. subtilis* genome. They also comprise antibiotic resistance genes for selection in both *B. subtilis* and *E. coli*. After plasmid amplification and isolation from *E. coli, B. subtilis* is transformed with the verified and linearized plasmids. In *B. subtilis* the plasmids are integrated into their respective target genes which are thereby interrupted and usually become nonfunctional. The non-essential genes *thrC* and *amyE* are commonly used for this purpose because their interruption can easily be verified in phenotypic assays. For integration in the *thrC* locus the presence of the promoter P_{hom} upstream of the integration site needs to be considered because it can cause transcriptional read-through in the integration site.[146] Integrating genetic parts into the genome is advantageous because varying plasmid copy numbers are thereby avoided. Instead, there is constantly one copy per cell.

1.2.2 The promoter P_{xyl}

P_{xyl} is a well-described inducible *B. subtilis* promoter often used for genetic modifications of *B. subtilis.* It is inhibited by the protein XylR in the absence of xylose (Figure 7).[147] In the presence of xylose, XylR is released from P_{xyl} and thus P_{xyl} is

activated. This mechanism ensures a xylose-concentration dependent control of gene expression.[146]

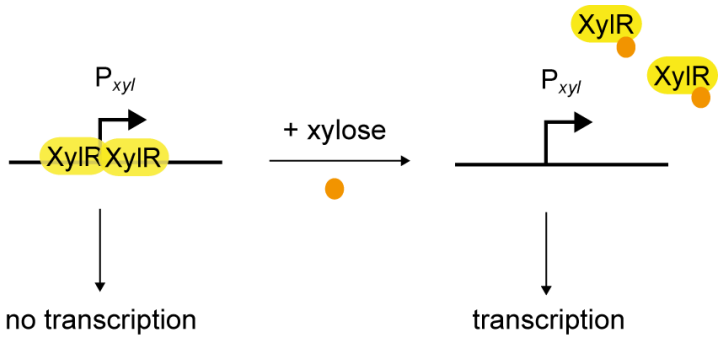

Figure 7: Scheme of P_{xyl} activity.
In the absence of xylose P_{xyl} is inhibited by XylR. XylR is released from P_{xyl} by xylose thereby inducing transcription from the P_{xyl} promoter.

1.2.3 The protein BlaI and the promoter P_{blaP}

BlaI and P_{blaP} both originate from *B. licheniformis*. BlaI proteins bind and repress the promoter P_{blaP} that contains two BlaI binding sites.[148] In *B. licheniformis*, BlaI represses β-lactamase gene (*blaP*) expression in the absence of β-lactam antibiotics. If β-lactam antibiotics are present, however, they are sensed by the transmembrane protein BlaR through acylation followed by its proteolytic autocleavage.[149, 150] The following steps that might involve BlaI autocleavage[151] are not fully understood yet but they finally lead to the release of BlaI from P_{blaP}.

In this work, only P_{blaP} and BlaI are utilized to gain a reverse reporter system. In the past, interactions between *blaI* and P_{blaP} have been employed for the integration of genes into the *B. subtilis* genome resulting in strains without a selection marker.[152] In *B. subtilis*, there exist no *blaP* homologues, but the P_{blaP} promoter is part of the early synthetic *B. subtilis* promoter $P_{pac\text{-}1}$.[153]

1.2.4 The reporter

In the following, the reporter genes utilized for the reporter system in this work are introduced.

1.2.4.1 Bioluminescence

Bioluminescence has been reported primarily from bacteria belonging to the genera *Photobacterium*, *Vibrio* and *Photorhabdus* (see [154, 155] for comprehensive reviews). Its generation is similar in all these bacteria: they contain two proteins responsible for

light production by forming a heterodimeric luciferase (LuxA and LuxB) with oxygen[156], myristyl aldehyde[157] and $FMNH_2$[158] consumption. The three proteins LuxC, LuxD and LuxE are needed for myristyl aldehyde regeneration.[159-161] In the reporter system, the *lux* genes from *Photorhabdus luminescens* are utilized.

As a reporter, the widely used bioluminescence readout has several advantages: it can be detected in bacteria without lysing the cells or adding substrate. With a plate reader it is also possible to generate time-resolved luminescence curves of single or multiple samples in parallel. Over a wide range, light intensity is directly dependent on the amount of luciferase protein.[155] Compared to fluorescence caused by GFP, bioluminescence is able to report promoter activity in real time.[162] The autoluminescence of *B. subtilis* strain W168 is negligible[155] while there is considerable autofluorescence of *B. subtilis* cells interfering with the GFP signal (own observations and [163]).

1.2.4.2 β-galactosidase activity

In nature, β-galactosidase originating from *E. coli* produces glucose and galactose from lactose, but it is also able to hydrolyze other β-galactopyranosides as *ortho*-nitrophenyl-β-galactoside (ONPG).[164] ONPG is cleaved by β-galactosidase to form galactose and the yellow product *ortho*-nitrophenol that can be quantified by measuring absorption at 420 nm. β-galactosidase activity displayed by ONPG hydrolysis is a commonly used and rather ancient reporter with a different mode of action and readout compared to bioluminescence. β-galactosidase activity can only be assayed after cell lysis and substrate addition. Compared to bioluminescence, additional pipetting steps are therefore necessary before signal detection is possible. As cell lysis is required, several samples have to be taken for time-course experiments.

2 Objectives

Despite the importance of riboswitches for their organisms, many riboswitches from pathogenic bacteria are not known or not well-investigated so far. Accordingly, the existence and position of guanine riboswitches from the gram-positive pathogen *B. anthracis* have only been hypothesized from sequence homologies at the beginning of this work.

The first aim of this thesis was to test the activity of potential *B. anthracis* guanine riboswitches. Thus, following bioinformatics analysis the activity of the riboswitches was investigated experimentally. Besides the functional characterization of the riboswitches, their *in vivo* activities as well as their *in vitro* ligand binding affinities were compared. Additionally, the ligand specificities of the *B. anthracis* riboswitches were analyzed using several guanine-like compounds. For these purposes, a novel indirect *in vivo* reporter system was expected to convert the response of an OFF riboswitch into a positive readout. The model organism *B. subtilis* was used as chassis since it is non-pathogenic, related to *B. anthracis*, and can be genetically modified.

So far, no reverse *in vivo* high-throughput screening for novel riboswitch ligands is known. It was intended to close this gap by optimizing the above-mentioned reporter system for high-throughput screening in 384-well format. To be able to identify false-positive hits, it is also of high importance to develop a secondary assay as well as counter assays.

In summary, the goal of this work was not only to provide an overview about several *B. anthracis* riboswitches in terms of mode of action, activity and selectivity, but also to establish a high-throughput-applicable *in vivo* screening system to provide new means for the identification of novel riboswitch ligands. In the future this could form the basis for using *B. anthracis* guanine riboswitches as drug targets and extend the number of well-understood riboswitches available for applications in synthetic biology.

3 Material and Methods

3.1 Material

3.1.1 Instruments

Table 1: Instruments used in this thesis.

Purpose	Name	Supplier
gel electroporation and analysis	Hoefer™ Mighty Small™ II system	Harvard bioscience (Holliston, USA)
	power supply pharmacia biotech EPS-600	GE healthcare (Chalfort St. Giles, GB)
	peqlab gel system and power supply	VWR (Radnor, USA)
	benchtop UV transilluminator 3UV™	Analytik Jena (Jena, Germany)
	gel imaging system G:BOX	Syngene (Cambridge, GB)
	UVLS-24 EL series UV lamp	Analytik Jena
centrifuges	SIGMA 1-14 Microfuge	SciQuip (Shrewsbury, GB)
	SIGMA 1-14K	SciQuip
	SIGMA 1-16K	SciQuip
electroporation	MicroPulser electroporation apparatus	Bio-Rad (Hercules, USA)
incubators	New Brunswick™ Scientific Innova 4320	Eppendorf (Hamburg, Germany)
	Multitron Standard	Infors HT (Bottmingen, Schweiz)
	New Brunswick™ Scientific I26	Eppendorf
	incubator	memmert (Schwabach, Germany)
microplate reader and accessories	Spark® 10M	Tecan (Männedorf, Switzerland)
	EnVision multilabel reader	PerkinElmer (Waltham, USA)
For *in vitro* assays	96-well plates PS, FLUOTRAC™ 200	Greiner^{R} Bio-One (Frickenhausen, Germany)
For *in vivo*	96-well plates PS, black, µ-	Greiner^{R} Bio-One

Purpose	Name	Supplier
assays	clear 384-well plates PS, black, µ-clear	Greiner^{R} Bio-One
PCR	T100™ thermal cycler	Bio-Rad
	MJ Mini™ thermal cycler	Bio-Rad
photometers	NanoPhotometer Classic	Implen (München, Germany)
	NanoDrop™ 2000c	Thermo Fisher Scientific (Wilmington, USA)
	Ultrospec™ 10	GE healthcare
pH-meter	inoLab® pH 720	WTW (Weilheim, Germany)
pipettes	accu-jet® pro	Brand (Wertheim, Germany)
	Research® plus 2.5 µl	Eppendorf
	Research® plus 10 µl	Eppendorf
	Research® plus 200 µl	Eppendorf
	Research® plus 1000 µl	Eppendorf
	Multipette® M4	Eppendorf
	Ovation Pipette ESC 25-1250 µl	VistaLab technologies (Brewster, USA)
scales	Sartorius BP 4100 S	DWS (Elk Grove, USA)
	Sartorius TE 124 S	DWS
screening robotics	MultiFlo™ dispenser	BioTek (Winooski, USA)
	Sciclone G3 liquid handling workstation	PerkinElmer
stirrers	MR Hei-Standard	Heidolph Instruments (Schwabach, Germany)
heating and sterilization	drying oven DRY-Line® 53	VWR
	autoclave Classic Media	Prestige Medical (Coventry, GB)
	ThermoMixer® comfort	Eppendorf
shakers	lab dancer	VWR
	REAX 2000	Heidolph Instruments

3.1.2 Chemicals, enzymes and kits

If not stated otherwise, chemicals were purchased from Carl Roth (Karlsruhe, Germany), VWR, AMRESCO (Solon, USA), New England Biolabs (Ipswich, USA), Thermo Fisher Scientific, Merck (Darmstadt, Germany) and AppliChem (Darmstadt, Germany). For the screening, the small-molecule library including an FDA-approved drug library of the Assay development and screening platform at the Helmholtz Zentrum München was used.[165] Compounds for the hit verification were purchased from TCI (Tokyo, Japan), Cayman chemical (Ann Arbor, USA), Sigma-Aldrich (St. Louis, USA) and Molekula (Newcastle Upon Tyne, UK).

Enzymes were used according to manufacturer´s instructions. Plasmids were amplified in *E. coli* and isolated using the peqGold Plasmid Miniprep Kit (VWR) or the Monarch Plasmid Miniprep Kit (NEB, Ipswich, USA). DNA preparations were purified by means of the Wizard SV Gel and PCR Clean-up system (Promega), the PeqGold Gel extraction Kit (VWR) or the Cycle-Pure Kit (VWR). Sequencing was done by GATC biotech (Konstanz, Germany).

Table 2: Enzymes used in this thesis.

Purpose	Name	Supplier
cell wall digestion	lysozyme	Merck
PCR (polymerase chain reaction)	*Pfu* polymerase	Promega (Madison, USA)
	Phusion polymerase	NEB
	Q5 polymerase	NEB
	GoTaq polymerase	Promega
digestion	restriction enzymes	NEB
	antarctic phosphatase	NEB
ligation	HC ligase	Promega
	DNA ligase	NEB
RNA preparation	RNase inhibitor (murine)	NEB
	inorganic pyrophosphatase (*E. coli*)	NEB
	T7 RNA polymerase	laboratory stock
	DNase (RNase-free)	NEB

3.1.3 Media

Table 3: Media used in this thesis.

Name	Composition
expression mix	2.4% (weight per volume ; w/v) yeast extract
	2.4% (w/v) casamino acids
	1.17 mM tryptophan
	0.387 µM chloramphenicol (if required)
***in vitro* reaction buffer pH 7.5**	40 mM HEPES (4-(2-hydroxyethyl)-1-piperazineethane-sulfonic acid)
For *in vitro* riboswitch binding assay	125 mM KCl
	3 mM $MgCl_2$
	30 µM DFHBI
LB	0.5% (w/v) NaCl
	1% (w/v) peptone
	0.5% (w/v) yeast extract
Lugol´s iodine	0.12 M KI
	1% (w/v) iodine
modified CSE[146, 166]	40.0 mM MOPS (3-(*N*-morpholino)propanesulfonic acid)
(C minimal medium with sodium succinate and potassium glutamate)	25.0 mM $(NH_4)_2SO_4$
	0.385 mM KH_2PO_4
	0.615 mM K_2HPO_4
	10.4 µM $MnSO_4$
	0.50 mM $MgSO_4$
	245 µM tryptophan
	42.0 mM threonine
	43.2 µM potassium glutamate
	84.0 µM ammonium ferric citrate
	37.0 µM sodium succinate
	139 µM fructose
	1% (w/v) casamino acids
MNGE medium	52.1 mM K_2HPO_4
	38.5 mM KH_2PO_4

Name	Composition
	2.85 mM $MgSO_4$
	2.97 mM sodium citrate
	0.105 M glucose
	10.3 mM potassium glutamate
	39.9 µM ammonium ferric citrate
	233 µM tryptophan
	399 µM threonine
SC buffer pH 7.0	0.15 M NaCl
	0.01 M sodium citrate
SOC medium (super optimal broth with catabolite repression)	0.5% (w/v) yeast extract
	2% (w/v) peptone
	10 mM NaCl
	2.5 mM KCl
	10 mM $MgSO_4$
	10 mM $MgCl_2$
	20 mM glucose
starch plates	0.75% (w/v) nutrient broth
	0.5% (w/v) starch
	1.5% (w/v) agar
50 x TAE buffer	2 M Tris (tris(hydroxymethyl)aminomethane)
	1 M glacial acetic acid
	50 mM EDTA (ethylenediaminetetraacetic acid)
10 x TBE buffer (Tris-Borate-EDTA buffer)	900 mM Tris
	900 mM boric acid
	10 mM EDTA pH 8.0
TBE-urea acrylamide gel	10% (volume per volume; v/v) 10 x TBE buffer
	7.0 M urea
	6% (w/v) acrylamide/bisacrylamide (19:1)
	0.12% (v/v) tetramethylethylenediamine
	3.5 mM ammonium persulfate
TE buffer (Tris-EDTA buffer)	10 mM Tris-HCl pH 7.5
	1 mM EDTA pH 8.0

Name	Composition
5 x *in vitro* transcription buffer	0.15 M HEPES pH 8.0 10 mM spermidine 50 mM dithiothreitol 0.05% (w/v) triton X100
working buffer pH 7.0	60 mM Na_2HPO_4 40 mM NaH_2PO_4 10 mM KCl 1 mM $MgSO_4$ 20 mM β-mercaptoethanol

3.1.4 Primers

Oligonucleotides and synthesized genes were ordered from metabion (Planegg, Germany), biomers.net (Ulm, Germany) or Thermo Fisher Scientific. The working concentration of synthesized oligonucleotides was 10 pmol/µl.

Table 4: Primers and oligonucleotides used in this thesis.

No.	Name[a]	Nucleotide sequence (5´ → 3´)[b]
for cloning		
o136	P_{blaP}-*Eco*RIfor	ATA*GAATTC*CTTCCCTCCGTTCATTTGTCCCCG
o138	BlaIfor	ATGAAAAAAATACCTCAAATCTCTGATG
o139	BlaIrev *Hind*III	*AAGCTT*TCATTCCTTCTTTCTGTTCTTATGTTC
o142	BS-purineRSfor	ATTAATTAAAATAGGAACACTCATATAATCGCGTG
o143	BS-purineRS-BlaIrev	**CATCAGAGATTTGAGGTATTTTTTTCAT**CCTGTCT ACCTCCGTTATG
o251	P_{blaP}-GFP rev	CTCATCTAGAATCCTCCTTA**GTATGAATATTTGAT TGATCGTGACTAGCTG**
o252	P_{blaP}-GFP fwd	**GTCACGATCAATCAAATATTCATAC**TAAGGAGGA TTCTAGATGAGTAAAGG
o253	GFPrev (*Hin*dIII)	GCT*AAGCTT*GCATGCCTGCAGGTCGAC
o259	*Ba*Xpt RS (*Bsa*I)	TAT*GGTCTC*AATCCAATAAATAGTTAGCTACACTC ATATAATCGCGGGGATATGGCCTGCAAGTTTCTAC CGAAGTACCGTAAATACTTTGACTATGAGTGAGGA CGAATATATTTGCTTGTTTAGCATTCTTTTTTGCGA AACTCCAAAAGCGCGTCTCTCACTTGTAACGAGT GGTGGCGGCTTTTGGAGTTTTTTTATTGCATAAGA

No.	Name[a]	Nucleotide sequence (5´ → 3´)[b]
		GGGGGAACAAACATGAA*GAGACC*ATT
o294	*BaGuaA* RS (*Bsa*I)	TAT*GGTCTC*AATCCAAGATAATATAAAACGATCCTT CATATATCCTCAAAGATAAGGTTTGAGAGTCTCTA CCGGGTTACCGTAAACAACCTGACTATGAAGGCA GTGTGTCTTATATTTATAAAGAGCGGAAGACTATC TTTCTTTATAAAGCCAGACCCCTGCCTTTTCTTTGT TATGAGACTAGAGGCGGAGGACTGGCTTTTTTTAT TATATTGGTAATGCTTTTCGCCAAATTGGTGAAAAT ATTTATATACGAGAACTAACGTTGGGGTGATTATTA TGAA*GAGACC*ATT
o295	*BaXpt* RS (*Bsa*I)	TAT*GGTCTC*AATCCAATAAATAGTTAGCTACACTC ATATAATCGCGGGGATATGGCCTGCAAGTTTCTAC CGAAGTACCGTAAATACTTTGACTATGAGTGAGGA CGAATATATTTGCTTGTTTAGCATTCTTTTTTGCGA AACTCCAAAAGCGCGTCTCTCACTTGTAACGAGT GGTGGCGGCTTTTGGAGTTTTTTTATTGCATAAGA GGGGGAACAAACATGAA*GAGACC*ATT
o301	pXT-*blaI*GGCFwd (*Bsa*I)	TAT*GGTCTC*AATGAAAAAAATACCTCAAATCTCTG ATGC
o302	pXT-P_{xyl}GGCRev (*Bsa*I)	TAT*GGTCTC*AGGATCCTCTAGAGTCGACCTGC
o309	*Lux*fwd_*Xba*I	GAT*TCTAGA*TGAAATTTGGAAACTTTTTGCTTAC
o310	*Lux*rev_*Sal*I	AAA*GTCGAC*ATATCAACTATCAAACGCTTCGG
o355	*purE* RS from *B. anthracis* (*Bsa*I)	TAT*GGTCTC*AATCCGAAAGAATAATATATAAGACC TCATATAATCGCGGGGATATGGCCTGCAAGTCTC TACCTAACGACCGTTATTCGTTAGACTATGAGGGA AAGTCACTCGGTATTTTTCTATTCACAAGGGATAC GTATGCCTGAGTAGAGCGCTTTCTCTCATAGTAAA AGAGAAACTGTTCTATTTCAGGCTTTTTTATTTGAA TCGGGGGGATTCTAATATGAA*GAGACC*ATT
o356	COG1972 RS from *B. anthracis* (*Bsa*I)	TAT*GGTCTC*AATCCAATACGGACGATGTTACCTCA TATATACTCGATAATATGGATCGAGAGTTTCTACC CGGCAACCTTAAATTGCTGGACTATGGGGAAAAC TAATGAATATTAGCCTATGTGCAAAAAAGGACTCA TATTGATTACTTTCTCTCATAGATGAAAGTGAATCC ATATGGGTCTTTTTTTATTTTTATTTTTCTAAAAGGT CAGACATCTTACGTATGACATAAAACCTCTTTGTTT TATTTTTAGTAATATAACGAGCGTTTTATGTACAAA CTTTATACGAACTTCTGAAAGGGGCAACTACATGA

No.	Name[a]	Nucleotide sequence (5´ → 3´)[b]
		A*G**AGACC*ATT
o357	COG2252 RS from *B. anthracis* (*Bsa*I)	TAT*GGTCTC*AATCCGAAAAGTGAATATTATGCCGT CGTATAATATCGGGGATATGGCCCGAAAGTTTCTA CCTAGCTACCGTAAATGGCTTGACTACGAGGCGT TTTTATAAAGGTGAGGGGAATCTTATCTTTATTCAT AGAACGCTTCCATGTATATGCAATGGAAGCCTTTT TTATTTTTAATAAATAAAAGAGGGCTAGGGGAATTA CGGCGAGTAATCATATAACGGGGGAAACGTAAGA TGAA*G**AGACC*ATT
o363	ΔRS SD$_{xptB.ant}$ ctr rev (*Bsa*I)	TAT*GGTCTC*ATCATGTTTGTTCCCCCTCTTGGATC CTCTAGAGTCGAC
o364	*Bsa*I-SD$_{opt}$-*blaI Fwd*	AAA*GGTCTC*ATAAGGAGGATTCTAGATGAAAAAAA TACCTCAAATCTCTG
o365	*Bsa*I-*P$_{xyl}$Rev*	ATA*GGTCTCC*CAGATGCATTTTATTTCATATAGTAA GTACATC
o366	*Bsa*I-SD$_{opt}$_*blaIfwd ctr*	AAA*GGTCTC*ATCTGTAAGGAGGATTCTAGATGAAA AAAATACCTCAAATCTCTG
o367	*guaA*RS1_Fwd (*Bsa*I)	ATA*GGTCTC*ATCTGACGATCCTTCATATATCCTCA AAG
o368	*guaA*RS1_Rev (*Bsa*I)	ATA*GGTCTC*ACTTAAATAAAAAAAGCCAGTCCTCC G
o369	*Bsa*I*xptB.ant*1_Fwd	AAA*GGTCTC*ATCTGCTACACTCATATAATCGCGG
o370	*Bsa*I*xptB.ant*1_Rev	ATA*GGTCTC*ACTTAAATAAAAAAACTCCAAAAGCC GC
o371	*Bsa*I_*purE*RS1_Fwd	AAA*GGTCTC*ATCTGCCTCATATAATCGCGGGG
o372	*Bsa*I_*purE*RS1_Rev	ATA*GGTCTC*ACTTAAAATAAAAAAGCCTGAAATAG AACAG
o373	*Bsa*I_COG2252 RS1_Fwd	AAA*GGTCTC*ATCTGATGCCGTCGTATAATATCGG
o374	*Bsa*I_COG2252 RS1_Rev	ATA*GGTCTC*ACTTAAAAATAAAAAAGGCTTCCATT GC
o375	*Bsa*I_COG1972 RS1_Fwd	AAA*GGTCTC*ATCTGCCTCATATATACTCGATAATAT G
o376	*Bsa*I_COG1972 RS1_Rev	ATA*GGTCTC*ACTTAAGAAAAATAAAAATAAAAAAAG ACCC
o419	*Bsa*I-P$_{xyl}$fwd	AAA*GGTCTC*ATGATCAGCGATATCCACTTCATC
o420	*Bsa*I-*thrC*rev	ATA*GGTCTCC*CGAAGGCAGCAGTTTTTTGG

No.	Name[a]	Nucleotide sequence (5´ → 3´)[b]
o422	*Bsa*I-*xpt*3Fwd	AAA*GGTCTC*ATCTGAAATAGTTAGCTACACTCATA TAATC
o423	*Bsa*I-*xpt*4Rev SD_{opt}	ATA*GGTCTC*ACTTATGCAATAAAAAAACTCCAAAA GC
o425	*Bsa*I*guaA*3Fwd	AAA*GGTCTC*ATCTGATAATATAAAACGATCCTTCAT ATATC
o426	*Bsa*I*guaA*4Rev SD_{opt}	ATA*GGTCTC*ACTTAGTTCTCGTATATAAATATTTTC ACC
o428	*Bsa*I_1972 RS3Fwd	AAA*GGTCTC*ATCTGGACGATGTTACCTCATATATA C
o429	*Bsa*I_1972 RS4Rev SD_{opt}	ATA*GGTCTC*ACTTAGAAGTTCGTATAAAGTTTGTA CATAAAAC
o434	*Bsa*I_2252 RS3Fwd	AAA*GGTCTC*ATCTGAGTGAATATTATGCCGTCGTA TAATATC
o435	*Bsa*I_2252 RS4Rev SD_{opt}	ATA*GGTCTC*ACTTATATGATTACTCGCCGTAATTC
o437	*Bsa*I_*purE*3Fwd	AAA*GGTCTC*ATCTGATATATAAGACCTCATATAATC GCG
o438	*Bsa*I_*purE*4RevSD_{opt}	ATA*GGTCTC*ACTTATTCAAATAAAAAAGCCTGAAAT AG
o469	*xptB.sub*2_Fwd	AAA*GGTCTC*ATCTGATAATAGGAACACTCATATAA TCGC
o471	*xptB.sub*3_rev	ATA*GGTCTC*ACTTAATGAGAATAAAAAAAGCATTG CC
o353	$\Delta P_{xyl}\Delta$RS rev *Bsa*I	AAA*GGTCTC*ACTTAAAGAAATACTAAGGGATTTAA AAAGAG
	LysS terminator sequence	AAA*GGTCTC*ATTCGTAAAAAAGAGCGGTATCCTCC ATAGGGAAAGGATGCCGCTCTTTTTAAATCCCTTA GTATTTCTTGATT*GAGACC*GAT
for *in vitro* assays		
o465	spinach2_BA_*xpt*-4	GATGTAACTGAATGAAATGGTGAAGGACGGGTCC Acatataatcgcggggatatggcctgcaagtttctaccgaagtaccg taaatactttgactatgTTGTTGAGTAGAGTGTGAGCTCC GTAACTAGTTACAT
o467	oT7spinach	ccaagTAATACGACTCACTATAGATGTAACTGAATG AAATGG
o468	spinach_Rev	ATGTAACTAGTTACGGAGCTC

No.	Name[a]	Nucleotide sequence (5´ → 3´)[b]
o529	BA-*purE*-Spinach2	GATGTAACTGAATGAAATGGTGAAGGACGGGTCC Aatataatcgcggggatatggcctgcaagtctctacctaacgaccgt tattcgttagactatTTGTTGAGTAGAGTGTGAGCTCCGT AACTAGTTACAT
o530	BA-COG2252-Spinach2	GATGTAACTGAATGAAATGGTGAAGGACGGGTCC Agtataatatcggggatatggcccgaaagtttctacctagctaccgta aatggcttgactacTTGTTGAGTAGAGTGTGAGCTCCGT AACTAGTTACAT
o531	BA-COG1972-Spinach2	GATGTAACTGAATGAAATGGTGAAGGACGGGTCC Aatatatactcgataatatggatcgagagtttctacccggcaacctta aattgctggactatTTGTTGAGTAGAGTGTGAGCTCCGT AACTAGTTACAT
o532	BA-*guaA*-Spinach2	GATGTAACTGAATGAAATGGTGAAGGACGGGTCC Aatatatcctcaaagataaggtttgagagtctctaccgggttaccgta aacaacctgactatTTGTTGAGTAGAGTGTGAGCTCCG TAACTAGTTACAT
o534	BS-*xpt*-Spinach2	GATGTAACTGAATGAAATGGTGAAGGACGGGTCC Aatataatcgcgtggatatggcacgcaagtttctaccgggcaccgta aatgtccgactatTTGTTGAGTAGAGTGTGAGCTCCGT AACTAGTTACAT

a. COG1972 refers to *nupC* and COG2252 refers to *pbuG*. SD means Shine-Dalgarno sequence.
b. Restriction sites are underlined, recognition sites are in italics. Overlapping sequences for fusion PCRs are in bold. Small letters mark the guanine riboswitch part in the spinach fusion constructs.

3.1.5 Vectors and plasmids

Table 5: Vectors and plasmids used in this thesis.

Name	Description[a]	Construction / Reference
pXT	*thrC*'…'*thrC*, P_{xyl}, MCS, *spc*, *erm*, *bla*	Derré *et al*., 2000[145]
pUC18	*lacZ*α, MCS, ori(pMB1), *bla*	Messing, 1983[167]
pSB_{BS}1C-*lacZ*	*amyE*'…'*amyE*, *cm*, MCS, *lacZ*, *bla*	Radeck *et al*., 2013[146]
pSB_{BS}3C	*sacA´…sacA´*, *cat*, MCS, *luxABCDE*, *bla*	Radeck *et al*., 2013[146]
pAT3803	*erm*, *bla*, P_{lial}-*gfp*, ColE1	Toymentseva *et al*., 2012[168]
#157	pSB_{BS}1C-P_{blaP}-*lacZ*	Kirchner, Schneider, 2017[169]

Name	Description[a]	Construction / Reference
#171	pXT-BS-RS-*blaI*	*B. subtilis xpt* riboswitch amplified from W168 with o142/o143 and *blaI* amplified from *B. licheniformis* with o138/o139 was cloned into pXT with *Hin*dIII
#197	pSB_{BS}1C-P_{blaP}-*gfp*	P_{blaP} amplified from #157 with o136/o251 and *gfp* amplified from pAT3803 with o252 and o253 were fused by fusion-PCR and cloned with *Eco*RI and *Hin*dIII into a pSB_{BS}1C-*lacZ*-derivative containing a *Hin*dIII-restriction site before the *Blp*I-site
#207	W168 *thrC*::pXT-*B.ant_xpt*RS-*blaI*	plasmid #171 amplified with primer pair o301/o302 and o259 cloned with golden gate cloning (*Bsa*I)
#209	pSB_{BS}1C-P_{blaP}-*luxABCDE*	*luxABCDE* amplified from pSB_{BS}3C with o309/o310 and cloned into plasmid #197 with *Xba*I/*Sal*I
#233	pXT-*purE_B.ant-blaI*	plasmid #171 amplified with o301/302 and o355 cloned with golden gate cloning (*Bsa*I)
#247	pXT-P_{xyl}-*nupC* RS1-SD_{opt}-*blaI*	*nupC* RS segment (o356) amplified with o375/o376 and plasmid #233 amplified with primer pair o364/365 cloned with golden gate cloning (*Bsa*I)
#248	pXT-P_{xyl}-*purE* RS1-SD_{opt}-*blaI*	*purE* RS segment (o355) amplified with o371/o372 and plasmid #233 amplified with primer pair o364/365 cloned with golden gate cloning (*Bsa*I)
#249	pXT-P_{xyl}-*guaA* RS1-SD_{opt}-*blaI*	*guaA* RS segment (o294) amplified with o367/o368 and plasmid #233 amplified with primer pair o364/365 cloned with golden gate cloning (*Bsa*I)
#250	pXT-P_{xyl}-SD_{opt}-*blaI*	plasmid #233 amplified with primer pair o365/366 cloned with golden gate cloning (*Bsa*I)
#251	pXT-P_{xyl}-*pbuG* RS1-SD_{opt}-*blaI*	*pbuG* RS segment (o357) amplified with o373/374 and plasmid #233 amplified with o364/365 cloned with golden gate cloning (*Bsa*I)
#252	pXT-P_{xyl}-*xpt B.ant* RS1-SD_{opt}-*blaI*	*xpt* RS segment (o295) amplified with o369/o370 and plasmid #233 amplified with o364/365 cloned with golden gate cloning (*Bsa*I)
#253	*thrC*::pXT-P_{xyl}-	pXT- backbone amplified with o301/o363 cloned

Name	Description[a]	Construction / Reference
	$SD_{B.ant\ xptRS}$-*blaI*	with golden gate cloning (*Bsa*I)
#294	pXT-term-P_{xyl}-*xpt* RS1 *B.ant*-SD_{opt}-*blaI*	*B. subtilis lysS* terminator (from gene synthesis; sequence: see primer table) and PI#252 amplified with o419/o420 cloned with golden gate cloning (*Bsa*I)
#299	pXT-term-P_{xyl}-*nupC* RS4-SD_{opt}-*blaI*	*nupC* RS4 amplified from o356 with o428/o429 and plasmid #294 amplified from $pSB_{BS}3C$ with o364/o365 cloned with golden gate cloning (*Bsa*I)
#300	pXT-term-P_{xyl}-*guaA*RS4-SD_{opt}-*blaI*	*guaA* RS4 amplified from o294 with o425/o426 and plasmid #294 amplified with o364/o365 cloned with golden gate cloning (*Bsa*I)
#303	pXT-term-P_{xyl}-*pbuG* RS4-SD_{opt}-*blaI*	*pbuG* RS4 amplified from o357 with o434/o435 and plasmid #294 amplified with o364/o365 cloned with golden gate cloning (*Bsa*I)
#304	pXT-term-P_{xyl}-*purE* RS4-SD_{opt}-*blaI*	*purE* RS4 amplified from o355 with o437/o438 and plasmid #294 amplified with o364/o365 cloned with golden gate cloning (*Bsa*I)
#306	pXT-term-P_{xyl}-*xpt*RS*B.ant*4-SD_{opt}-*blaI*	*xpt* RS *B.ant*4 amplified from o295 with o422/o423 and plasmid #294 amplified with o364/o365 cloned with golden gate cloning (*Bsa*I)
#312	pXT-term-P_{xyl}-SD_{opt}-*blaI*	plasmid #294 amplified with o365/o366 and religated with golden gate cloning (*Bsa*I)
#318	pXT-term-P_{xyl}-*xpt* RS3 *B.sub*-SD_{opt}-*blaI*	*xpt* RS3 *B.sub* amplified from PI#171 with o469/o471 and plasmid #294 amplified with o364/o365 cloned with golden gate cloning (*Bsa*I)
#354	pXT-term-ΔP-ΔRS-SD_{opt}-*blaI*	Plasmid #300 amplified with o364/o535 cloned with golden gate cloning (*Bsa*I)

a. RS means riboswitch; SD means Shine-Dalgarno sequence; MCS means multiple cloning site.

3.1.6 Bacterial strains

Table 6: *E. coli* and *B. subtilis* strains used in this thesis.

Name	Genotype[a]	Source
E. coli strains		
XL1-Blue	*recA1 endA1 gyrA96 thi-1 hsdR17 supE44 relA1 lac* [F´ *proAB lacI*^{q}*ZΔM15* Tn*10* (Tet^{r})]	laboratory stock
DH5α	F– Φ80Δ*lac*ZΔM15 Δ(*lac*ZYA-*arg*F) U169 *rec*A1 *end*A1 *hsd*R17 (rK–, mK+) *pho*A *sup*E44 λ– *thi*-1 *gyr*A96 *rel*A1	laboratory stock
XL10-Gold	Tet^{r}Δ(*mcrA*)183 Δ(*mcrCB-hsdSMR-mrr*)173 *endA1 supE44 thi-1 recA1 gyrA96 relA1 lac* Hte [F´ *proAB lacI*^{q}*ZΔM15* Tn*10*(Tet^{r}) Amy Cam^{r}]	laboratory stock
B. subtilis strains		
W168	wild type, *trpC2*	laboratory stock
BS2	W168 *amyE*::pSB$_{BS}$1C-P$_{blaP}$-*lacZ* (Pl#157)	this work
BS41	W168 *amyE*::pSB$_{BS}$1C-P$_{blaP}$-*luxABCDE* (Pl#209)	this work
BS44	W168 *amyE*::pSB$_{BS}$1C-P$_{blaP}$-*lacZ thrC*::pXT-*B.ant_xpt*RS-*blaI* (Pl#207)	this work
BS47	W168 *amyE*::pSB$_{BS}$1C-P$_{blaP}$-*luxABCDE thrC*::pXT-*B.ant_xpt*RS-*blaI* (Pl#207)	this work
BS115	W168 *amyE*::pSB$_{BS}$1C-P$_{blaP}$-*luxABCDE thrC*:: pXT-P$_{xyl}$-*guaA* RS1-SD$_{opt}$-*blaI* (Pl#249)	this work
BS116	W168 *amyE*::pSB$_{BS}$1C-P$_{blaP}$-*luxABCDE thrC*:: pXT-P$_{xyl}$- *pbuG* RS1-SD$_{opt}$-*blaI* (Pl#251)	this work
BS117	W168 *amyE*::pSB$_{BS}$1C-P$_{blaP}$-*luxABCDE thrC*::pXT-P$_{xyl}$-*xpt B ant* RS1-SD$_{opt}$-*blaI* (Pl#252)	this work
BS118	W168 *amyE*::pSB$_{BS}$1C-P$_{blaP}$-*luxABCDE thrC*::pXT-P$_{xyl}$-SD$_{B.\ ant\ \ xpt\ \mathrm{RS}}$-*blaI* (Pl#253)	this work
BS119	W168 *amyE*::pSB$_{BS}$1C-P$_{blaP}$-*luxABCDE thrC*::pXT-P$_{xyl}$-*nupC* RS1-SD$_{opt}$-*blaI* (Pl#247)	this work
BS120	W168 *amyE*::pSB$_{BS}$1C-P$_{blaP}$-*luxABCDE thrC*::pXT-P$_{xyl}$-*purE* RS1-SD$_{opt}$-*blaI* (Pl#248)	this work
BS140	W168 *amyE*::pSB$_{BS}$1C-P$_{blaP}$-*lacZ thrC*::pXT-P$_{xyl}$-SD$_{B.antxpt\mathrm{RS}}$-*blaI* (Pl#253)	this work
BS190	W168 *amyE*::pSB$_{BS}$1C-P$_{blaP}$-*luxABCDE thrC*::pXT-term-P$_{xyl}$-*nupC* RS4-SD$_{opt}$-*blaI* (Pl#299)	this work

Name	Genotype[a]	Source
BS192	W168 *amyE*::pSB$_{BS}$1C-P$_{blaP}$-*luxABCDE thrC*::pXT-term-P$_{xyl}$-*guaA* RS4-SD$_{opt}$-*blaI* (Pl#300)	this work
BS194	W168 *amyE*::pSB$_{BS}$1C-P$_{blaP}$-*luxABCDE thrC*::pXT-term-P$_{xyl}$-*xpt* RS*B.ant*4-SD$_{opt}$-*blaI* (Pl#306)	this work
BS196	W168 *amyE*::pSB$_{BS}$1C-P$_{blaP}$-*luxABCDE thrC*:: pXT-term-P$_{xyl}$-*purE* RS4-SD$_{opt}$-*blaI* (Pl#304)	this work
BS198	W168 *amyE*::pSB$_{BS}$1C-P$_{blaP}$-*luxABCDE thrC*::pXT-term-P$_{xyl}$-*pbuG* RS4-SD$_{opt}$-*blaI* (Pl#303)	this work
BS209	W168 *amyE*::pSB$_{BS}$1C-P$_{blaP}$-*luxABCDE thrC*::pXT-term-P$_{xyl}$-*xpt* RS3*B.sub*-SD$_{opt}$-*blaI* (Pl#318)	this work
BS210	W168 *amyE*::pSB$_{BS}$1C-P$_{blaP}$-*luxABCDE thrC*::pXT-term-P$_{xyl}$-SD$_{opt}$-*blaI* (Pl#312)	this work
BS257	W168 *amyE*::pSB$_{BS}$1C-P$_{blaP}$-*luxABCDE thrC*::pXT-term-ΔP-ΔRS-SD$_{opt}$-*blaI* (Pl#354)	this work

a. Pl means plasmid.

3.2 Methods

3.2.1 Bacterial growth and storage conditions

For cloning purposes, bacteria were grown at 37 degree celsius (°C) with agitation in Luria-Bertani (LB) medium. For plate reader and β-galactosidase assays as well as the screening a modified CSE medium based on MOPS buffer with 1% casamino acids and fructose as carbon source was used. The *Escherichia coli* strains DH5α, XL10-Gold and XL1-Blue were electro-transformed and selected using 100 µg/ml ampicillin. All *B. subtilis* strains are based on strain W168 and were grown with 100 µg/ml spectinomycin and/or 5 µg/ml chloramphenicol when appropriate. For LB and MNGE plates the medium was supplemented with 2% agar. For long-term storage, overnight cultures of the bacteria in LB medium with selection were supplemented with glycerol to a final concentration of 25% and stored at –80 °C.

3.2.2 Cloning

3.2.2.1 PCRs

Standard PCRs were performed with Phusion polymerase or Q5 polymerase. The melting temperatures were calculated using the online tool oligocalc.[170] Usually, primers contained up to three bases 5´ of their restriction sites to support an efficient cleavage.

For fusion-PCRs, the parts were amplified in separate PCRs with primers containing overlapping tails (overlaps correspond to a melting temperature of 65 – 70 °C). The purified PCR products were deployed in equimolar amounts in a subsequent overlap primer extension PCR using the flanking primers. The PCR program contained a ramp of 0.5 °C/second in the annealing steps of the first two cycles.

PCR products were analyzed with agarose gels (1% agarose in 1 x TAE buffer) and purified using agarose gels and PCR purification kits. If necessary, genomic DNA was removed through *Dpn*I digestion.

3.2.2.2 Golden gate cloning

For scarless insertion of riboswitch parts into a plasmid, golden gate cloning was performed based on Engler *et al*., 2008[171] and Engler *et al*., 2009.[172] All primer contained a *Bsa*I recognition site and a non-palindromic restriction site that differed

in two or more bases in one reaction. After PCR-amplification of plasmid backbones and inserts, 40 fmol of the purified DNA fragments were incubated with *Bsa*I (20 U) and a highly concentrated ligase (20 U) in CutSmart buffer for 30 thermal cycles (37 °C, 5 minutes (min.) followed by 20 °C, 2 min.). As the pXT backbone contains an internal *Bsa*I restriction site it is crucial to end with a ligation step. The golden gate samples were stored at 4 °C until electro-transformation of *E. coli*.

3.2.2.3 Conventional cloning using restriction enzymes

Purified inserts and plasmids were both digested with appropriate amounts of restriction enzymes at 37 °C for 2 hours (h). For dephosphorylation, 500 ng plasmid backbones were incubated at 37 °C for 30 min. with 1 µl antarctic phosphatase. After an additional purification step, plasmid and insert were ligated using a three-fold excess of the insert with 1 µl DNA ligase and incubation over night at 4 °C. The preparation was used for transformation of *E. coli*.

3.2.2.4 **E. coli *transformation***

45 µl electro-competent cells were thawed on ice and 2 µl of a ligated plasmid mixture was added. The cells were electroshocked in an electroporation cuvette with a 2.5 kV pulse and re-suspended in pre-warmed SOC medium. After incubation at 37 °C for 20 – 40 min., the cells were plated on LB plates supplemented with ampicillin.

3.2.2.5 Colony-PCRs and control digestions

For plasmid verification, colony-PCRs and control digestions were performed. Colony-PCRs were prepared using GoTaq G2 polymerase according to manufacturer´s instructions with adding cells of interest as template into the PCR mixture. For control digestions, the purified plasmid of interest (3 µl) was digested with 0.3 µl of each selected restriction enzyme at 37 °C for 30 min. Both colony-PCRs and control digestions are followed by agarose gel electrophoresis to verify the lengths of the resulting DNA fragments.

3.2.3 Isolation of *B. subtilis* genomic DNA

B. subtilis genomic DNA was prepared based on Cutting and Vander Horn[173] from appropriate overnight cultures. The cells were mixed with an equal volume of SC buffer, pelleted and re-suspended in SC buffer. Lysozyme (final concentration (conc.) 0.1 mg/ml solved in SC buffer) was added and the mixture was incubated at

37 °C under agitation for 30 – 60 min. After NaCl addition (1.9 M final conc.), the suspension was carefully mixed and filtered using a 0.45 µm filter before storage at –20 °C.

3.2.4 Transformation of *B. subtilis*

The *B. subtilis* transformation was performed as described by Radeck *et al*., 2013:[146] MNGE medium was inoculated to an optical density at 600 nm (OD_{600}; abbreviated with "OD") of 0.1 using overnight cultures and grown at 37 °C with agitation until the late logarithmic growth phase. Eventually, *B. subtilis* genomic DNA or *Sca*I-linearized plasmids were added to the cells. After one hour of incubation, ¼ volume expression mix was added. After incubation for one hour the cells were plated on LB plates with selection.

3.2.4.1 Test for integration into the thrC *locus*

To test the integration into the *B. subtilis thrC* locus threonine auxotrophy was verified. For this purpose, MNGE medium with and without threonine was prepared as medium or as plates with agar. It was supplemented with the cells to test and incubated at 37 °C over night. Colonies with the desired *thrC* integration were able to grow in MNGE medium with threonine but not without. W168 and a strain carrying a *thrC* insertion were used as controls.

3.2.4.2 Test for integration into the amyE *locus*

To verify integrations in the *amyE* locus, the colonies in question were streaked on starch plates together with a verified *amyE* insertion strain and W168 as controls. The plates were incubated over night at 37 °C and subsequently flooded with Lugol´s iodine solution for several seconds. After removal of the iodine solution, the plates were examined. Colonies containing an insertion in the *amyE* locus are not surrounded by non-stained zones because they are not able to degrade starch.

3.2.5 Luciferase assays

Day cultures were inoculated 1:100 in modified CSE medium from overnight cultures in LB medium with selection, if appropriate. They were incubated at 37 °C and 200 rpm (rounds per minute) until OD = 1.5 – 3 was reached. The cultures were re-diluted to OD = 0.05 and additional chemicals were added, if necessary (final concentrations: 0 – 1 mM guanosine, 1 mM nucleoside analoga, 1%, 2% or 5% (v/v) dimethyl sulfoxide (DMSO), 0.1 – 0.005% (w/v) xylose or 0.01 µM – 1 mM

gemcitabine). For dose response curves, 1:2 serial dilutions of guanosine were prepared. 96-well plates were filled with 100 µl per well and measured in a microplate reader. Subsequently they were incubated at 37 °C using double orbital shaking (108 rpm) and luminescence and OD were measured every ten minutes. The data of three wells containing medium were averaged over time and used to blank bioluminescence and OD in each experiment. The relative luminescence units (RLU) divided by the optical density yielded the luciferase activity [RLU/OD]. Note: due to different path lengths, the optical densities measured in plate readers cannot be directly compared to values determined with photometers.

3.2.6 Screening procedure

Overnight cultures were grown for seven hours at 37 °C with agitation in CSE medium with antibiotic selection. For the screening, 384-well plates were filled with 50 µl per well. Each plate contained 16 wells with the positive control (cells, 0.01% xylose, 1 mM guanosine and 1% DMSO), the negative control (cells, 0.01% xylose and 1% DMSO), CSE medium and CSE medium plus guanosine (1 mM). All other wells were filled with CSE medium containing cells (starting-OD = 0.05), xylose (0.01%) and compounds solved in DMSO (final concentration (conc.): 10 µM compound and 1% DMSO). Subsequently, the initial luminescence and OD were determined before incubation of the plates for 3 – 3.5 h at 37 °C. Afterwards, the final luminescence and OD were measured in two end-point measurements (FDA-approved drug library) or a single end-point measurement (small-molecule library). For evaluation, the OD and luminescence values of all wells with CSE (blank) were averaged and subtracted from the respective values of compound-containing wells. Finally, the adjusted luminescence values were divided by the OD of the same well (= bioluminescence/OD) to account for different cell numbers. For hit selection, the average and standard deviations of all wells containing negative controls of all plates screened on one day were calculated.

3.2.7 β-galactosidase assays

Day cultures for β-galactosidase assays were inoculated to OD = 0.25 from overnight cultures grown in MCSE medium with antibiotic selection, if necessary. 10 ml day cultures containing 0.01% xylose, 1 mM guanosine, 0.1% DMSO and 0.1,

1, 10 or 100 µM gemcitabine, if appropriate, were grown at 37 °C with agitation for 6 h before pelleting the cells. Pellets were stored at –20 °C before usage.

The assay was performed according to Miller, 1972:[174] cells were re-suspended in working buffer and diluted to OD = 0.2 – 0.8. Lysozyme (0.12 mg/ml, solved in working buffer without β-mercaptoethanol) was added and the solutions were incubated at 37 °C until they were clear. A freshly prepared *ortho*-nitrophenyl-β-galactoside solution (ONPG; solved in working buffer without β-mercaptoethanol) was added to the lysed cells (final conc.: 2 mM). After ONPG addition, the samples were incubated at room temperature until they turned yellow (maximum: 1 h) and the reaction was stopped with Na_2CO_3 (final conc.: 294 mM). The absorptions at 420 and 550 nm were measured and the Miller units (MU) were calculated according to the following formula: $\mathrm{MU} = \frac{1000*(A_{420}-(1.75*A_{550}))}{(t*0.8\ \mathrm{ml}*OD_{600})}$, where A_{420} and A_{550} means absorption at 420 nm or 550 nm, respectively, and t means the time from ONPG induction until Na_2CO_3 addition in minutes.

3.2.8 Determination of binding constants

The binding constants were determined based on a method published by Kellenberger and Hammond.[113] There, the riboswitch aptamers of interest are fused to the spinach aptamer by exchange of the spinach aptamer´s P2 stem with the P1 stem of the riboswitch aptamer domains. The P1 stems of the riboswitches were shortened to 3 bp here. Thus, folding of the riboswitch aptamer due to ligand binding enables spinach aptamer folding. This can be monitored by fluorescence caused by binding of 3,5-difluoro-4-hydroxybenzylidene imidazolinone (DFHBI) to the spinach aptamer. Therefore, riboswitch folding leads to fluorescence which can be detected by microplate readers. To be able to perform these experiments, RNA has to be transcribed and purified first.

3.2.8.1 In vitro *transcription*

Templates for *in vitro* transcription were generated by PCR using single-stranded DNA as template (o465, o529 – o532, o534) and primer pair o467/o468 with Q5 polymerase and enhancer. The PCR products were purified using the PCR purification kit and stored in sterile water.

The subsequent *in vitro* transcriptions contained the following compounds:

Table 7: Composition of *in vitro* transcription mixtures.

Component	Final conc.
purified PCR product	3 µg/ml
1 M $MgCl_2$	32 mM
nucleosidetriphosphates (NTPs), 25 mM each NTP	1.5 mM each
5 x *in vitro* transcription buffer	1 x
0.1 U/µl inorganic pyrophosphatase (optional)	0.5 U/ml
40 U/µl RNase inhibitor	200 U/ml
T7 RNA polymerase (~0.6 µg/µl)	~30 µg/ml

The samples were incubated for 2 h at 37 °C and stored at −80 °C or purified directly.

3.2.8.2 RNA isolation

To remove template DNA, the *in vitro* transcription samples (1 mL each) were treated with 5 µl DNase and incubated at 37 °C for 30 min. Then, the RNA was precipitated by adding 50 µl sodium acetate (3 M, pH 5.3) and 1 ml cold ethanol (100%, −20 °C) and mixing. The suspension was stored at −80 °C for several hours before centrifugation (4 °C, 20 min., 16,602 g). The thereby-generated pellet was washed with 70% ethanol, dried at room temperature and re-suspended in 100 µL TE buffer. After addition of RNA loading buffer, the mixture was heated to 70 °C for 5 min., loaded onto a TBE-urea acrylamide gel and the gel was run at 200 V for 45 min. The RNA bands were identified under ultraviolet light by their shades on fluorescent thin-layer chromatography plates. They were cut out of the gel and purified using electrophoresis (150 V, 50 mA, 40 min.) in a purpose-built chamber where the RNA was extracted from the gel into an 8 M ammoniumacetate solution. The RNA-ammoniumacetate mixture was removed from the electrophoresis chamber and the RNA was precipitated by addition of cold 100% ethanol (−20 °C) and storage at −80 °C. The precipitated RNA was pelleted by centrifugation (4 °C, 20 min., 16,602 g), washed with 70% ethanol (−20 °C) and dried at room temperature. The purified RNA was solved in TE buffer and stored at −80 °C.

To determine RNA concentrations accurately and to avoid hypochromicity effects, the neutral pH thermal hydrolysis assay was performed.[175] The RNA samples were incubated with 50 mM Na_2CO_3 and 1 mM EDTA (pH 7.0) for 1.5 h at 95 °C and

cooled to room temperature. The absorbance at 260 nm (A_{260}) was measured and the RNA concentrations were calculated according to the following formula:

$$\text{RNA conc.} = \frac{A_{260}}{\text{path length} * \sum_{i = A,U,C,G} n_i \varepsilon_{260,i}}.$$

n means the number of a nucleotide in the RNA sequence, i is the nucleotide identity, and $\varepsilon_{260,i}$ is the molar extinction coefficient of the respective nucleotide.

3.2.8.3 In vitro *riboswitch binding assays*

Ligand affinities were determined using fluorescence as readout that was caused by DFHBI binding to the spinach aptamer. Before the measurement, serial dilutions of the riboswitch ligand guanine in 40 mM HEPES buffer (pH 7.5) were made. Prior to usage, RNA was denatured by incubation at 70 °C for 3 min. and subsequently cooled to room temperature for 5 min. The RNA samples, buffer and ligand dilutions were pipetted into 96-well plates yielding *in vitro* reaction buffer with 0.02 µM final RNA concentration and 0 – 10 µM ligand in a total volume of 80 µl. For every riboswitch three control wells per plate were filled with reaction buffer containing RNA and DFHBI but no ligand. The reactions were incubated in a microplate reader at 37 °C with agitation and double orbital shaking (90 rpm). The fluorescence (absorption: 457 nm; emission: 503 nm) was determined every 30 min. while removing the lid for the measurement. All tested riboswitches reached equilibrium in the course of one hour after beginning of the incubation. For evaluation, the average fluorescence results of RNA samples without ligand were subtracted from the ligand-containing samples. The data of three independent experiments was used to plot guanine concentrations against relative fluorescence. Dissociation constants were determined based on these binding curves using the software Prism.

3.2.9 Computational methods and statistical analysis

The riboswitch DNA sequences were taken from *B. anthracis* strain Ames[96] (NC_003997) at GenBank[176], the European Bioinformatics Institute[177, 178] and MicrobesOnline,[179] upstream of the genes *guaA* (accession NP_842821.1), *nupC* (NP_842879.1), *pbuG* (NP_842822.1), *purE* (NP_842838.1), *ymfC* (NP_846173.1) and *xpt* (NP_844040.1). Software used is listed in Table 8. Sequence alignments were done with RNAalifold,[180, 181] Clustal Omega,[182] and BioEdit.[183] RNA folding was analyzed using the programs RNAfold[184] and Mfold.[185-187] To calculate the ligand-

bound riboswitch structures *in silico* without simulating the ligand, the aptamer domains and the expression platforms were calculated separately and fused afterwards. Mfold was used to determine the Gibbs free energies of the terminators. RNA sequence identity was calculated with the EMBOSS Needle nucleotide alignment tool.[188] P values were calculated with unpaired t-tests with Welch´s correction using the software Prism. Figures were generated using the softwares Prism, Adobe Illustrator, BioEdit[183] and R2R.[189]

For the screening development, samples containing cells and 0.01% xylose were used as negative control (neg) and samples containing cells, 0.01% xylose and 1 mM guanosine as positive control (pos). Signal-to-background (S/B) ratios were calculated according to the formula $\mathrm{S/B} = \frac{\emptyset_{\mathrm{pos}}}{\emptyset_{\mathrm{neg}}}$ where Ø represents the mean values. Z´ factors were calculated according to the formula $\mathrm{Z'} = 1 - \frac{3(\sigma_{\mathrm{pos}}+\sigma_{\mathrm{neg}})}{|\emptyset_{\mathrm{pos}}-\emptyset_{\mathrm{neg}}|}$ where σ represents the standard deviations.[190] Signal windows (SW) were calculated according to the formula $\mathrm{SW} = \frac{\emptyset_{\mathrm{pos}}-\emptyset_{\mathrm{neg}}-3(\sigma_{\mathrm{pos}}+\sigma_{\mathrm{neg}})}{\sigma_{\mathrm{pos}}}$.[191]

Table 8: Tools and software used for this thesis.

Software	Source
tools for data analysis and creation of figures and text	
Adobe Illustrator CS4	Adobe (San José, USA)
BioEdit version 7.2.5	[183]
ChemDraw Professional 15.0	PerlinElmer (Waltham, USA)
EndNote X4.0.2	Alfasoft AB (Göteborg, Sweden)
Microsoft Office Standard 2010 (Excel, Word, PowerPoint)	Microsoft (Redmond, USA)
Prism ver. 5.0.2	GraphPad (La Jolla, USA)
PyMOL Molecular Graphics System, Version 1.8	Schrödinger (New York City, USA)
R2R	[189]
online tools	
Clustal Omega	[182]

4 Results and Discussion

4.1 Analysis of *B. anthracis* guanine riboswitches

In *B. anthracis*, six potential riboswitches were proposed to be guanine-responsive due to aptamer sequence homologies and a conserved cytidine (C74).[21] Apart from their proposed existence and class they were not studied (Section 1.1.4.2). Therefore, one purpose of this work is to verify their function and to characterize them.

4.1.1 *In silico* analysis

To identify the expression platforms and suggest probable working modes of the putative riboswitches their RNA sequences were first examined *in silico*.

4.1.1.1 Aptamer domain

Based on the position of the guanine riboswitch aptamer domains postulated in 2007,[21] the aptamer domains of the potential *B. anthracis* guanine riboswitches were aligned and a consensus structure was calculated (Figure 8 A and B). The junctions (which form the ligand cavity) are mostly, but not completely, conserved, whereas the sequences vary predominantly in the P2 and P3 helices. These findings are largely in accordance with previous findings comparing guanine aptamer sequences from other organisms.[10] The conserved C74 is supposed to be responsible for guanine binding.

The *B. anthracis* riboswitch aptamer domains have 67.5 – 82.1% nucleotide identity compared to the model *B. subtilis xpt* riboswitch with the *B. anthracis xpt* riboswitch being the most similar one (Table 9). The *pbuG* riboswitch aptamer domain is similar to its *B. subtilis* homolog, whereas the *B. anthracis purE* aptamer displays comparably low homologies to the *B. subtilis xpt* and *B. subtilis purE* aptamer domains (72.8 / 74.4%).

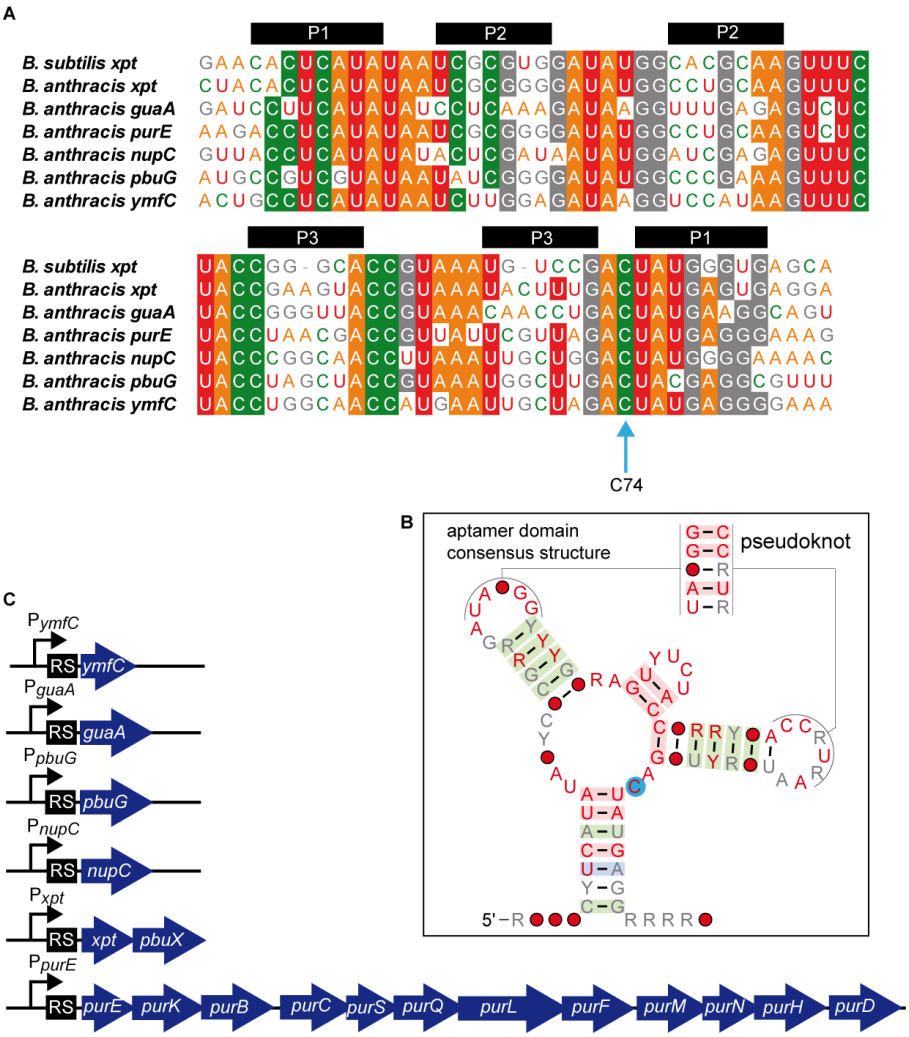

Figure 8: Sequence alignment, genomic localization and consensus of the aptamer domains of postulated *B. anthracis* guanine riboswitches.

(A) Sequence alignment of all six proposed *B. anthracis* guanine riboswitches and the *B. subtilis xpt* riboswitch. Nucleotides present in five or more riboswitches are shaded. Residues belonging to the three helices P1 – P3 in the *B. subtilis xpt* riboswitch are indicated by black bars. The conserved residue C74 presumably forming a Watson-Crick base pair with the ligand guanine is indicated by a light blue arrow.

(B) Consensus structure of the aptamer domains of the six proposed *B. anthracis* guanine riboswitches. The guanine-binding cytidine is labelled by a light blue circle. Red dots represent nucleotides present in all riboswitches. The nucleotide identity is depicted by light grey (5 out of 6 riboswitches) and red (all riboswitches) characters. Green, blue or red-shaded base pairs have covarying or compatible mutations[193] or are completely conserved, respectively. The possible pseudoknot formed upon ligand binding is depicted on top of the structure. The figure was generated with the software R2R. R = A or G; Y = C or U.

(C) Position and regulon of the proposed *B. anthracis* guanine riboswitches. Promoters are represented by black arrows; genes by blue arrows and the riboswitches by black boxes (RS). The genes are not true to scale.

Table 9: Nucleotide identity of the potential *B. anthracis* (BA) riboswitch aptamer domains compared to the *B. subtilis* (BS) *xpt* riboswitch (left) and their homologous *B. subtilis* riboswitches (right).
The RNA sequences depicted in Figure 8 A as well as *B. subtilis pbuG* and *purE* aptamers with comparable lengths and positions were compared. The other proposed *B. anthracis* riboswitches do not have a corresponding *B. subtilis* guanine riboswitch homolog.

Riboswitch aptamer	Identity compared to BS *xpt* [%]	Identity compared to the corresponding BS homolog if present [%]
BA *xpt*	82.1	82.1
guaA	63.4	
nupC	69.1	
pbuG	64.0	81.0
purE	72.8	74.4
ymfC	67.5	

4.1.1.2 Regulated genes

The functions of *B. anthracis* genes regulated by purine riboswitches (Figure 8 C) are solely proposed due to homologies to *B. subtilis* genes. The genes are named accordingly here: the single genes *guaA* (encoding for a putative GMP synthase),[60] *pbuG* (hypoxanthine-guanine permease),[59] *nupC* (nucleoside transporter),[64] *ymfC* (putative transcription regulator) and the operons *xpt-pbuX* (xanthine phosphoribosyl-transferase and xanthine permease)[37] and *purE-purK-purB-purC-purS-purQ-purL-purF-purM-purN-purH-purD* (adenylosuccinate lyase (*purB*) and proteins responsible for *de novo* purine biosynthesis).[58] Apart from the *ymfC* homolog that encodes a putative GntR family transcriptional regulator, all riboswitches control genes probably directly involved in nucleotide synthesis or transport.

4.1.1.3 Putative modes of action

To unravel the modes of action of the *B. anthracis* purine riboswitches the RNA sequences downstream of their proposed aptamer domains were analyzed. Possible secondary structures of these sequences and their corresponding folding energies were determined by computational analysis. In Firmicutes like *B. anthracis* riboswitches mainly act through transcription attenuation.[21] Therefore, it was especially searched for rho-independent transcription terminators. These are characterized by a GC-rich stem loop structure in the RNA followed by a number of

uridines[194] (see [195] for a comprehensive review). Such structures could be found in the expression platforms of five potential riboswitches in front of the *xpt*, *guaA*, *nupC*, *pbuG* and *purE* genes (Figure 9).

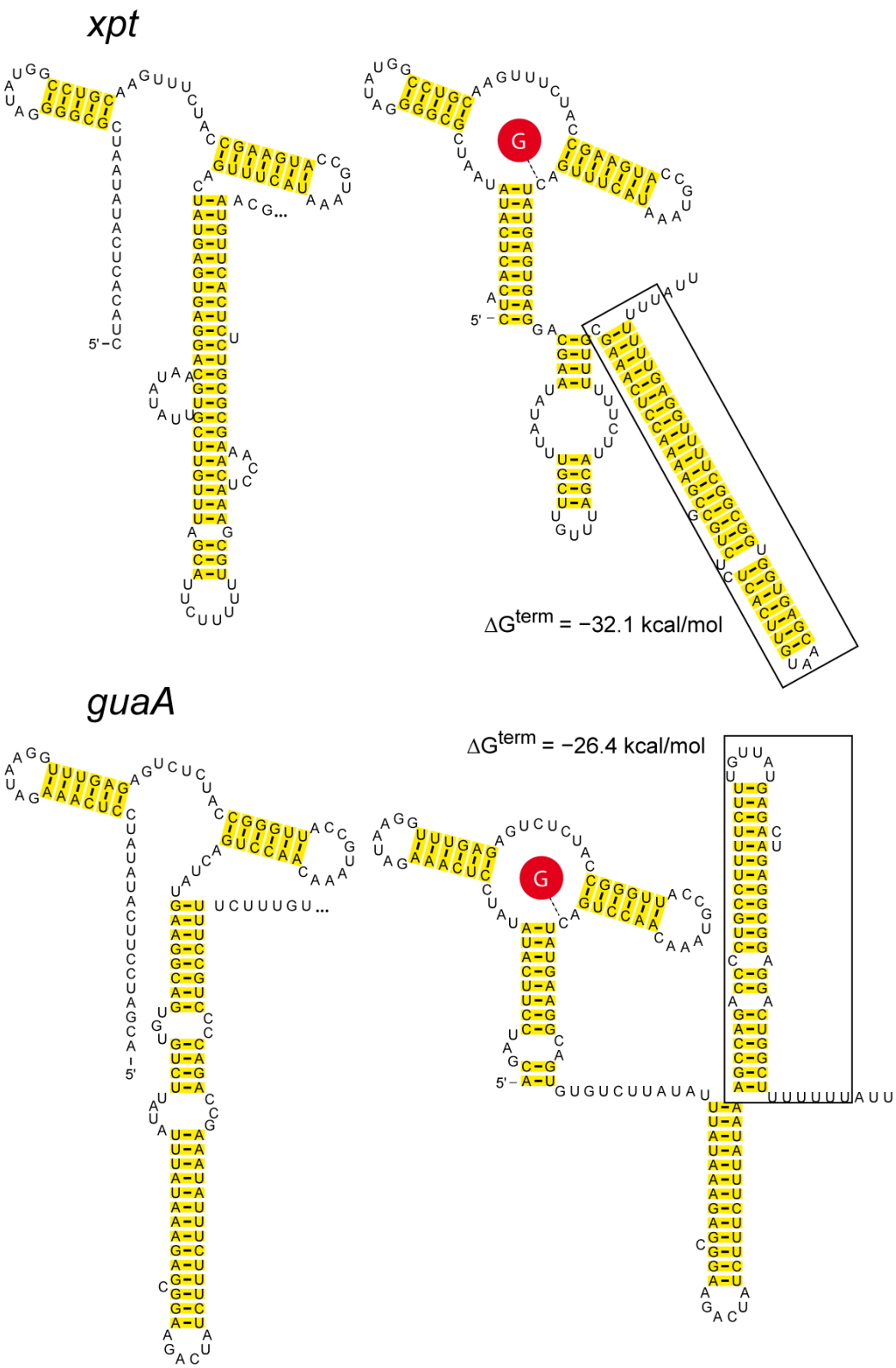

nupC

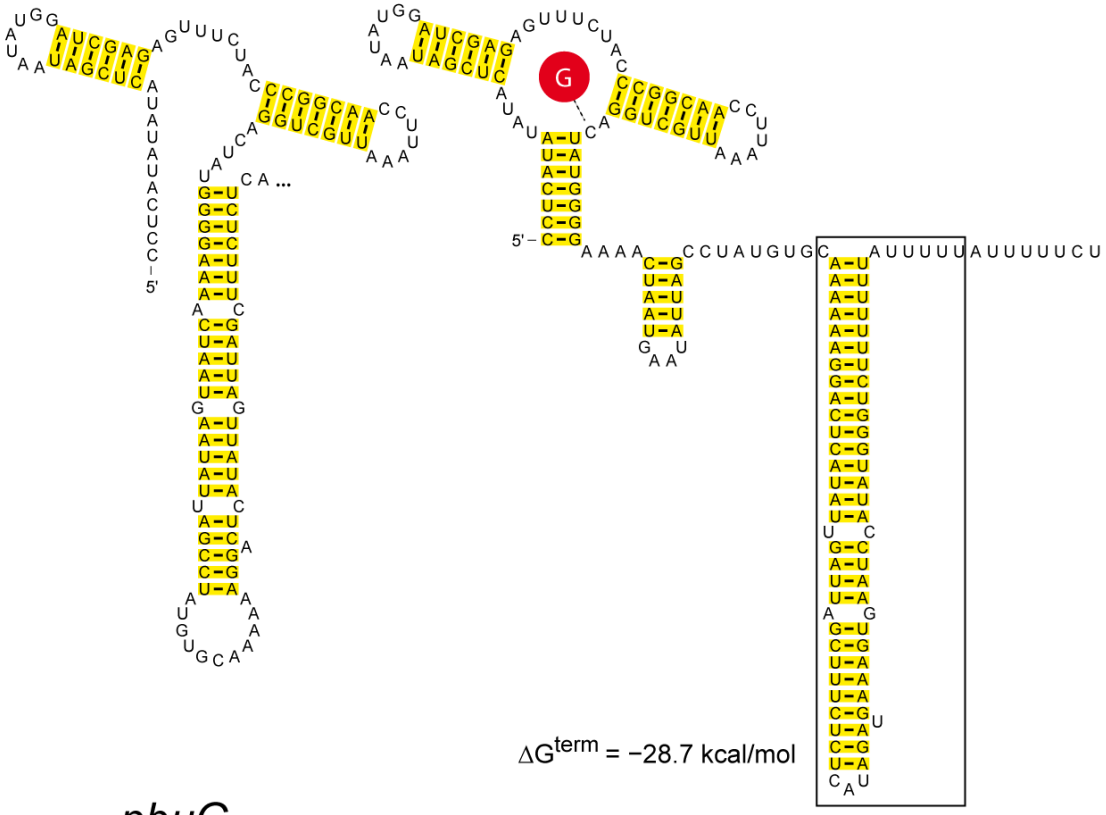

pbuG

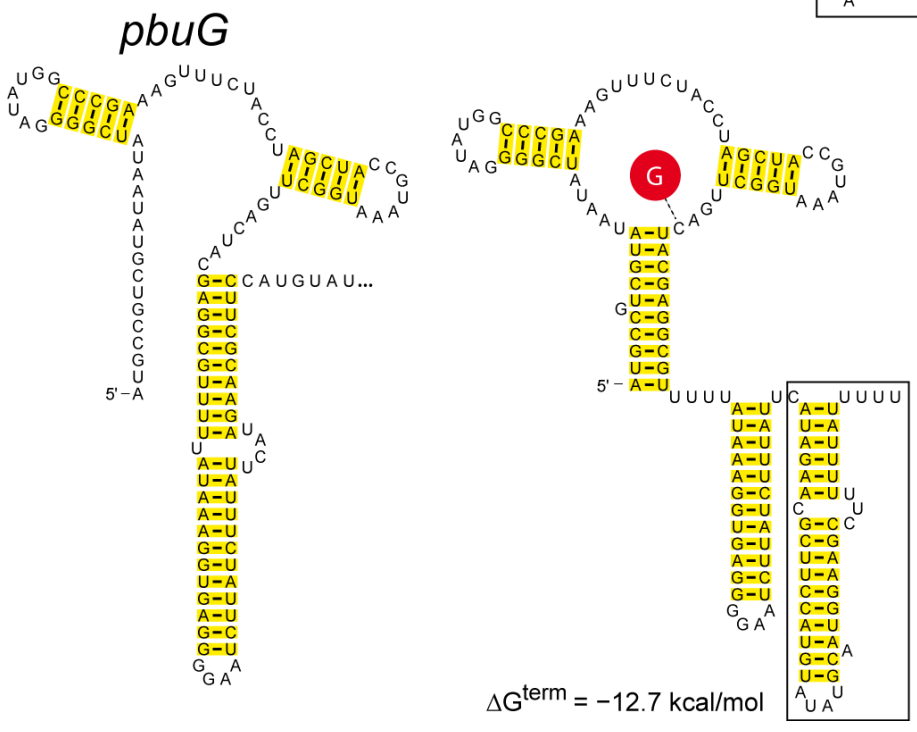

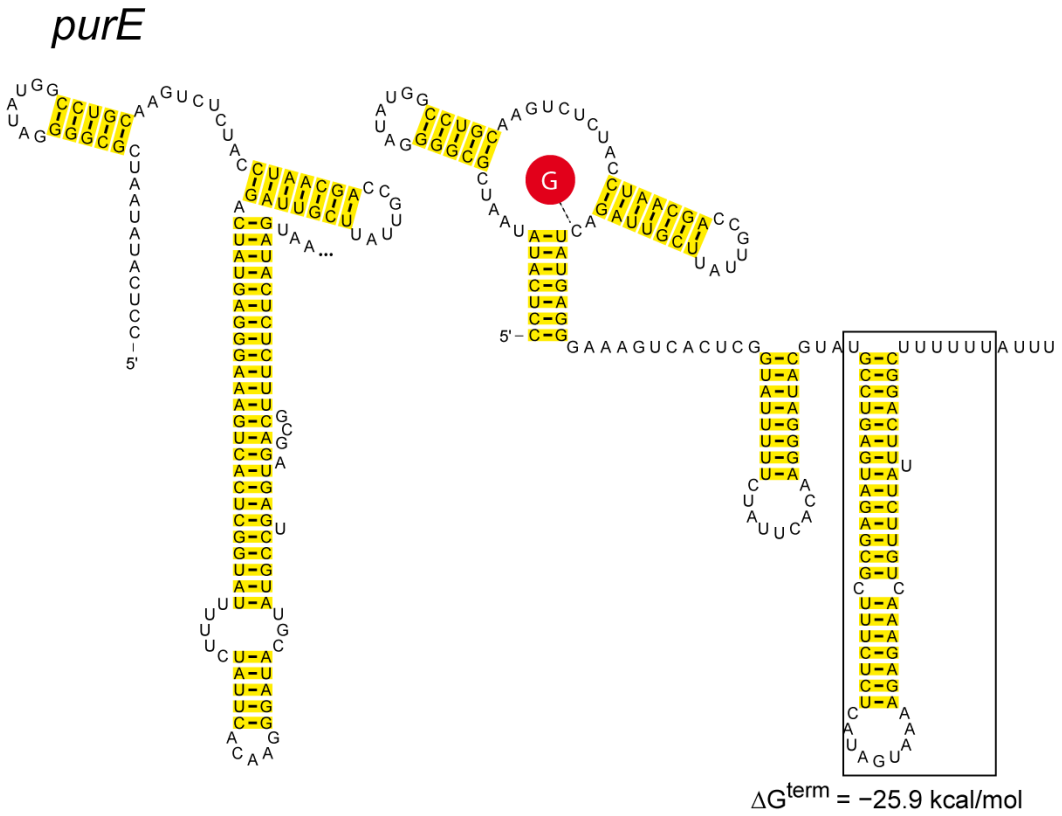

Figure 9: Topology of five *B. anthracis* purine riboswitches without (left) and with ligand (right) and the predicted free folding energies of their terminators.

Paired bases are marked in yellow and the ligand is represented by a red circle (G). Schematic representations were generated with the software R2R.[196] The relative free energies of the terminator stems (black boxes) were calculated using the program mfold.[185]

The calculated stabilities of the terminator domains differ considerably from ΔG^{term} = −32.1 kcal/mol (*xpt* riboswitch) to ΔG^{term} = −12.7 kcal/mol (*pbuG* riboswitch). Since additional tertiary interactions could influence the free energy, the values given here represent only estimates.

4.1.2 The proposed *B. anthracis ymfC* riboswitch

The sixth potential *B. anthracis* guanine riboswitch (*ymfC*) behaved different than the other riboswitches *in silico* as well as *in vivo*. In the following, the findings concerning this RNA element are briefly summarized:

- The *ymfC* riboswitch aptamer domain displayed the lowest nucleotide identity compared to the *B. subtilis xpt* riboswitch (Table 9).
- The gene regulated by the putative riboswitch (a potential transcription regulator) is unusual as there is no known connection between the function of

the gene and the proposed ligand guanine — in contrast to the other five potential *B. anthracis* guanine riboswitches.

- Initial *in vitro* transcription experiments demonstrated only very weak, if any, binding of guanine to the aptamer domain.

The following results were obtained assuming that the *ymfC* RNA element is a transcriptional OFF riboswitch (Figure 10 A), like the other *B. anthracis* guanine riboswitches:

- The potential terminator is unusual due to the low GC-ratio of the base pairs in front of the U-stretch and the fact that most of the uridines can be integrated into the stem.
- The potential antiterminator domain presumably does not fulfill its function as it does not fully hinder the formation of the P1 helix of the aptamer domain.
- The corresponding *in vivo* riboswitch activity (preliminary data not shown) was tested with four constructs with different lengths that all comprised the putative aptamer domain and transcription terminator (the shortest one is indicated by black dashed lines in the right part of Figure 10 A). All of these constructs gave very weak responses (5 - 15-fold induction) to ligand addition. In addition, two of them displayed a high background and all caused a clearly higher (2 - 4-fold) non-induced than ligand-induced signal. This behavior is in contrast to that observed from the other *B. anthracis* guanine riboswitches (Figure 13).

Considering these findings it seemed rather improbable that this putative mode of action is true.

Further analysis of the RNA sequence led to the proposition that the *ymfC* riboswitch might control translation by hiding the RBS in absence of the ligand (Figure 10 B). If this was true, the riboswitch would be a translational ON switch in contrast to the putative modes of action of the other five *B. anthracis* guanine riboswitches. This mode of action was tested *in vivo* with longer constructs — in a direct as well as an indirect reporter gene setup — containing the natural RBS and also part of the *ymfC* gene in a translational fusion with the downstream genes.

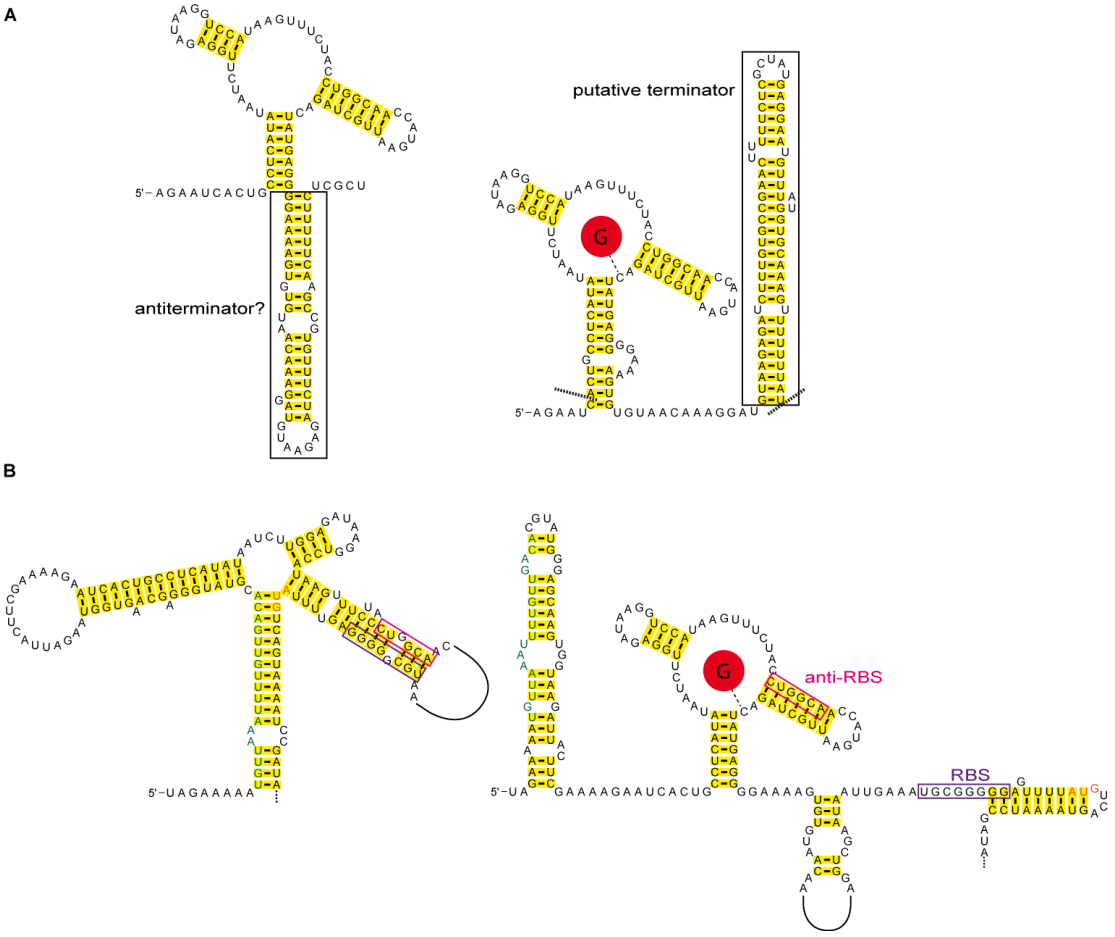

Figure 10: Two functional models of the putative *ymfC* riboswitch.

(A) Model for a transcriptional OFF riboswitch without (left) and with ligand (right). Putative antiterminator and terminator sequences are indicated. Dashed lines mark the beginning and end of the smallest construct tested.

(B) Model for a translational ON riboswitch without (left) and with ligand (right). The RBS is shown in lilac; the anti-RBS in pink. The AUG start codon is highlighted in orange. Sequences complementary to the AUG start codon and the beginning of the *ymfC* gene are indicated in dark green. Parts of the sequence are represented by black lines. The ligand guanine is indicated by a red circle.

The indirect reporter assay (data not shown) demonstrated a small effect caused by ligand addition indicating that the riboswitch is indeed an ON switch. As the overall effect of ligand addition was rather low, the system was re-cloned into direct promoter-riboswitch-reporter gene constructs. However, the experimental data of these constructs suggested that the riboswitch is an OFF switch instead of an ON switch.

There are two probable explanations for these observations: first, it is possible that the RNA element is either non-functional or has changed its function so that it is no

longer primarily guanine-responsive. Second, there might be an essential part of the riboswitch missing in the constructs tested here; for example a tandem arrangement with another RNA element is imaginable. Due to the puzzling and inconclusive *in silico* and *in vivo* data, the purpose and activity of this RNA element remains a mystery. The *ymfC* riboswitch was therefore excluded from further investigations here.

4.1.3 Creation of a reporter system to investigate transcriptional OFF riboswitches

For investigating the five putative transcription-terminating (OFF) *B. anthracis* guanine riboswitches a reverse reporter gene system was developed to convert the proposed negative consequence of ligand binding (transcription termination) into a positive (elevated) output signal. In addition, a beneficial interplay between promoters present only once per cell and multiple RNAs / proteins should amplify the riboswitch ligand response. The riboswitches were investigated not in their pathogenic host organism, but in the non-pathogenic model organism *B. subtilis*.

4.1.3.1 Working mode

The individual parts of the reverse reporter system are described in the introduction (Section 1.2) and the genetic setup of the system can be seen in Figure 11. It consists of two parts, P_{xyl}-riboswitch-*blaI* and P_{blaP}-reporter, which are both single-inserted into different loci of the *B. subtilis* genome. The riboswitch length and identity as well as the reporter genes can be varied appropriately. The interplay between the parts of the system works as follows:

The system can be activated by inducing the promoter P_{xyl} with xylose. In the absence of a riboswitch ligand (Figure 11, upper part), this leads to transcription of an mRNA composed of a riboswitch RNA (black) and *blaI* (blue arrow). Consequently, BlaI translation is initiated from a RBS between riboswitch and *blaI*. The thereby produced BlaI proteins bind the promoter P_{blaP} and inhibit reporter gene expression.

In the presence of a riboswitch ligand (Figure 11, lower part) the transcriptional OFF riboswitch stops transcription before *blaI* mRNA production. Consequently, no BlaI is produced and the active P_{blaP} causes reporter gene expression. Thus, the

response of a transcriptional OFF riboswitch to its ligand leads to a positive output signal.

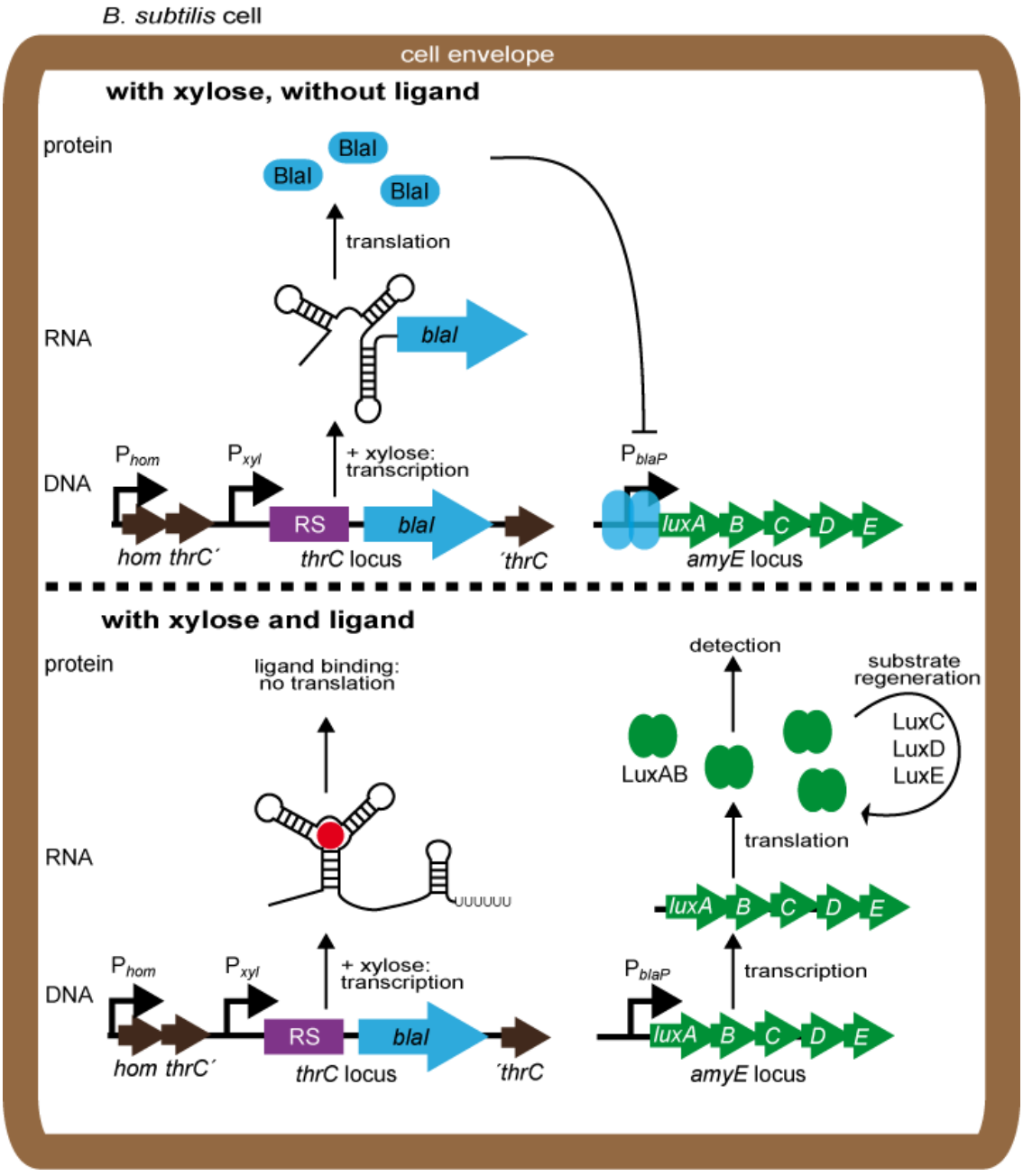

Figure 11. Scheme of the reverse reporter system.

In *B. subtilis* (cell envelope in brown) two parts of the system are integrated into the *thrC* and the *amyE* locus. P_{xyl} (promoters shown by black arrows) regulates a riboswitch (RS; lilac) and *blaI* (blue) as a transcriptional fusion. P_{hom} regulates the expression of Hom and ThrC and might cause read-through in the *thrC* locus. P_{blaP} controls the reporter genes (here: *luxABCDE*, green). The riboswitch ligand is represented by a red circle.

4.1.3.2 Proof of principle

To test the functionality of the reverse reporter system, the response to xylose and ligand was tested using the proposed *xpt* riboswitch from *B. anthracis*. For this purpose, a full-length (fl) riboswitch construct was utilized starting from 13 bp before the proposed start of the P1 stem, including the native *B. anthracis xpt* RBS (= Shine-Dalgarno (SD) sequence) and ending right before the *xpt* gene. This construct was cloned into a system containing the *luxABCDE* cassette[162] for bioluminescence readout (*xpt* fl *lux*; BS47). Guanosine was added to the cells instead of the putative riboswitch ligand guanine because of its better solubility. It is taken up by *B. subtilis* guanosine transporters like NupNOPQ or NupG and converted into the active compound guanine intracellularly by PupG.[63, 65, 66]

After induction, the bioluminescence signal of *xpt* fl *lux* treated with xylose gradually decreased and reached a basal level (~10 RLU/OD) about 7 h after induction (Figure 12 A, upper graph, black curve) while the signal from the xylose and guanosine sample (red curve) increased for about 3.3 h until > 10^5 RLU/OD before it diminished. The decrease of the luciferase activity after 3.3 h could be either attributed to a decrease of P_{blaP} activity[197] or to a reduced oxygen concentration at the onset of stationary phase despite continuous shaking during incubation. Cells treated with guanosine displayed a slight growth delay of about half an hour (Figure 12 A, lower graph, red curve). Growth inhibition due to naturally occurring nucleosides is common in many bacteria.[57] This, however, should not influence the luciferase activity values as they were calculated by normalizing the measured luminescence by the OD. These results reveal that the proposed *B. anthracis xpt* riboswitch is indeed functional and able to respond to guanine.

After these promising first results, the optimal xylose concentration was determined next. Theoretically, the lower the xylose concentration the lower is the intracellular riboswitch concentration. For a constant ligand concentration a lower riboswitch concentration is supposed to give a better signal because there are more ligands per target. On the other hand the xylose concentration should be high enough to produce enough BlaI to reduce the luciferase activity if treated with xylose only. Therefore the lowest xylose concentration able to suppress the bioluminescence signal is most suitable.

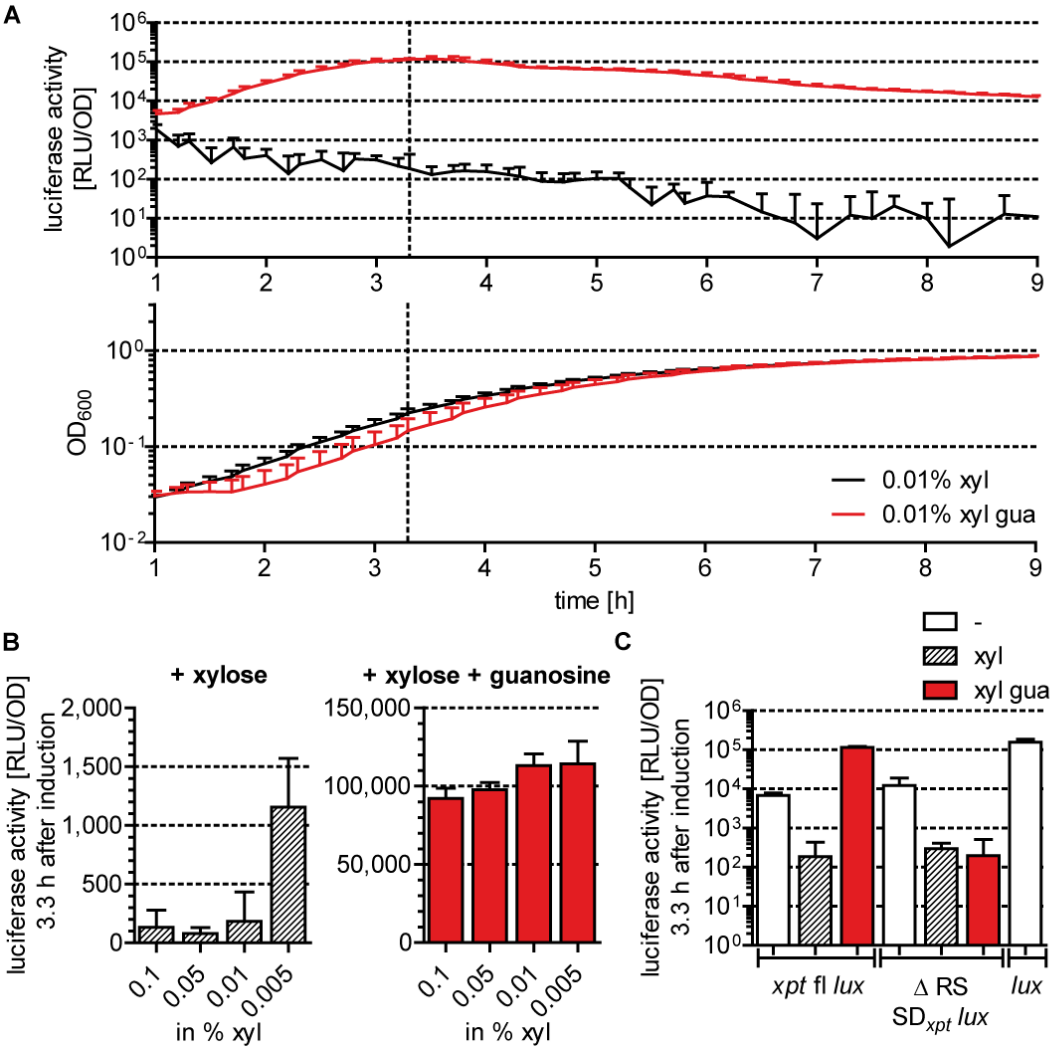

Figure 12: Functional characterization of the reverse reporter system.

(A) Time response of the *xpt* fl *lux* strain (containing the *B. anthracis xpt* riboswitch) displayed by luciferase activity (upper part; [RLU/OD]) and growth (lower part; [OD]) 1 – 9 h after induction with 0.01% xylose or 0.01% xylose and 1 mM guanosine. Both graphs are plotted on logarithmic scales. The time 3.3 h is indicated by a black dotted line.

(B) Luciferase activity [RLU/OD] of the *xpt* fl *lux* strain 3.3 h after induction with xylose (left; 0.1 – 0.005%) or xylose and 1 mM guanosine (right). Luciferase activity on linear scales.

(C) Luciferase activity [RLU/OD] of the strains *xpt* fl *lux,* Δ RS SD_{xpt} *lux* and *lux* 3.3 h without treatment or after induction with 0.01% xylose or xylose and 1 mM guanosine. Luciferase activity on a logarithmic scale.

Non-treated samples ("–") are represented by white bars, samples treated with xylose (xyl) in black (or black striped bars) and xylose plus guanosine samples (xyl gua) in red. For comparability, data varying over a wide range as well as OD curves are displayed on logarithmic scales. Data points and error bars represent the means and standard deviations of at least three biological replicates.

To find the best xylose concentration, the samples were treated with 0.1, 0.05, 0.01 and 0.005% (w/v) xylose with and without 1 mM guanosine (Figure 12 B). 3.3 h after induction, all tested xylose concentrations (Figure 12 B, black striped bars) exhibited a significantly different luciferase activity compared with those treated with 0.1 – 0.005% xylose plus 1 mM guanosine (Figure 12 B, red bars; $P < 10^{-5}$). Moreover, 0.1, 0.05 and 0.01% xylose gave similarly low luciferase activity (< 200 RLU/OD) while the 0.005% xylose signal was more than five-fold higher. As expected, the signal of xylose plus guanosine samples increased with decreasing xylose concentrations from 9×10^4 RLU/OD (0.1% xylose) to 11×10^4 RLU/OD (0.005% xylose). 0.01% was the lowest xylose concentration giving a very satisfactory induction (> 600-fold) and was therefore chosen for further use.

The riboswitch dependence of the system was verified with Δ RS SD_{xpt} *lux* (BS118), which differs from the *xpt* fl *lux* strain only in the absence of the riboswitch. The Δ RS SD_{xpt} *lux* strain displays a xylose response similar to the *xpt* fl *lux* strain (~300 RLU/OD) but lacks a response to guanosine (200 RLU/OD; Figure 12 C) proving that the reverse reporter setup functions as intended.

As guanine is naturally present in *B. subtilis* cells, guanine molecules could bind the riboswitches and lead to a constant *blaI* repression. In the extreme case, naturally occurring guanine could cause constantly high reporter gene readout independent of external ligand addition, thereby hindering the function of the reverse reporter gene system. However, the results demonstrate that the intracellular guanine concentration does not perturb the reporter gene readout. This can be explained by the high copy numbers of riboswitch RNA produced by the strong promoter P_{xyl} causing a favorable ratio between BlaI and P_{blaP}. The intracellular guanine concentration (which has not been measured in *B. subtilis* so far) is obviously not sufficient to trigger reporter gene expression.

Readthrough from the promoter P_{hom} in front of the *thrC* locus (Section 1.2.1) can cause riboswitch and *blaI* transcription in the absence of xylose. To reduce this undesired effect, it was tried to limit the activity of the P_{hom} promoter using two strategies: first, the growth medium was supplemented with casamino acids as it is known that casamino acids repress P_{hom} activity.[146] To see whether this strategy works, the *lux* strain (BS41), which contains only the P_{blaP}-*lux* part of the system, was

included in the study as a control (Figure 12 C). It displayed the highest luminescence in this assay (1.5 x 10^5 RLU/OD), which is due to the lack of the transcriptional repressor BlaI in this strain. The finding that the untreated *xpt* fl *lux* strain has a clearly lower signal (6.8 x 10^3 RLU/OD) demonstrates that there are BlaI proteins present in these cells although P_{xyl} is not activated. This finding can be traced back to either P_{xyl} leakiness or an active P_{hom} promoter in front of P_{xyl}.

In a second attempt to limit readthrough from P_{hom}, the *B. subtilis* transcription terminator *lysS* (ΔG = –25.3 kcal/mol)[198, 199] was cloned in front of P_{xyl}. To this end, two controls were tested (that both contained an optimal SD[200] in front of *blaI*): in Δ P_{xyl} Δ RS SD_{opt} *lux* (BS257) both the promoter P_{xyl} and the riboswitch were deleted (Figure 13 A). With no P_{hom} or P_{xyl} promoter activity one would expect high luciferase activity originating from a highly active P_{blaP} promoter at about 1.5 x 10^5 RLU/OD (level of the *lux* strain; Figure 12). Instead, Δ P_{xyl} Δ RS SD_{opt} *lux* exhibits background activities (< 180 RLU/OD) without ("–", white bars) and with xylose (black striped bars) as well as with xylose and guanosine (red bars). The other control strain, Δ RS SD_{opt} *lux* (BS210) with P_{xyl} but lacking a riboswitch displayed an elevated luciferase activity in the sample without xylose (4 x 10^3 RLU/OD) compared to the xylose sample (57 RLU/OD). Considering the working mode of P_{xyl} (Section 1.2.2) these results can be explained by hypothesizing that XylR acts as a roadblock to prevent readthrough from P_{hom} in the non-induced state. These results suggest that P_{blaP} inhibition is, at least in part, caused by *blaI* transcription from the P_{hom} promoter that the combined usage of casamino acids and the *lysC* terminator could not prevent. Due to the differences between the non-treated Δ RS SD_{opt} *lux* signal and the *lux* strain signal (1.5 x 10^5 RLU/OD) it is likely that P_{xyl} is also leaky to some extent. However, since the system function is not strictly dependent on P_{xyl} inducibility the residual expression can be neglected.

4.1.4 Characterization of *B. anthracis* riboswitches

In the following, the *B. anthracis* guanine riboswitches should be compared and characterized in different aspects like activity, sensitivity and selectivity using the reporter system established above.

To be able to compare the riboswitches, their sequences were cloned alike beginning ten bases upstream of the putative P1 stems as predicted by the *in silico*

calculations, and until, but not including, the putative RBS. The regions between the putative terminator and the RBSs were included to reflect the natural riboswitch surroundings as much as possible. Riboswitches with this length will be abbreviated with "1" in the following. To exclude effects due to differences in the RBS, an optimal *B. subtilis* SD[200] was cloned between the riboswitches and *blaI* instead of the natural RBSs, thereby assuming that the riboswitch actions are indeed independent of their RBS sequences. In addition, the above-mentioned transcription terminator *lysS*[198, 199] was placed in front of P_{xyl} to limit the transcriptional read-through from the P_{hom} promoter (Section 4.1.3.2).

4.1.4.1 In vivo *activity*

To ensure that no additional promoters are present in the riboswitch sequences, Δ P_{xyl} RS constructs were cloned and compared to the Δ P_{xyl} Δ RS control (Figure 13 A). Here, the untreated and xylose-treated samples are comparable because the xylose-responsive element has been removed. If there was a promoter in one of the riboswitch sequences one would expect lower bioluminescence caused by the non- or xylose-treated riboswitch strain compared to the corresponding Δ P_{xyl} Δ RS control sample. All Δ P_{xyl} RS strains displayed a higher bioluminescence as the Δ P_{xyl} Δ RS control either in the absence or presence of xylose or both (Figure 13 A). Taking the low signal level of the Δ P_{xyl} Δ RS strain (about W168-level) into account, these results have to be considered with caution. Nevertheless they hypothesize that there are no hidden promoters in the riboswitch sequences.

Next, the responses of the five putative *B. anthracis* riboswitches to the presence of their potential ligand guanine were examined and compared to the well-investigated *B. subtilis xpt* riboswitch (BS *xpt* 1 *lux*). For this purpose, the luminescence activity of the riboswitch reporter constructs 3.3 h after induction was analyzed. Upon xylose treatment (Figure 13 B, black striped bars), all *B. anthracis* riboswitch constructs displayed a decreased luciferase activity to a similar basal level (50 – 161 RLU/OD). After xylose and guanosine addition (red) all signals increased significantly ($P < 0.00001$), leading to up to thousandfold inductions compared to the signals in the absence of guanosine (see Table 10). The lowest luciferase activity was caused by the *guaA* 1 *lux* strain (~2,800 RLU/OD) and the highest by the BA *xpt* 1 *lux* strain (~53 x 10^3 RLU/OD). In comparison with the *B. anthracis* riboswitches the *B. subtilis xpt* model riboswitch displays the highest residual

luciferase activity as well as the highest activity in the presence of xylose or xylose and guanosine, respectively. Due to the high xylose signal the corresponding guanosine induction rate was low (67-fold) compared to its *B. anthracis* homolog (~10^3-fold). In summary, all riboswitch constructs tested here indeed respond to guanosine addition but they differ greatly in strength.

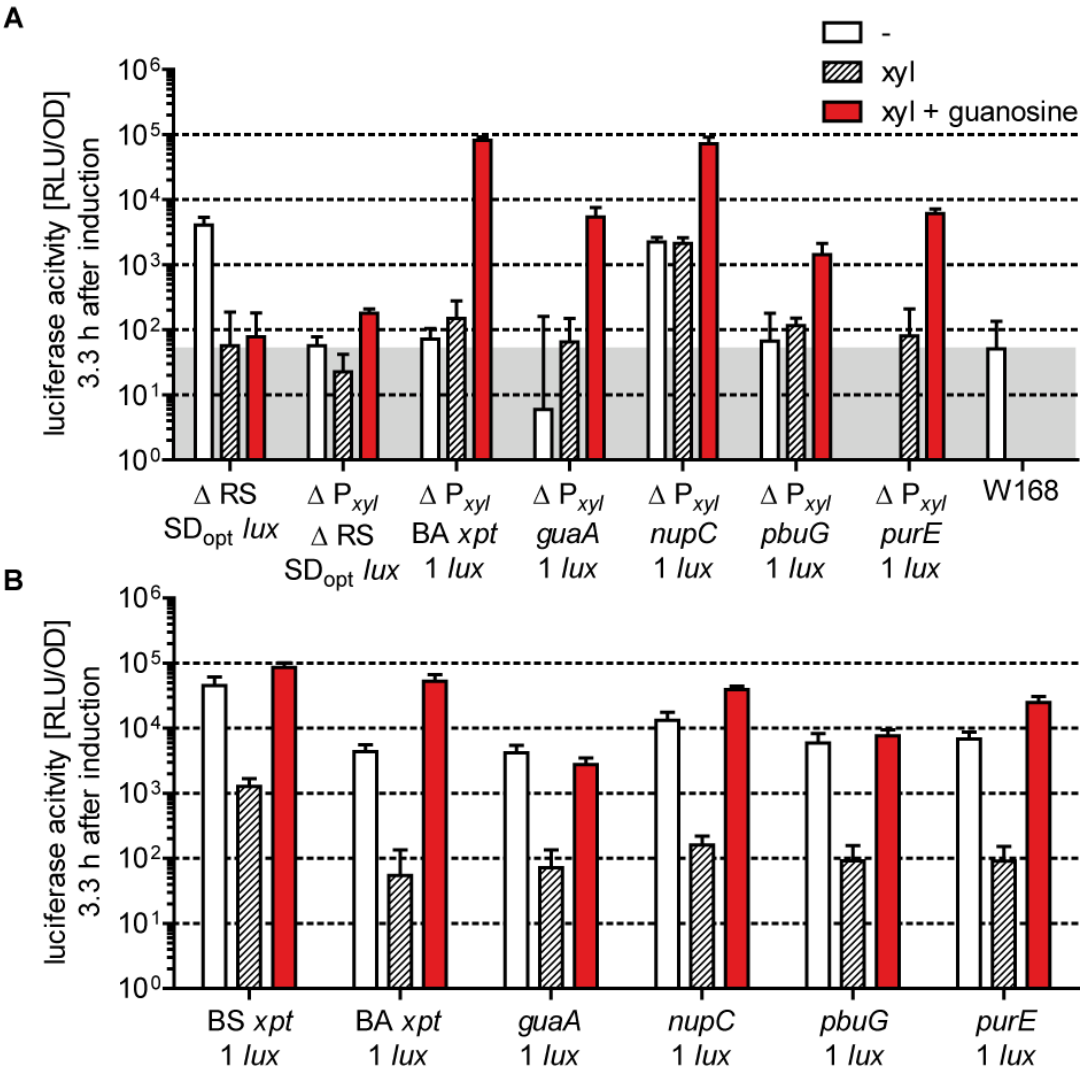

Figure 13: Activity of the *B. anthracis* guanine riboswitches.

(A) Control strains: the luciferase responses of Δ RS, Δ P_{xyl} Δ RS, the Δ P_{xyl} *B. anthracis* riboswitch constructs and W168 ("–" sample only) without treatment, with xylose and with xylose and guanosine. The W168-level is shaded in grey.

(B) The luciferase responses to no treatment, xylose or xylose and guanosine caused by the *B. anthracis* riboswitch constructs and the *B. subtilis xpt* riboswitch.

Abbreviations and color code as in Figure 12. The luciferase activities [RLU/OD] 3.3 h after induction are given on logarithmic scales. Data points and error bars represent the means and standard deviations of at least three biological replicates. Note: negative values cannot be displayed on logarithmic scales.

Table 10: Overview of the average xylose (xyl) and xylose + guanosine (xyl + gua) results obtained 3.3 h after induction and their corresponding induction ratios.

Riboswitch	Luciferase activity xyl sample 3.3 h after induction [RLU/OD]	Luciferase activity xyl + gua sample 3.3 h after induction [RLU/OD]	Ratio $\frac{\text{xyl + gua}}{\text{xyl}}$
BS *xpt*	1,275	85,787	67
BA *xpt*	54	52,798	971
guaA	72	2,775	39
nupC	161	39,100	243
pbuG	91	7,662	84
purE	91	24,916	274

In the *in vivo* experiments, some factors potentially influencing riboswitch behavior in their native state such as tertiary interactions of the riboswitch RNAs to their native 5´ RNAs could not be taken into account.

4.1.4.2 Ligand specificity

To determine the ligand specificity of the guanine riboswitches their response to several guanine-like molecules was assessed. The ligand candidates adenine, hypoxanthine, 2,6-diaminopurine, 2,5,6-triaminopyrimidin-4-one (PC1) and 2,6-diaminopyrimidin-4-one (PC2) were chosen from literature since they were shown to bind purine riboswitches (chemical structures: Figure 2).[38, 39] Compound PC1 has additionally been shown to have antibacterial properties (although these are not solely due to its riboswitch binding).[38, 53]

The results of the *in vivo* assays with the riboswitch 1 *lux* constructs (Figure 14) demonstrate that none of the investigated *B. anthracis* guanine riboswitches responded to adenine (≤ 237 RLU/OD; dark green bars). Upon hypoxanthine addition, the BS *xpt* 1 *lux*, the *nupC* 1 *lux* and the *purE* 1 *lux* strains displayed a significant response (BS *xpt*: P = 0.00002; *nupC*: P = 0.002 and *purE*: P = 0.038; light green bars). The *nupC* 1 and the BS *xpt* 1 riboswitches demonstrate a significant response to 2,6-diaminopurine (*nupC*: P = 0.015; BS *xpt*: P = 0.0016; brown bars). Strikingly, the BS *xpt* 1 riboswitch is the only one sensitive to the compound PC2 (P = 0.022; orange bars).

PC1 could not be investigated with the reverse reporter gene setup because *B. subtilis* did grow in the presence of 1 mM PC1 only after a huge growth delay

(data not shown). This presumably interfered with the assay as no bioluminescence was observed even from the *B. subtilis xpt* riboswitch. For this reason, PC1 could not be investigated further.

It has been demonstrated previously that guanine riboswitches do respond to adenine very weakly.[10, 106] By comparison, the *B. subtilis xpt* riboswitch binds hypoxanthine[10] stronger, as observed here for two guanine riboswitches from *B. anthracis*. Thus, the results here are consistent with existing studies. Interestingly there is a huge difference in the response to PC2 between the *B. anthracis* riboswitches (no observable response) and the *B. subtilis xpt* riboswitch (significant response) that indicates structural differences in their aptamer domains.

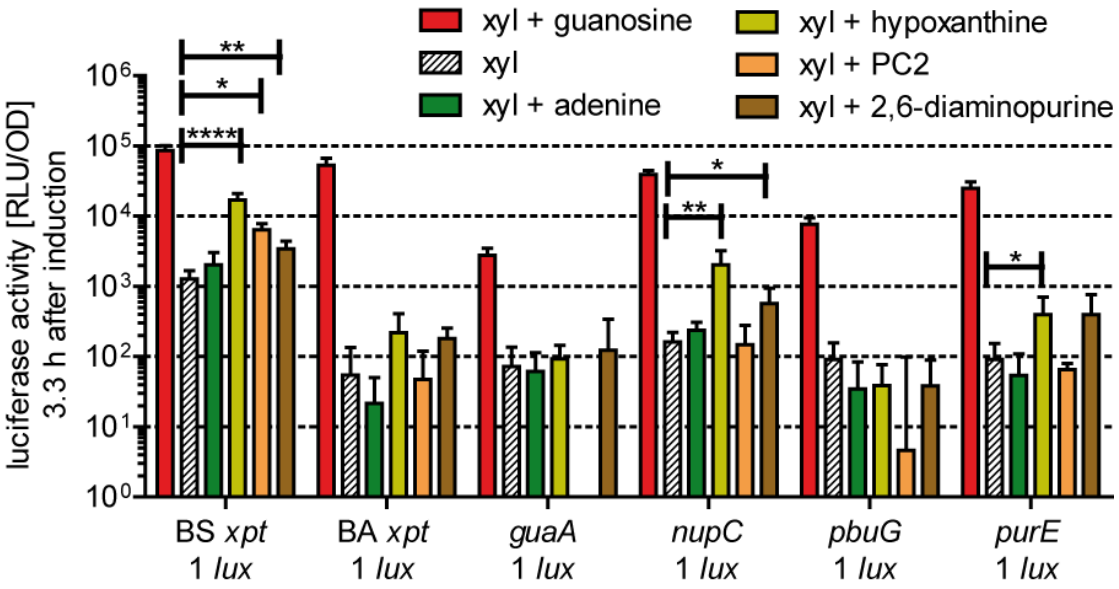

Figure 14: Riboswitch response to guanine-like compounds.
Riboswitch responses to 0.01% xylose (xyl; black striped bars), xylose and 1 mM guanosine (red), adenine (dark green), hypoxanthine (light green), PC2 (orange) or 2,6-diaminopurine (brown). Significant changes of secondary ligands compared to the xyl values are marked by asterisks. The luciferase activities [RLU/OD] 3.3 h after induction are given on a logarithmic scale. Data points and error bars represent the means and standard deviations of at least three biological replicates.

4.1.4.3 Ligand sensitivity

With the reverse reporter setup, the dynamic range of the riboswitches can be investigated by varying the ligand concentrations in the medium. The ligand concentrations can only be compared relatively to each other as there is no

information about the impact on the intracellular guanine concentrations. Nevertheless these should be equal in all strains tested. For better comparison, the response observed in the presence of 1 mM guanosine was set to 100% and the dose-dependent responses were plotted relatively to this.

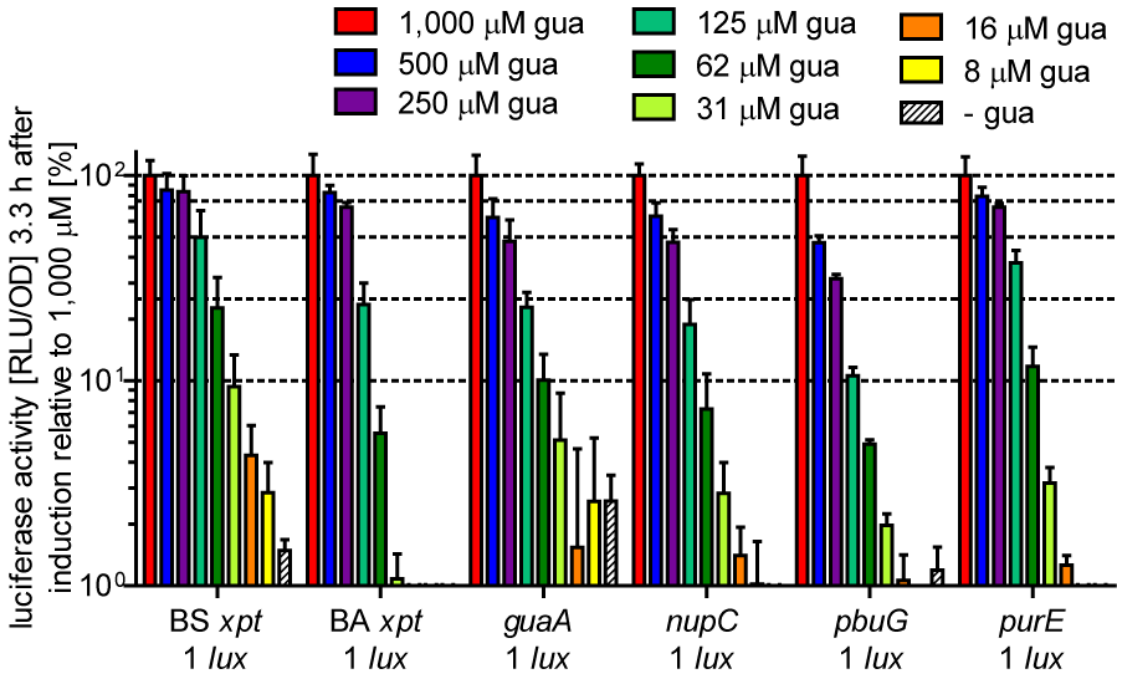

Figure 15: Dose-dependent riboswitch response.
Response of the 1 *lux* riboswitches treated with xylose and addition of guanosine (gua; red: 1,000 µM, blue: 500 µM, violet: 250 µM, turquoise: 125 µM, dark green: 62 µM, light green: 31 µM, orange: 16 µM, yellow: 8 µM) or without guanosine (black striped bars). Luciferase activity relative to the averaged 1,000 µM guanosine values (100%) of each riboswitch is given and 10, 25, 50, 75 and 100% are indicated by dashed lines. The luciferase activities [RLU/OD] 3.3 h after induction are given on a logarithmic scale. Data points and error bars represent the means and standard deviations of at least three biological replicates.

The relative riboswitch responses to 0 – 1,000 µM guanosine are depicted in Figure 15. The riboswitches demonstrate different ligand sensitivities: while the responses to 250 µM guanosine (violet bars) reached about 70% for BA *xpt* 1 and *purE* 1, the *pbuG* 1 riboswitch displayed only a response of 30%. This demonstrates that the *purE* and BA *xpt* riboswitches react more sensitively to changes in higher concentrations than the others. The results indicate that the riboswitches strongly differ in the ligand concentration range where smaller changes in ligand concentration trigger high differences in luciferase activity. Similar observations were

made in previous RT-qPCR (reverse-transcription quantitative PCR) experiments where three *B. subtilis* guanine riboswitches were investigated.[106]

The *B. subtilis xpt* riboswitch responded more sensitively to relatively low (e.g. 62 µM) guanosine concentrations compared with the *B. anthracis* riboswitches: from 0 – 31 µM guanosine, an evenly graded luciferase activity can be observed which ranges from 1 – 9% of the maximal *B. subtilis xpt* response. The corresponding relative *B. anthracis* riboswitch responses are much lower (≤ 5.1%).

4.1.4.4 In vitro *ligand binding*

The guanosine-dependent activity of riboswitches observed *in vivo* needs to be investigated *in vitro* to prove that ligand sensing is performed by the RNA itself and not by secondary effects such as additional protein factors. Considering the fact that guanosine binding by purine riboswitches has previously been observed[36] it is also necessary to verify the assumption that the *B. anthracis* riboswitches do indeed bind guanine. Therefore, the riboswitch-guanine dissociation constants were determined in an *in vitro* spinach aptamer-riboswitch fusion assay (Section 1.1.5). In this assay, riboswitch ligand binding causes folding of the riboswitch aptamer that enables folding of the spinach aptamer and its binding to DFHBI. The thereby generated spinach aptamer-DFHBI complex is fluorescent and can be monitored in a plate reader. By measuring serial ligand dilutions and plotting the ligand concentration against the fluorescence signal, K_D values were determined.

Table 11: K_D values of riboswitch-guanine binding determined by riboswitch-spinach fusions.

Riboswitch	K_D [µM][a]
BS *xpt*	0.04 ± 0.01
BA *xpt*	0.04 ± 0.01
guaA	4.10 ± 3.72
nupC	0.27 ± 0.12
pbuG	1.18 ± 0.33
purE	3.52 ± 1.22

a. The mean and standard deviations of three independent measurements are given.

The obtained apparent K_D values range from 40 nM (BA *xpt* and BS *xpt*) to 4.1 µM (*guaA*) and therefore reflect large differences in riboswitch-guanine binding affinities.

Due to the method setup rather large K_D standard deviations were obtained especially for riboswitches with low binding affinity. Comparisons between these K_D values should therefore only be drawn with caution. Nevertheless, it can be stated that all riboswitches displayed a guanine-dependent response. Therefore, the K_D measurements do prove that the five *B. anthracis* riboswitches indeed bind guanine without any additional protein factors involved.

Previous investigations revealed that guanine riboswitches can have large differences in their ligand binding affinity.[106] In accordance with these results, the *B. anthracis* riboswitches exhibited distinct variations in their K_D values here. Apparent 2AP dissociation constants of the *B. subtilis xpt, purE* and *pbuG* riboswitches determined in a former study by fluorescence spectroscopy are similar.[106] Compared to their homologous *B. subtilis* riboswitches, the corresponding *B. anthracis* riboswitches gave a clearly different picture here with K_D values ranging from 0.04 µM (*xpt*) to 3.52 µM (*purE*). It becomes evident that the dissociation constants vary relatively to each other from one to another *Bacillus* species. This can be explained considering the comparably low sequence identity of the *purE* riboswitch aptamer domains of 74.4%.

Known *B. subtilis xpt* K_D values obtained by in-line probing ($K_D \leq 5$ nM)[10] differ from the dissociation constant determined here (40 nM). The discrepancy can be attributed to different methods as well as reaction conditions (40 mM HEPES pH 7.5, 125 mM KCl, 3 mM $MgCl_2$, 37 °C here versus (vs.) 50 mM Tris pH 5.8, 20 mM $MgCl_2$, 100 mM KCl, 25 °C[10]). In fact, it was observed previously that K_D values obtained by spinach-riboswitch fusions were higher than those from in-line probing or gel-shift assays.[110, 201] Therefore, the absolute K_D values here cannot be compared directly to K_D values measured by different means. However, the *B. anthracis* riboswitches can be ranked relatively to the BS *xpt* aptamer included in this study.

K_D values give the equilibrium ligand concentration where half of the riboswitches are ligand-bound. If equilibrium is not reached (kinetic regime), less ligands are bound to aptamers at the same total ligand concentration compared to the situation in equilibrium (thermodynamic regime). But does riboswitch ligand binding follow a thermodynamic or a kinetic regime in the cells? Riboswitches causing transcription termination upon ligand binding are likely to be kinetically governed because there is

a limited time frame during transcription after formation of the aptamer domain and before the RNA polymerase has reached the transcription terminator.[34] Thus, several factors have to be kept in mind:[33, 34] first, the length of the RNA between aptamer domain and the terminator influences the time available for folding. In case of the *B. anthracis* riboswitches, the distance from the aptamer domain until the U-stretch ranges from 67 bases (*pbuG*) to 95 bases (*guaA* and *purE*) (see Table 12). Consequently, the former have a lower probability of being governed by a thermodynamic regime than the latter. Second, transcriptional pause sites have to be considered that prolong the time needed for transcription and therefore can shift the riboswitch towards a thermodynamic regime. Third, transcription factors as NusA can trigger RNA polymerase pausing and transcription termination.[202] In addition, the NTP concentration influences the transcription rate.[203] Due to the variety of factors influencing co-transcriptional riboswitch folding it cannot be decided here if the riboswitches follow a kinetic or a thermodynamic regime.

Table 12: Distances from aptamer to U-stretch of terminator domains and ΔG^{term} determined *in silico*.

Riboswitch	Distance from aptamer to U-stretch [bases]	ΔG^{term} [kcal/mol]
BS *xpt*	72	–23.0
BA *xpt*	89	–32.1
guaA	95	–26.4
nupC	86	–28.7
pbuG	67	–12.7
purE	95	–25.9

How far do the *in vitro* and *in silico* studies really reflect the *in vivo* data? Strong riboswitches give a high *in vivo* signal upon ligand addition in the setup presented here. They are expected to have a potent terminator and a high *in vitro* ligand binding affinity. Indeed, although the K_D values using spinach aptamer-riboswitch aptamer-fusion RNAs are not very precise and reflect only the state of equilibrium some correlations can be drawn between the strengths of the terminators, the apparent K_D values and the *in vivo* data (Table 13). The highest *in vivo* activity was observed from the *B. anthracis xpt* riboswitch (~53,000 RLU/OD) that also displayed the lowest K_D value (0.04 µM) and a strong terminator (–32.1 kcal/mol). The same is

true for *nupC* (~39,000 RLU/OD; K_D = 0.27 µM; ΔG^{term} = –28.7 kcal/mol). The lowest *in vivo* activity was observed from the *guaA* riboswitch (~2,800 RLU/OD) that has a moderate terminator (ΔG^{term} = –26.4 kcal/mol) but a very low *in vitro* binding affinity (K_D = 4.10 µM). Compared to the *purE* riboswitch, the *pbuG* riboswitch displays a lower *in vivo* guanosine signal despite a lower K_D (3.52 µM vs. 1.18 µM). This can be explained by the different aptamer-U-stretch distances (*pbuG*: 67 b; *purE*: 95 b) and terminator strengths (*pbuG*: -12.7 kcal/mol; *purE*: -25.9 kcal/mol).

Table 13: Overview of results obtained from *B. anthracis* riboswitches.
Summary of Tables 10-12. xyl = xylose; xyl gua = xylose and guanosine.

Ribo-switch	Luciferase activity 3.3 h after induction [RLU/OD]		Luciferase ratio $\frac{\text{xyl} + \text{gua}}{\text{xyl}}$	K_D [µM]	Distance aptamer → U-stretch [bases]	ΔG^{term} [kcal/mol]
	xyl	xyl + gua				
BA *xpt*	54	52,798	971	0.04 ± 0.01	89	–32.1
guaA	72	2,775	39	4.10 ± 3.72	95	–26.4
nupC	161	39,100	243	0.27 ± 0.12	86	–28.7
pbuG	91	7,662	84	1.18 ± 0.33	67	–12.7
purE	91	24,916	274	3.52 ± 1.22	95	–25.9

4.1.4.5 Verifying the modes of action

To prove the mode of action proposed in Section 4.1.1.3, minimal riboswitch sequences were cloned into the reporter system described in Section 4.1.3 (without a transcription terminator in front of P_{xyl}). They start directly 5´ to the P1 sequence and end after the last U probably still belonging to the proposed terminator. The constructs comprise all bases shown in the ligand-bound structures in Figure 9 and will be abbreviated with “2” in the following. Again, the natural RBSs were changed into an optimal *B. subtilis* SD to exclude the possible impact of variations in the RBS.

The relative increase in bioluminescence upon guanosine addition compared to the xylose samples was generally similar in 1 *lux* and 2 *lux* strains. The absolute xylose and guanosine values of the 2 *lux* constructs are in the same range as the longer constructs (1 *lux*). While some constructs like the xylose- and xylose and guanosine-

treated *nupC* 2 and *purE* 2 as well as the xylose-treated *pbuG* 2 yielded smaller signals compared to their construct 1 counterparts the xylose and guanosine signal of *guaA* increased considerably from 2.8 x 10^3 RLU/OD (*guaA* 1 *lux*) to 2.2 x 10^4 RLU/OD (*guaA* 2 *lux*). Lower construct 2 signals can be explained by a small fraction of the terminator missing in the minimal constructs. The *guaA* 2 behavior resembles those from the strains Δ P_{xyl} *nupC* 1 *lux* and BS *xpt* 1 *lux* and can probably be explained by alternative RNA folding. In case of the *guaA* riboswitch the effect of the transcription terminator in construct 1 could thereby be lowered leading to an elevated BlaI level in the cells and consequently to a lower luciferase signal independent of ligand binding in construct 1. That finding confirms the decision to use longer constructs for riboswitch comparison to include unforeseen tertiary interactions as much as possible. In summary, all construct 2 riboswitches displayed a clear response to ligand addition. The results therefore support the above-mentioned model of the riboswitches (Section 4.1.1.3) in length as well as their mode of action as transcriptional OFF switches.

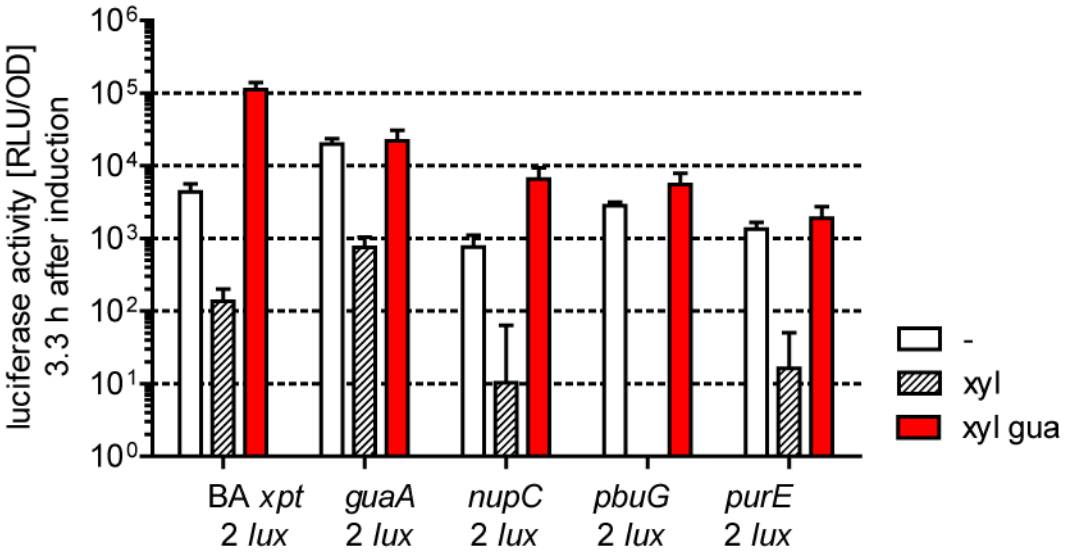

Figure 16: Activity of short *B. anthracis* riboswitches.

All short riboswitch constructs are still ligand-responsive. Colors and axes as in Figure 13. Data points and error bars represent the means and standard deviations of at least three biological replicates. Note: negative values cannot be displayed on logarithmic scales.

4.2 Development of a high-throughput screening

Riboswitches are seen as good potential drug targets (Section 1.1.6.2). Therefore it is of high interest to find molecules targeting *B. anthracis* guanine riboswitches—novel compounds as well as known drugs already used for the treatment of other diseases.

The general procedure of a high-throughput screening of large compound libraries is depicted schematically in Figure 17. First, a compound library, a target and appropriate reporters have to be chosen. Here, a screening facility and a compound library previously reported were utilized.[165, 204] The library consists of a collection of FDA-approved drugs and a small-molecule library. The compounds in the small-molecule library had been selected on the following criteria: predicted DMSO-solubility, diverse chemical scaffolds and satisfying drug properties based on Lipinski´s rule of five (Section 1.1.6.2).[204] Putative unstable or toxic compounds as well as frequent hitters had been excluded.

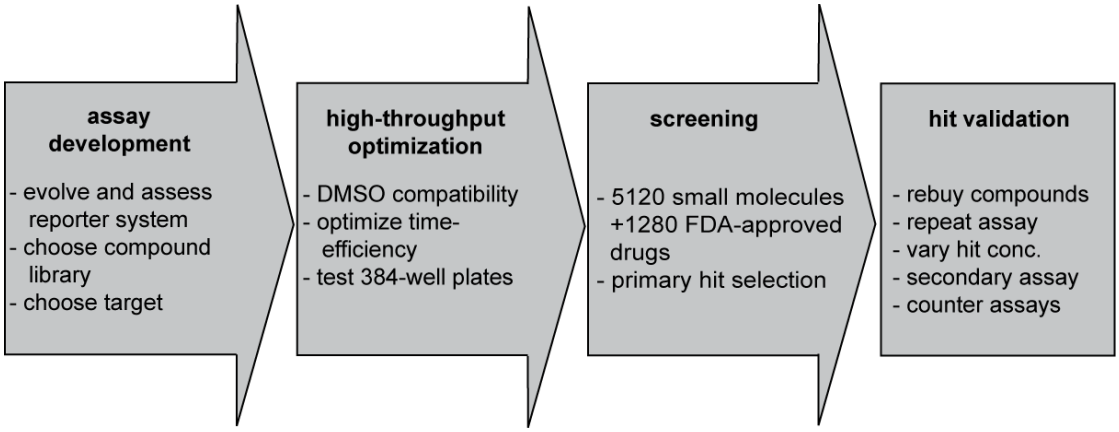

Figure 17: Procedure of a high-throughput screening.
After assay development and high-throughput optimization the screening is performed and the hits are validated.

The *B. anthracis xpt* riboswitch is a good target because of its high response to ligand addition. One compound targeting the homologous *xpt* riboswitch from *B. subtilis* has already been shown to have antimicrobial activities against *S. aureus* and *Clostridium difficile*,[38] although its action is not solely riboswitch-dependent.[53] It is not known whether an *xpt*-riboswitch targeting compound could inhibit growth or pathogenicity of *B. anthracis*, but it is probable that it would do so if the compound targets some or all *B. anthracis* guanine riboswitches simultaneously.

The reverse reporter system established in this thesis is well-suited to screen for novel synthetic riboswitch ligands due to the large signal difference in xylose and xylose plus guanosine-treated samples. The luciferase reporter was selected for the screening and the orthogonal *lacZ* reporter (Section 1.2.4.2) is suitable for secondary assays. The reporter construct used for the screening (*xpt* fl *lux*; Section 4.1.3.2) consists of the *B. anthracis xpt* riboswitch with its native RBS upstream of *blaI* and the luciferase genes controlled by P_{blaP}. Since the *lysS* terminator is not able to completely hinder P_{hom} readthrough as presented in Section 4.1.4.1 it was omitted here.

One potential problem in this screening for guanine riboswitch ligands is cell death caused by hit compounds leading to false-negative results. Compounds causing cell death, for example by interfering with the cellular metabolism, cannot be identified in this screening. A more specific cause for impaired cell growth could occur upon addition of compounds able to target guanine riboswitches in general whose binding to *B. subtilis* guanine riboswitches could disturb the bacterial metabolism and lead to reduced growth. Yet, previous studies showed that antibacterial guanine analogues do inhibit *B. subtilis* growth less in rich than in minimal medium.[38, 129] The modified CSE medium used here can be considered as suitable because it permits growth of the compounds PC1 and PC2 similarly to previously observed growth behavior.[38] Consequently, false-negative results due to cross-reactivity between the *B. anthracis xpt* riboswitch and *B. subtilis* guanine riboswitches are limited here as far as possible.

4.2.1 High-throughput optimization

Before applying a method to a high-throughput mode it is necessary to ensure that the positive and negative signals are well-separated and that the signals are reproducible. To this end, assay performance measures as Z´ factor or signal window (SW) are used (Section 3.2.9) to judge the suitability of the system for high-throughput applications. They quantify the amount of separation of the positive and the negative controls taking the corresponding variability into account (see [205] or [206] for more information). For this purpose, the data of the target strain *xpt* fl *lux* (shown in Figure 12 C) were analyzed: the > 600-fold increase in luciferase activity upon guanosine addition corresponds to a signal window (SW) of 13.44 and a Z´ of 0.81,

which clearly fulfills the acceptance values for screening assays (SW > 2; Z´ > 0.5) claimed by Iversen *et al*.[205] Thus, the assay is generally suitable for a screening.

Typically, compound libraries are solved in DMSO. DMSO can denature RNA[207] as well as affect RNA-ligand binding affinities.[208] It may also impair *B. subtilis* growth or change gene expression levels. Therefore, the DMSO tolerance of the system will be examined in the following using the *xpt* fl *lux* strain described in Section 4.1.3.2. To ensure a compound concentration of 10 µM during the screening, the system needs to tolerate at least 1% (v/v) DMSO. Thus, the reporter gene activities of samples treated with xylose and 1 – 5% DMSO, with and without guanosine, were compared. The corresponding luciferase activities were in the same range with and without 1% DMSO both in time course (Figure 18 A) as well as 3.3 h after induction (Figure 18 B; + xylose: 183 and 234 RLU/OD; + xylose and guanosine: 11 x 10^4 RLU/OD and 8 x 10^4 RLU/OD for 0 and 1% DMSO, respectively). With increasing DMSO concentrations (0 – 5%; Figure 18 B, lilac) the xylose signal increased while the xylose guanosine signal decreased. Consequently, the signal-to-background ratios (S/B) diminished from > 600 without DMSO to ~350 with 1% DMSO. Nevertheless, the S/B ratio of 1% DMSO as well as the corresponding SW and Z´ (11.42 and 0.79) are still satisfactory for screening purposes.

To be able to screen many compounds in parallel, 384-well plates have to be used and the workflow has to be adjusted to enable parallel preparation, incubation and read-out of the samples. It is also important to pay attention to spatial uniformity of the plates. Edge or drift effects can occur, for example, due to evaporation from outer wells or temperature gradients during incubation.[206] To adapt the system for the high-throughput procedure in 384-well plates (Figure 18 C), two successive pre-cultures were replaced by a short overnight culture. For parallelization, time-course measurements were substituted by two successive end-time measurements 3 and 3.5 h after induction. For incubation, plates were shaken in an incubator. To ensure proper mixing, cells and xylose were diluted separately and distributed to the 384-well plates in comparably high volumes. With this improved work flow, tests were run in 384-well plates containing cells treated with xylose (negative control) or with xylose and guanosine (positive control). Although there was an edge effect visible, three independent experiments still gave satisfactory assay performance

measures (Z´ = 0.72 ± 0.09 and SW = 10 ± 5) and therefore the setup was ready to be tested in a screening.

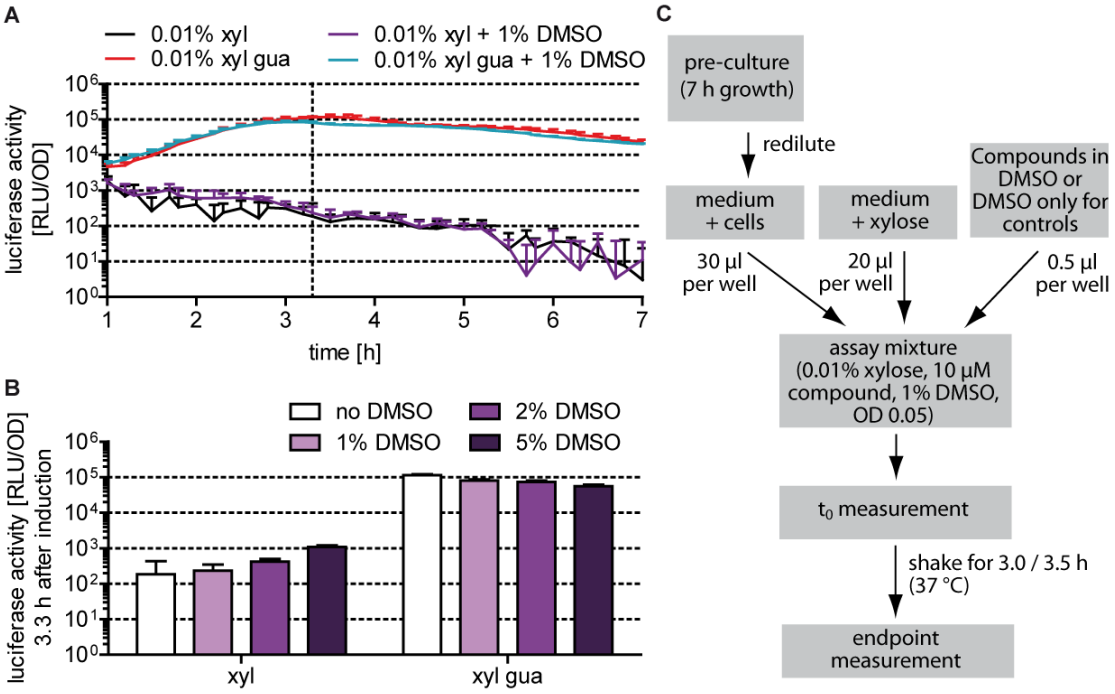

Figure 18: DMSO tolerance *xpt* fl *lux* and optimized screening workflow.

(A) Time course (1 – 7 h after induction) of the luciferase activity [RLU/OD] of xylose and xylose guanosine samples treated with (lilac and blue) or without 1% DMSO (black and red).

(B) Luciferase activity [RLU/OD] 3.3 h after induction. Samples were treated with xylose (left) or xylose and guanosine (right) without (white) or with 1 – 5% DMSO (lilac).

(C) Workflow of the screening.

Abbreviations as in Figure 12. The luciferase activities [RLU/OD] are given on logarithmic scales. Data points and error bars represent the means and standard deviations of at least three biological replicates.

4.2.2 Screening

A library of 1,280 FDA-approved drugs and 5,120 small compounds in 20 384-well plates was subjected to a screening following the workflow in Figure 18 C. Every plate included 16 wells containing negative control (xylose) and 16 wells with positive control (xylose and guanosine). For illustration, the results of the FDA-approved drug screening plates are shown in Figure 19. The corresponding controls are visualized in Figure 19 A. An edge effect is visible especially in the positive controls (red) of plate 4. The data are nevertheless acceptable as displayed by the satisfactory Z´ values (0.77 ± 0.02; Figure 19 B) and signal windows (10.87 ± 1.46).

Only a few of the compound-treated samples displayed a luciferase activity above 407 RLU/OD (selection criterion 1; Figure 19 C).

It was possible to screen 5,120 small-molecule compounds in parallel, proving that the method is indeed high-throughput applicable. The corresponding 16 small-molecule screening plates yielded Z´ values above 0.54 with one outlier (0.45).

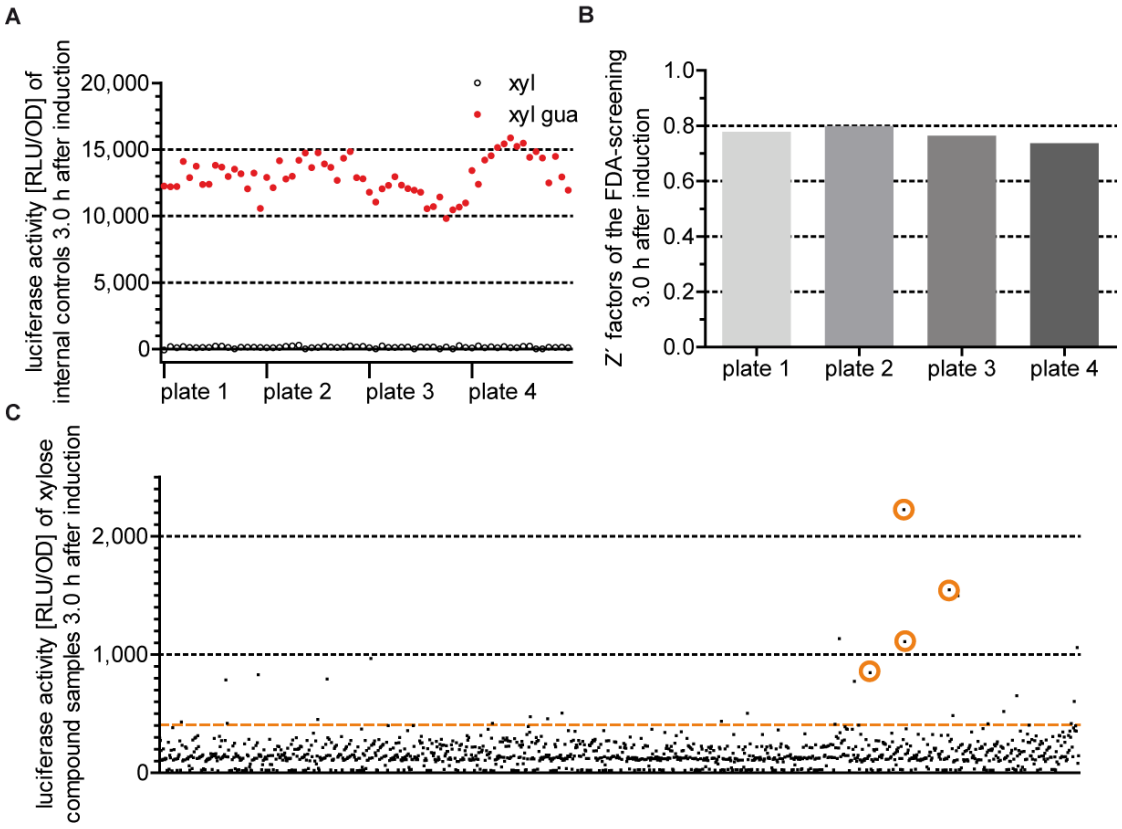

Figure 19: Results of the screening with FDA-approved drugs.

(A) Luciferase activity of internal positive (red dots) and negative controls (white dots) on the screening plates 3.0 h after induction.

(B) Z´ of the four FDA-screening plates 3.0 h after induction.

(C) Luciferase activity of compound and xylose samples 3.0 h after induction. The orange line at 407 RLU/OD represents hit selection criterion 1 (see below) and orange circles mark the four primary hit compounds.

The Z´ factors and luciferase activities [RLU/OD] 3.0 h after induction are given on linear scales.

4.2.3 Hit selection

Establishing an approach to select promising primary hits is vital for high-throughput screening evaluation. Here, the signals of the compound-containing wells were compared to the negative control wells containing cells and 0.01% xylose (negative

control; neg). The following selection criteria were applied for the evaluation of the screening of the FDA-approved drugs consisting of four 384-well plates:

1) luciferase activity 3 h after induction [RLU/OD] > $\emptyset_{neg}$ + 4 x σ_{neg} (here: ≙ 407 RLU/OD; represented by an orange line in Figure 19);
2) luciferase activity 3.5 h after induction [RLU/OD] > $\emptyset_{neg}$ + 3 x σ_{neg};
3) luminescence [RLU] prior incubation < $\emptyset_{neg}$ + 3 x σ_{neg};
4) wells had to display an elevated luminescence compared to their neighbors;
5) luminescence [RLU] 3 h after induction > $\emptyset_{neg}$ + 3 x σ_{neg};

where ∅ abbreviates the mean value, neg the negative control (xylose only) and σ the standard deviation.

Hit compounds should cause a long-lasting luciferase activity; that is ensured by the criteria 1 and 2. An essential part is the exclusion of false-positive hits that can be caused by autoluminescent compounds. This is included in criterion 3. Edge effects could also lead to false-positive results and are therefore considered in criterion 4. Another possible source of false-positive hits in this setup are compounds that do inhibit growth without causing an elevated luminescence signal. These can lead to elevated calculated luciferase activity values due to the calculation $\text{luciferase activity} = \frac{\text{luminescence [RLU]}}{\text{cell density } (OD_{600})}$. Criterion 5 is meant to exclude this source of errors.

For the small-molecule library (16 384-well plates in parallel) it was not possible to perform two end-point measurements due to time pressure. Instead, the final luciferase activity was determined once after three hours of incubation. Selection criterion 2 was therefore not applied for the small-molecule library. Instead, criterion 1 was tightened:

1) luciferase activity 3 h after induction [RLU/OD] > $\emptyset_{neg}$ + 4.5 x σ_{neg} (here: ≙ 381 RLU/OD).

Applying the aforementioned selection criteria, eight primary hits were found; four in the FDA-approved drug library (encircled in orange in Figure 19 C) and four in the small-molecule library (Figure 20). The final hit rate was satisfactory (0.125%) and similar to hit rates in common high-throughput screenings for enzyme agonists (< 0.5%).[135]

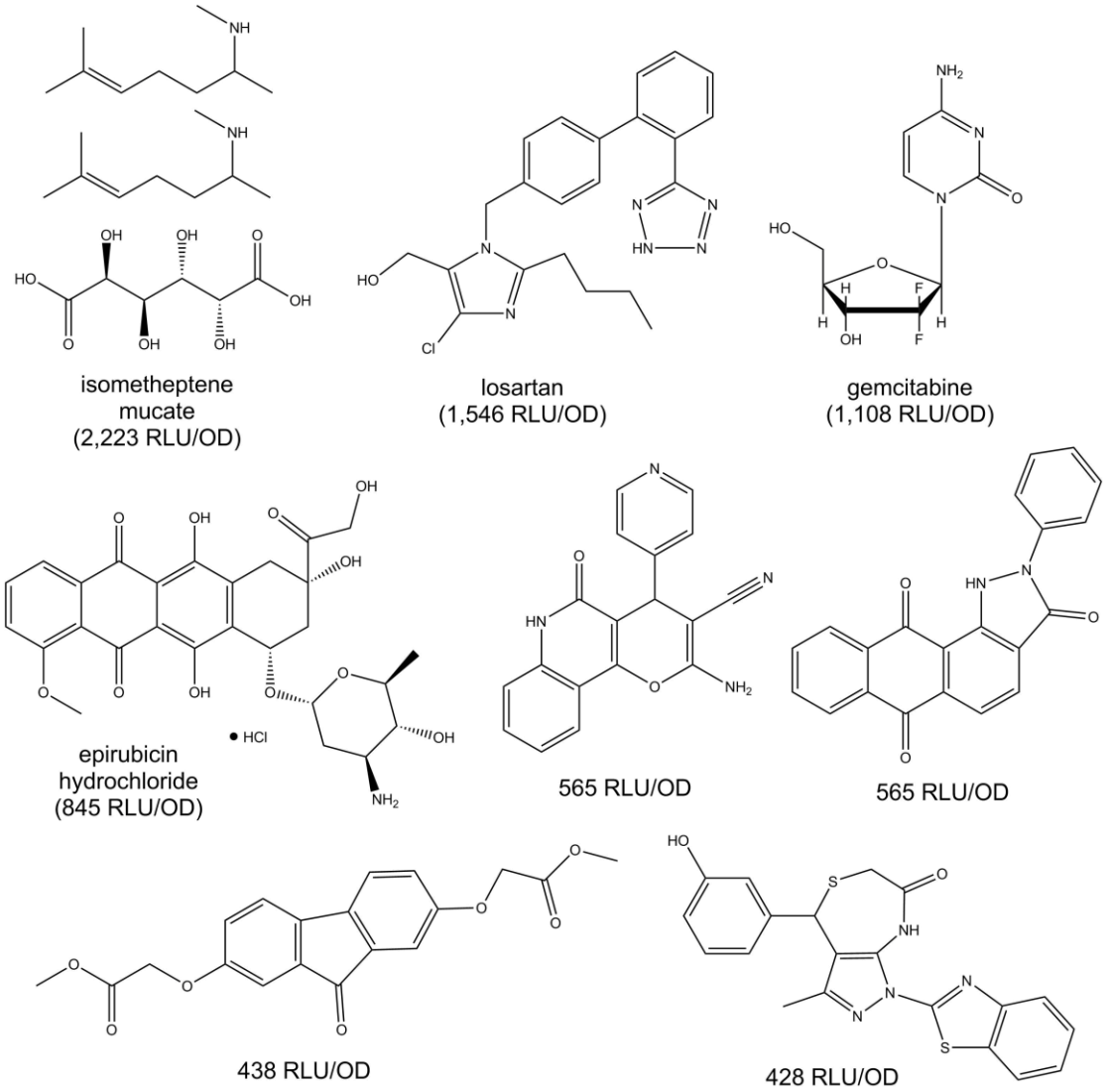

Figure 20: Primary hit compounds.

The chemical structures of the eight primary hit compounds and their corresponding luciferase activities after three hours of incubation are given. Only the names of the FDA-approved drugs are displayed.

4.2.4 Hit validation

The hit validation strategy starts with assaying primary hit compounds in time-course measurements using the screening strain *xpt* fl *lux* (primary assay). Different compound concentrations give information about a dose-dependency of the signal. Afterwards, the riboswitch-dependence of the signals is verified in counter assays. Finally, the signal independence on the reporter is confirmed with a secondary assay and its corresponding counter assays.

4.2.4.1 Primary assays

For hit validation, strain *xpt* fl *lux* was first treated with 5, 10 and 20 µM of the eight rebought primary hit compounds in time-course experiments (data not shown). Only one of the primary hits caused an elevated luciferase activity in the repetition experiment and was further investigated: the antitumor drug gemcitabine. The *xpt* fl *lux* strain displayed an increasing luciferase activity to about 12 x 10^3 RLU/OD 1 – 11 h after induction with 1 µM – 1 mM gemcitabine (Figure 21 A). When treated with lower gemcitabine concentrations, the corresponding luciferase activity stayed at a rather low level (0.1 µM; orange curve; ~900 RLU/OD) or decreased after three hours until a background level of < 10 RLU/OD was reached after 5.5 h (0.01 µM; brown curve). Higher gemcitabine concentrations did not display a dose-dependent signal. Compared to wild type W168 (Figure 21 B, black curve), the gemcitabine growth curves demonstrated growth defects even with the lowest gemcitabine concentration tested. 0.01 µM gemcitabine caused a three-hour growth delay while 100 and 1,000 µM gemcitabine prevented cell growth completely. Notably there seems to be a time correlation between cell growth and luciferase activity decrease.

A significant difference between the xylose- and the xylose and 10 µM gemcitabine-treated samples could be observed 3.3 h after induction (P = 0.0077; Figure 21 C), that became even larger 8.0 h after induction (Figure 21 D). These results prove that gemcitabine indeed causes an increased luciferase activity in the *xpt* fl *lux* strain. But is this observation riboswitch-driven or caused by off-target effects? To answer this question some control strains were tested.

As counter assays, the luciferase activities of the Δ RS SD_{xpt} *lux* and the wild type W168 upon 10 µM gemcitabine treatment were assayed (Figure 21 D). Both strains gave elevated luciferase signals 8 h after gemcitabine treatment (711 and 300 RLU/OD, respectively). However, these were significantly smaller than that observed from *xpt* fl *lux* (9,431 RLU/OD; P < 0.0001). These findings indicate that the signal increase upon addition of gemcitabine is indeed riboswitch-dependent.

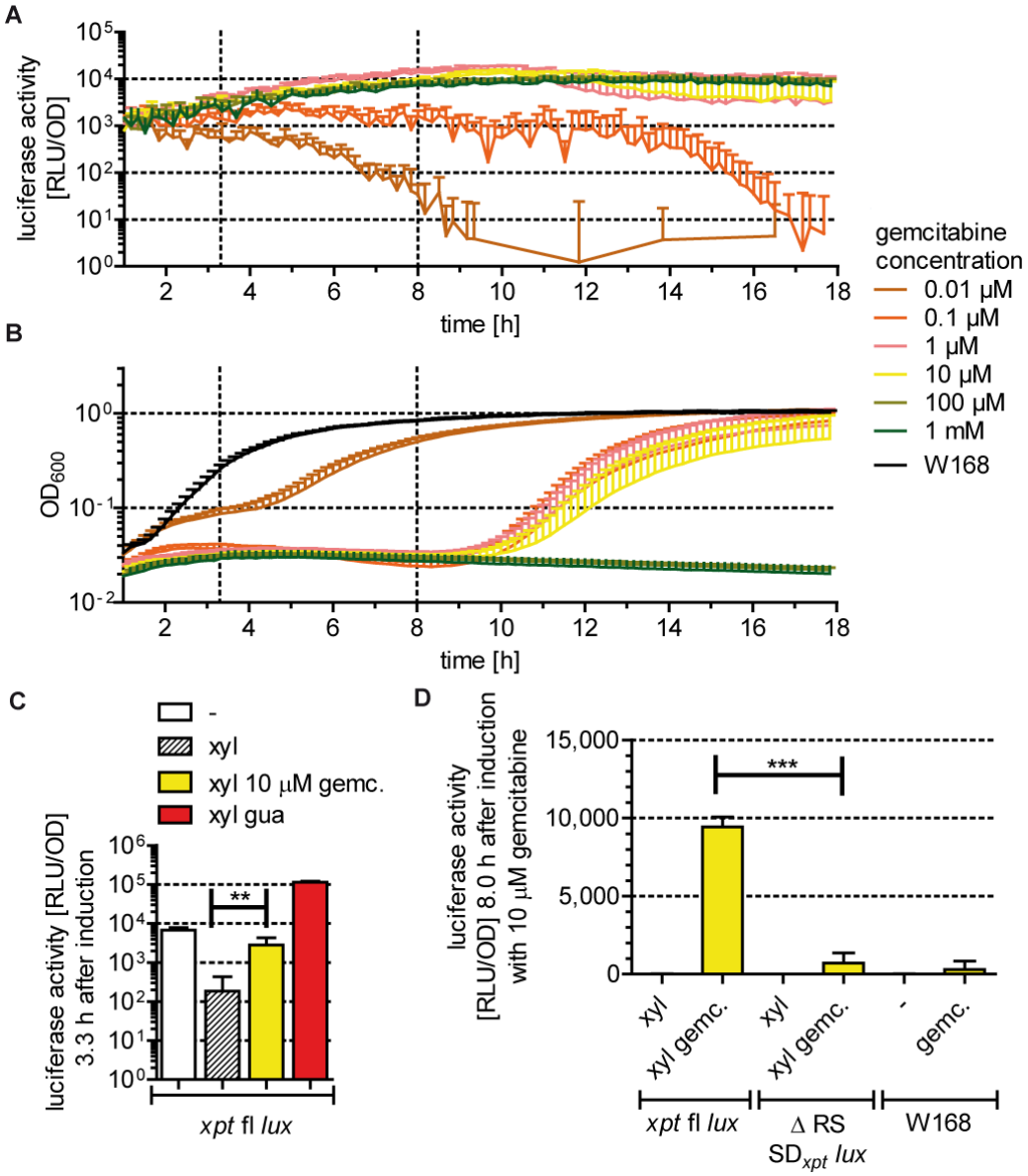

Figure 21: Hit validation using the primary assay.

(A) Luciferase activity of the *xpt* fl *lux* strain treated with gemcitabine (gemc.; 0.01 µM (brown), 0.1 µM (orange), 1 µM (light red), 10 µM (yellow), 100 µM (light green) or 1 mM (green)) 1 – 18 h after induction. 3.3 and 8 h are indicted by dotted lines.

(B) OD curves of the samples in A.

(C) *xpt* fl *lux* without treatment or treated with xylose (0.01%), xylose and 10 µM gemcitabine (gemc.; yellow) or xylose and guanosine (1 mM). The luciferase activity [RLU/OD] 3.3 h after induction is given on a logarithmic scale. Color code and abbreviations as in Figure 12.

(D) *xpt* fl *lux*, Δ RS SD_{xpt} *lux* and W168 treated with xylose or xylose and gemcitabine (10 µM). The luciferase activity [RLU/OD] 8.0 h after induction is given on a linear scale. Color code and abbreviations as in C.

Data points and error bars represent the means and standard deviations of at least three biological replicates. Important significant differences caused by gemcitabine treatment are marked by asterisks.

4.2.4.2 Secondary assays

β-galactosidase activity (Section 1.2.4.2) is orthogonal to bioluminescence and therefore well-suited to perform secondary reporter assays to verify the above-mentioned results in a different setup. For this reason, two more strains were constructed identically to *xpt* fl *lux* and the counter assay strain Δ RS SD_{xpt} *lux* but containing the *lacZ* reporter gene instead of the *luxABCDE* genes (BS44 (*xpt* fl *lacZ*) and BS140 (Δ RS SD_{xpt} *lacZ*)).

The secondary β-galactosidase assay was characterized by testing strains *xpt* fl *lacZ* and Δ RS SD_{xpt} *lacZ* with xylose or xylose and guanosine (Figure 22). Strain *xpt* fl *lacZ* displayed a low signal after xylose treatment which increased ~1,000-fold upon guanosine addition to the medium (SW = 8.61). As expected the corresponding counter assay with the riboswitch deletion strain (Δ RS SD_{xpt} *lacZ*) gave a similar xylose signal, but did not respond to guanosine addition.

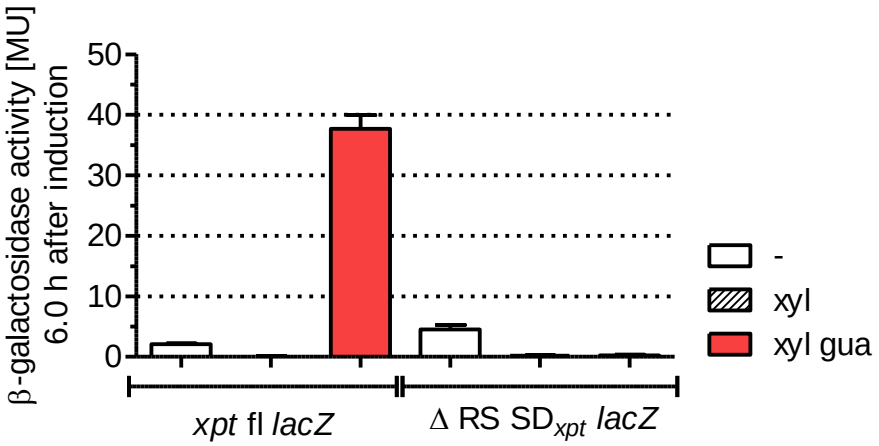

Figure 22: The secondary assay and its corresponding counter assay.
Strains *xpt* fl *lacZ* and Δ RS SD_{xpt} *lacZ* were tested without and with 0.01% xylose or with xylose and guanosine (1 mM). The β-galactosidase activity 6.0 h after induction is given on a linear scale. Data points and error bars represent the means and standard deviations of at least three biological replicates. Abbreviations and color code as in Figure 12.

After having verified the functionality of the secondary assay, the *xpt* fl *lacZ* strain was employed to test the β-galactosidase response upon 0.1 – 100 µM gemcitabine treatment (Figure 23 A). Interestingly, the signal decreased from 1 to 100 µM gemcitabine while the 0.1 µM gemcitabine sample displayed the lowest signal. As in the luciferase experiments, no dose-dependent response could be observed here.

The *lacZ* counter assays (Figure 23 B) with the wild type W168 and the Δ RS SD_{xpt} *lacZ* strain gave a similar picture as the corresponding bioluminescence assays. Again, both W168 and Δ RS SD_{xpt} *lacZ* displayed an elevated gemcitabine signal compared to the xylose- or non-treated samples. However, the *xpt* fl *lacZ* xylose gemcitabine signal was significantly higher (P = 0.02 for Δ RS SD_{xpt} *lacZ* and P = 0.0085 for W168).

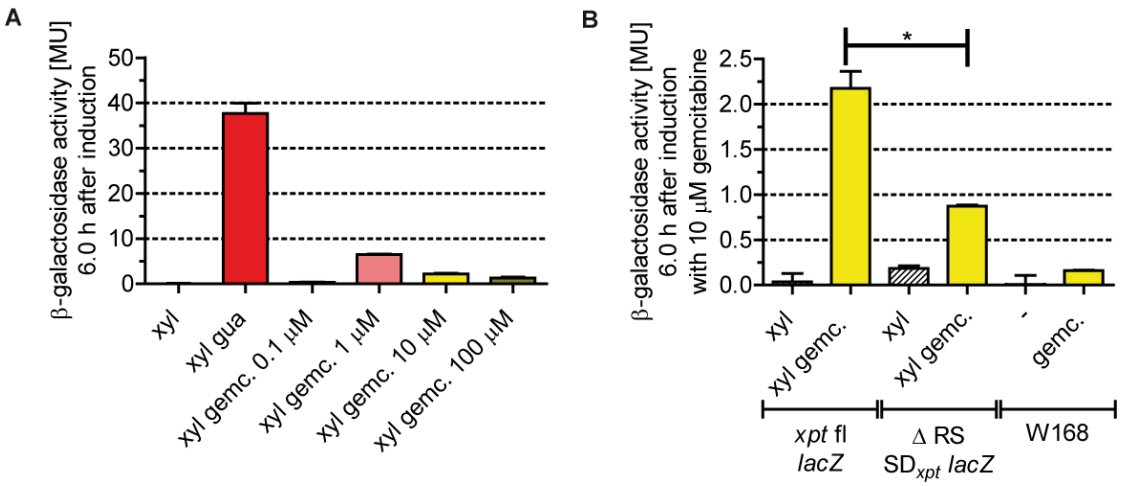

Figure 23: Hit validation with the secondary assay.

(A) Gemcitabine response of *xpt* fl *lacZ.* The β-galactosidase activities 6.0 h after induction with xylose, xylose and guanosine (red) or xylose and 0.1 – 100 µM gemcitabine (gemc.) are given on a linear scale.

(B) Counter assays: *xpt* fl *lacZ* and Δ RS SD_{xpt} *lacZ* treated with xylose (black striped bars) or xylose and gemcitabine (gemc.; yellow bars; 10 µM). W168 treated with (yellow) and without (white) gemcitabine. The β-galactosidase activity 6.0 h after induction is given on a linear scale. Important significant differences caused by gemcitabine treatment are marked by asterisks.

Data points and error bars represent the means and standard deviations of at least three biological replicates. Color code and abbreviations as in Figure 21.

Altogether, the results obtained from the *xpt* fl luciferase and β-galactosidase assays as well as the corresponding counter assays indicate that gemcitabine does cause an elevated riboswitch activity as the observed effect is largely riboswitch-dependent. The lacking dose-dependent behavior, however, suggests that the observed effects are not, or at least not solely, due to direct riboswitch binding but to indirect effects. To judge this alternative, the scientific knowledge about the hit compound gemcitabine should be summarized in the following.

4.2.4.3 The hit compound gemcitabine

In 1986, gemcitabine (2´,2´-difluorodeoxycytidine; Figure 24) was discovered as an antiviral drug.[209] Some years later, it was also shown to be a chemotherapeutic agent against pancreatic cancer, non-small-cell lung cancer and other types of cancer (see [210] for a review). It is administered through intravenous infusions.[211]

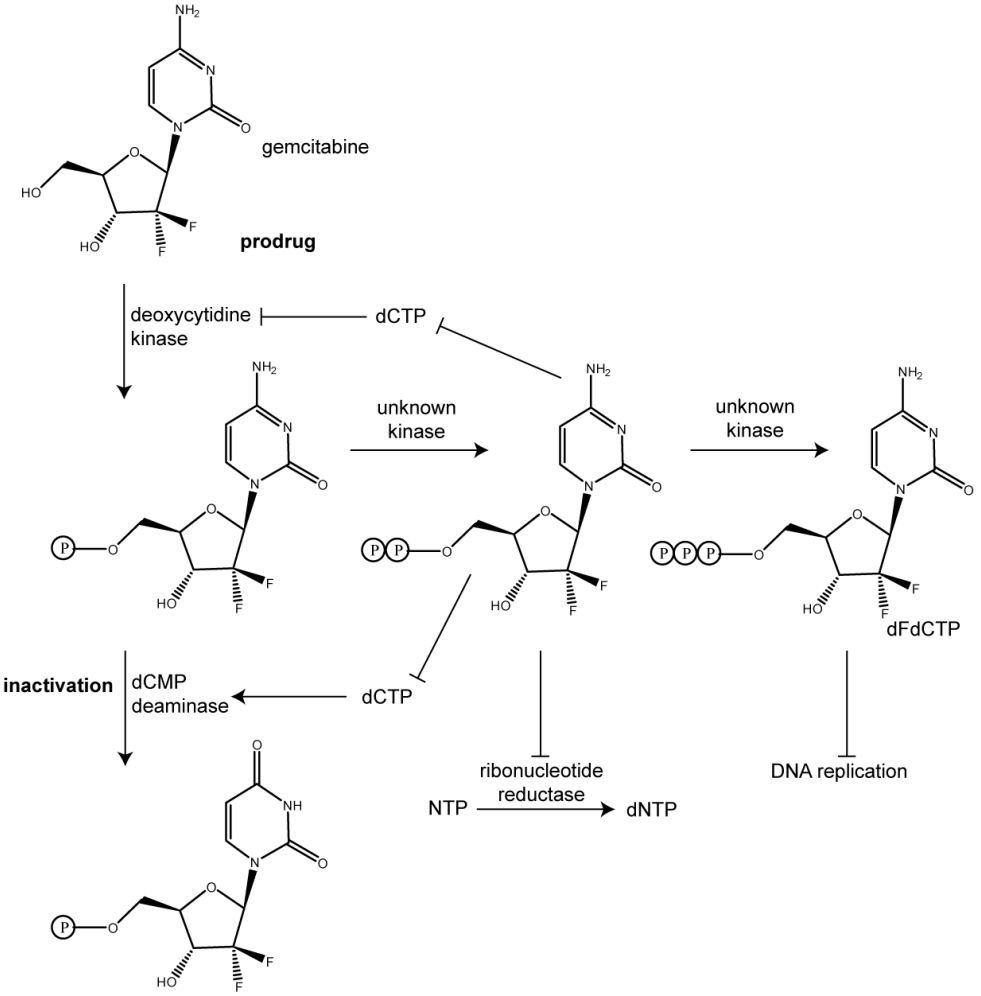

Figure 24: Metabolic products of gemcitabine.

The prodrug gemcitabine is phosphorylated and activated by the deoxycytidine kinase and so far unknown kinases. Gemcitabine diphosphate acts as a ribonucleotide reductase inhibitor and hinders the degradation of gemcitabine monophosphate by inhibiting the dCMP (deoxycytidine monophosphate) deaminase. Gemcitabine triphosphate, in turn, inhibits DNA replication.

Gemcitabine is a prodrug that needs to be activated by a deoxycytidine kinase (Figure 24).[212] During DNA synthesis, gemcitabine triphosphate is incorporated into the DNA, which leads to a replication pause one nucleotide after gemcitabine incorporation.[213] In addition, gemcitabine diphosphate inhibits the ribonucleotide

reductase and thereby prevents *de novo* dNTP (deoxynucleoside triphosphate) synthesis.[214] As the deoxycytidine kinase is inhibited by dCTP (deoxycytidine triphosphate),[215, 216] gemcitabine promotes its own activation by downregulating the dCTP concentration. At the same time, low dCTP concentrations reduce dCMP deaminase activity[217] and thereby hinder gemcitabine inactivation.[218]

The ribonucleotide reductase connects gemcitabine effects to the intracellular pool of DNA building blocks; for example 1 µM gemcitabine increases GTP pools in an ovary cancer cell line up to twofold.[219] Therefore, it is likely that the riboswitch-dependent enhanced reporter activity caused by gemcitabine might be due to indirect effects, leading for example to elevated intracellular guanine concentrations, rather than due to a direct binding of gemcitabine to the *B. anthracis xpt* riboswitch. This assumption is supported by the fact that most synthetic riboswitch ligands are mimics of the natural ligand. The cytidine analogue gemcitabine, however, is larger and structurally different from guanine.

Although presumably no *B. anthracis xpt* riboswitch-binding compound could be found in the screening evolved here, the identification of gemcitabine demonstrates that the reverse reporter system works in screenings for riboswitch ligands. In addition, the follow-up controls are able to distinguish riboswitch-dependent effects from off-target effects and to analyze the dose-dependent behavior of the primary hit compounds.

5 Conclusion and Outlook

In this work, a reverse *in vivo* reporter system was evolved to investigate transcriptional OFF riboswitches. Indeed the system responds to riboswitch ligand binding with a positive output and displays high differences between samples supplemented with and without ligand. Using this system, six proposed guanine riboswitches from *B. anthracis* were closely examined. While the regulatory mechanism of one of them is still unclear, five putative *B. anthracis* riboswitches could be identified as transcriptional OFF riboswitches. Their mode of action was verified by *in vivo* measurements and it was found that the riboswitches varied in their ligand specificities and ligand responses—in strength as well as in their gradual responses to different ligand concentrations. It could also be demonstrated that the *B. subtilis xpt* riboswitch-binding compound PC2 was not able to activate the *B. anthracis* riboswitches *in vivo*. Direct riboswitch-guanine binding could be affirmed by *in vitro* studies that also point out differences in ligand binding affinities.

In the future, the structures and dynamics of the *B. anthracis* guanine riboswitches could be determined to identify the reason for their differing *in vivo* and *in vitro* behaviors. It would also be interesting to unravel the folding pathways of the *B. anthracis* riboswitches and to find out if their ligand response is thermodynamically or kinetically governed. These data could be obtained using FRET (fluorescence resonance energy transfer) analysis, optical tweezers or high-resolution NMR (nuclear magnetic resonance). Further *in vitro* studies can help to investigate the binding of the antibacterial compound PC1 to the *B. anthracis* riboswitches, which could not be studied here *in vivo*. Other future tasks are, for example, to study the strengths of the native riboswitch promoters *in vivo* using reporter gene setups and to verify the function of the riboswitch-controlled metabolic genes experimentally. To identify the purpose and mode of action of the sixth putative *B. anthracis* guanine riboswitch will also be a future challenge.

The five riboswitches investigated here can be used as targets for antibacterial compounds. Furthermore, they can be utilized as inducible tools to regulate gene expression in the context of synthetic biology and for basic research in the gram-positive model organism *B. subtilis*.

In this work, the reverse *in vivo* reporter gene system has been optimized for a high-throughput mode and a screening of 6,400 compounds was conducted. The identification and verification of the compound gemcitabine have proven that it is possible to find molecules that modulate riboswitch activity with the setup established here. Nevertheless, the lacking dose-dependent behavior and the mode of action of the anticancer drug gemcitabine suggest indirect effects rather than direct binding of gemcitabine to the riboswitch. This assumption should be supported by *in vitro* experiments as in-line probing or gel-shift assays in the future.

Theoretically, any transcriptional OFF riboswitch can be used in future screenings instead of the chosen target. After performing the *in vivo* control experiments explained here, promising hit candidates should be tested with *in vitro* assays as in-line probing to prove direct compound-riboswitch binding. If this is the case, the exact binding mode of the new ligand could be determined, for example by structure determination. Using a pre-investigated translational OFF riboswitch it can also be attempted to adapt the system to another kind of regulation mechanism.

6 Acknowledgement

I want to thank…

…Dr. Sabine Schneider for giving me the opportunity to work with my favorite microorganism *Bacillus subtilis*, for her ideas for my project and for the freedom to realize my ideas in this project.

…Prof. Dr. Michael Groll for his interest in my work and many good suggestions. I am very grateful for having been part of his group and for having been allowed to use all his facilities.

…the GRK2062 not only for financial support but also for many greatly organized events, good feedback and for the chance to be part of such a nice interdisciplinary and international group of young researchers. Especially I want to thank Prof. Dr. Kirsten Jung and Dr. Beate Hafner for their constant support and for their many perfectly realized ideas for events, workshops and conferences. I also want to thank my TAC advisors Prof. Dr. Thomas Carell and Prof. Dr. Anja Hoffmann-Röder.

…Dr. Kenji Schorpp, Dr. Kamyar Hadian and Dr. Jan Vomacka for pleasant cooperation projects. They opened my eyes for very interesting research areas.

…the TUM and its graduate school for financial support and very interesting workshops.

I also want to thank…

…my colleagues and lab mates Vroni, Sabrina, Christine, Christopher and Leo. Thanks for the great time I had with you, for a nice atmosphere in the lab and for many fruitful talks and discussions!

…the whole Groll group for their support, many great seminars, PhD parties, lunches and talks. I especially want to acknowledge Astrid, Ute, Felix, Andrea, Chris, Philipp, Haissi, Eva, Marie-Theres, Bastian, Wolfgang and Katrin.

…the junior researchers and post-docs of the GRK2062 for interesting discussions, many great ideas regarding my project and for being such a positive-thinking and open-minded group!

…our HiWis Simon, Jenny, Yuliya and our technician Uschi. Thank you for helping me a lot!

…my excellent students Christopher, Michael and Sonja. I very much enjoyed the time you joined me in the lab.

…Matthias Stahl for introducing me to tecan readers.

…Thorsten Mascher and his group; especially Jara, Julia, Caro and Karen for teaching me how to work with *Bacillus subtilis*.

…Jonathan for his never-ending support and love.

This work would not have been possible without the steady love and support from my parents, my brother and my grandmother.

7 References

1. Crick F. Central dogma of molecular biology. Nature 1970; 227:561-3.
2. Tomizawa J, Itoh T*, et al.* Inhibition of ColE1 RNA primer formation by a plasmid-specified small RNA. Proc Natl Acad Sci USA 1981; 78:1421-5.
3. Conrad SE, Campbell JL. Role of plasmid-coded RNA and ribonuclease III in plasmid DNA replication. Cell 1979; 18:61-71.
4. Lee RC, Feinbaum RL*, et al.* The *C. elegans* heterochronic gene *lin-4* encodes small RNAs with antisense complementarity to *lin-14*. Cell 1993; 75:843-54.
5. Waters LS, Storz G. Regulatory RNAs in bacteria. Cell 2009; 136:615-28.
6. Nahvi A, Sudarsan N*, et al.* Genetic control by a metabolite binding mRNA. Chem Biol 2002; 9:1043.
7. Dambach MD, Winkler WC. Expanding roles for metabolite-sensing regulatory RNAs. Curr Opin Microbiol 2009; 12:161-9.
8. Sherwood AV, Henkin TM. Riboswitch-mediated gene regulation: novel RNA architectures dictate gene expression responses. Annu Rev Microbiol 2016; 70:361-74.
9. Winkler WC, Breaker RR. Genetic control by metabolite-binding riboswitches. Chembiochem 2003; 4:1024-32.
10. Mandal M, Boese B*, et al.* Riboswitches control fundamental biochemical pathways in *Bacillus subtilis* and other bacteria. Cell 2003; 113:577-86.
11. Serganov A, Yuan YR*, et al.* Structural basis for discriminative regulation of gene expression by adenine- and guanine-sensing mRNAs. Chem Biol 2004; 11:1729-41.
12. Batey RT, Gilbert SD*, et al.* Structure of a natural guanine-responsive riboswitch complexed with the metabolite hypoxanthine. Nature 2004; 432:411-5.
13. Baker JL, Sudarsan N*, et al.* Widespread genetic switches and toxicity resistance proteins for fluoride. Science 2012; 335:233-5.
14. Winkler WC, Nahvi A*, et al.* An mRNA structure that controls gene expression by binding *S*-adenosylmethionine. Nat Struct Biol 2003; 10:701-7.
15. Mironov AS, Gusarov I*, et al.* Sensing small molecules by nascent RNA: a mechanism to control transcription in bacteria. Cell 2002; 111:747-56.
16. Winkler W, Nahvi A*, et al.* Thiamine derivatives bind messenger RNAs directly to regulate bacterial gene expression. Nature 2002; 419:952-6.
17. Breaker RR. Prospects for riboswitch discovery and analysis. Mol Cell 2011; 43:867-79.
18. Davis JH, Dunican BF*, et al. glmS* riboswitch binding to the glucosamine-6-phosphate alpha-anomer shifts the pK_a toward neutrality. Biochemistry 2011; 50:7236-42.
19. Xin Y, Hamelberg D. Deciphering the role of glucosamine-6-phosphate in the riboswitch action of *glmS* ribozyme. RNA 2010; 16:2455-63.
20. Welz R, Breaker RR. Ligand binding and gene control characteristics of tandem riboswitches in *Bacillus anthracis*. RNA 2007; 13:573-82.
21. Barrick JE, Breaker RR. The distributions, mechanisms, and structures of metabolite-binding riboswitches. Genome Biol 2007; 8:R239.
22. Winkler WC, Nahvi A*, et al.* Control of gene expression by a natural metabolite-responsive ribozyme. Nature 2004; 428:281-6.
23. Caron MP, Bastet L*, et al.* Dual-acting riboswitch control of translation initiation and mRNA decay. Proc Natl Acad Sci USA 2012; 109:E3444-53.
24. Rodionov DA, Vitreschak AG*, et al.* Comparative genomics of the methionine metabolism in gram-positive bacteria: a variety of regulatory systems. Nucleic Acids Res 2004; 32:3340-53.
25. Cheah MT, Wachter A*, et al.* Control of alternative RNA splicing and gene expression by eukaryotic riboswitches. Nature 2007; 447:497-500.
26. Wachter A, Tunc-Ozdemir M*, et al.* Riboswitch control of gene expression in plants by splicing and alternative 3' end processing of mRNAs. Plant Cell 2007; 19:3437-50.
27. Bocobza S, Adato A*, et al.* Riboswitch-dependent gene regulation and its evolution in the plant kingdom. Genes Dev 2007; 21:2874-9.
28. Croft MT, Moulin M*, et al.* Thiamine biosynthesis in algae is regulated by riboswitches. Proc Natl Acad Sci USA 2007; 104:20770-5.

29. Mandal M, Lee M*, et al.* A glycine-dependent riboswitch that uses cooperative binding to control gene expression. Science 2004; 306:275-9.
30. Vitreschak AG, Rodionov DA*, et al.* Riboswitches: the oldest mechanism for the regulation of gene expression? Trends Genet 2004; 20:44-50.
31. Barrick JE, Corbino KA*, et al.* New RNA motifs suggest an expanded scope for riboswitches in bacterial genetic control. Proc Natl Acad Sci USA 2004; 101:6421-6.
32. Rieder R, Lang K*, et al.* Ligand-induced folding of the adenosine deaminase A-riboswitch and implications on riboswitch translational control. Chembiochem 2007; 8:896-902.
33. Wickiser JK, Winkler WC*, et al.* The speed of RNA transcription and metabolite binding kinetics operate an FMN riboswitch. Mol Cell 2005; 18:49-60.
34. Wickiser JK, Cheah MT*, et al.* The kinetics of ligand binding by an adenine-sensing riboswitch. Biochemistry 2005; 44:13404-14.
35. Kim JN, Roth A*, et al.* Guanine riboswitch variants from *Mesoplasma florum* selectively recognize 2'-deoxyguanosine. Proc Natl Acad Sci USA 2007; 104:16092-7.
36. Kim YB, Wacker A*, et al.* Ligand binding to 2'-deoxyguanosine sensing riboswitch in metabolic context. Nucleic Acids Res 2017.
37. Christiansen LC, Schou S*, et al.* Xanthine metabolism in *Bacillus subtilis*: characterization of the *xpt-pbuX* operon and evidence for purine- and nitrogen-controlled expression of genes involved in xanthine salvage and catabolism. J Bacteriol 1997; 179:2540-50.
38. Mulhbacher J, Brouillette E*, et al.* Novel riboswitch ligand analogs as selective inhibitors of guanine-related metabolic pathways. PLoS Pathog 2010; 6:e1000865.
39. Gilbert SD, Mediatore SJ*, et al.* Modified pyrimidines specifically bind the purine riboswitch. J Am Chem Soc 2006; 128:14214-5.
40. Mandal M, Breaker RR. Adenine riboswitches and gene activation by disruption of a transcription terminator. Nat Struct Mol Biol 2004; 11:29-35.
41. Ottink OM, Rampersad SM*, et al.* Ligand-induced folding of the guanine-sensing riboswitch is controlled by a combined predetermined induced fit mechanism. RNA 2007; 13:2202-12.
42. Gilbert SD, Stoddard CD*, et al.* Thermodynamic and kinetic characterization of ligand binding to the purine riboswitch aptamer domain. J Mol Biol 2006; 359:754-68.
43. Noeske J, Buck J*, et al.* Interplay of 'induced fit' and preorganization in the ligand induced folding of the aptamer domain of the guanine binding riboswitch. Nucleic Acids Res 2007; 35:572-83.
44. Chandra V, Hannan Z*, et al.* Single-molecule analysis reveals multi-state folding of a guanine riboswitch. Nat Chem Biol 2017; 13:194-201.
45. Brenner MD, Scanlan MS*, et al.* Multivector fluorescence analysis of the *xpt* guanine riboswitch aptamer domain and the conformational role of guanine. Biochemistry 2010; 49:1596-605.
46. Steinert H, Sochor F*, et al.* Pausing guides RNA folding to populate transiently stable RNA structures for riboswitch-based transcription regulation. Elife 2017; 6.
47. Singh P, Sengupta S. Phylogenetic analysis and comparative genomics of purine riboswitch distribution in prokaryotes. Evol Bioinform Online 2012; 8:589-609.
48. Ivánovics G, Marjai E*, et al.* The growth of purine mutants of *Bacillus anthracis* in the body of the mouse. J Gen Microbiol 1968; 53:147-62.
49. Jenkins A, Cote C*, et al.* Role of purine biosynthesis in *Bacillus anthracis* pathogenesis and virulence. Infect Immun 2011; 79:153-66.
50. Samant S, Lee H*, et al.* Nucleotide biosynthesis is critical for growth of bacteria in human blood. PLoS Pathog 2008; 4:e37.
51. Mei JM, Nourbakhsh F*, et al.* Identification of *Staphylococcus aureus* virulence genes in a murine model of bacteraemia using signature-tagged mutagenesis. Mol Microbiol 1997; 26:399-407.
52. Brubaker RR. Interconversion of purine mononucleotides in *Pasteurella pestis*. Infect Immun 1970; 1:446-54.
53. Kofoed EM, Yan D*, et al. De novo* guanine biosynthesis but not the riboswitch-regulated purine salvage pathway is required for *Staphylococcus aureus* infection *in vivo*. J Bacteriol 2016; 198:2001-15.

54. Kobayashi K, Ehrlich SD*, et al.* Essential *Bacillus subtilis* genes. Proc Natl Acad Sci USA 2003; 100:4678-83.
55. Kappock TJ, Ealick SE*, et al.* Modular evolution of the purine biosynthetic pathway. Curr Opin Chem Biol 2000; 4:567-72.
56. Zalkin H. *De novo* purine nucleotide synthesis. In: Sonenshein AL, Hoch JA*, et al.*, eds. *Bacillus subtilis* and other gram-positive bacteria: biochemistry, physiology, and molecular genetics. Washington: American Society for Microbiology, 1993.
57. Nygaard P. Purine and pyrimidine salvage pathways. In: Sonenshein AL, Hoch JA*, et al.*, eds. *Bacillus subtilis* and other gram-positive bacteria: biochemistry, physiology, and molecular genetics. Washington: American Society for Microbiology, 1993.
58. Ebbole DJ, Zalkin H. Cloning and characterization of a 12-gene cluster from *Bacillus subtilis* encoding nine enzymes for *de novo* purine nucleotide synthesis. J Biol Chem 1987; 262:8274-87.
59. Saxild HH, Brunstedt K*, et al.* Definition of the *Bacillus subtilis* PurR operator using genetic and bioinformatic tools and expansion of the PurR regulon with *glyA*, *guaC*, *pbuG*, *xpt-pbuX*, *yqhZ-folD*, and *pbuO*. J Bacteriol 2001; 183:6175-83.
60. Mäntsälä P, Zalkin H. Cloning and sequence of *Bacillus subtilis purA* and *guaA*, involved in the conversion of IMP to AMP and GMP. J Bacteriol 1992; 174:1883-90.
61. Endo T, Uratani B*, et al.* Purine salvage pathways of *Bacillus subtilis* and effect of guanine on growth of GMP reductase mutants. J Bacteriol 1983; 155:169-79.
62. Kanzaki N, Miyagawa K. Nucleotide sequence of the *Bacillus subtilis* IMP dehydrogenase gene. Nucleic Acids Res 1990; 18:6710.
63. Schuch R, Garibian A*, et al.* Nucleosides as a carbon source in *Bacillus subtilis*: characterization of the *drm-pupG* operon. Microbiology 1999; 145:2957-66.
64. Saxild HH, Andersen LN*, et al. Dra-nupC-pdp* operon of *Bacillus subtilis*: nucleotide sequence, induction by deoxyribonucleosides, and transcriptional regulation by the *deoR*-encoded DeoR repressor protein. J Bacteriol 1996; 178:424-34.
65. Belitsky BR, Sonenshein AL. CodY-mediated regulation of guanosine uptake in *Bacillus subtilis*. J Bacteriol 2011; 193:6276-87.
66. Johansen LE, Nygaard P*, et al.* Definition of a second *Bacillus subtilis pur* regulon comprising the *pur* and *xpt-pbuX* operons plus *pbuG*, *nupG* (*yxjA*), and *pbuE* (*ydhL*). J Bacteriol 2003; 185:5200-9.
67. Zhu H, Yang SM*, et al.* Metabolic and genetic factors affecting the productivity of pyrimidine nucleoside in *Bacillus subtilis*. Microb Cell Fact 2015; 14:54.
68. Saxild HH, Nygaard P. Genetic and physiological characterization of *Bacillus subtilis* mutants resistant to purine analogs. J Bacteriol 1987; 169:2977-83.
69. Schultz AC, Nygaard P*, et al.* Functional analysis of 14 genes that constitute the purine catabolic pathway in *Bacillus subtilis* and evidence for a novel regulon controlled by the PucR transcription activator. J Bacteriol 2001; 183:3293-302.
70. Stülke J, Hillen W. Regulation of carbon catabolism in *Bacillus* species. Annu Rev Microbiol 2000; 54:849-80.
71. Vogels GD, Van der Drift C. Degradation of purines and pyrimidines by microorganisms. Bacteriol Rev 1976; 40:403-68.
72. Weng M, Nagy PL*, et al.* Identification of the *Bacillus subtilis pur* operon repressor. Proc Natl Acad Sci USA 1995; 92:7455-9.
73. Saxild HH, Nygaard P. Regulation of levels of purine biosynthetic enzymes in *Bacillus subtilis*: effects of changing purine nucleotide pools. J Gen Microbiol 1991; 137:2387-94.
74. Mock M, Fouet A. Anthrax. Annu Rev Microbiol 2001; 55:647-71.
75. Ashford D, Beyer W*, et al.* Anthrax in humans and animals. In: Turnbull P, ed.: World Health Organization, 2008.
76. Uchida I, Hashimoto K*, et al.* Virulence and immunogenicity in experimental animals of *Bacillus anthracis* strains harbouring or lacking 110 MDa and 60 MDa plasmids. J Gen Microbiol 1986; 132:557-9.
77. Welkos SL. Plasmid-associated virulence factors of non-toxigenic (pX01-) *Bacillus anthracis*. Microb Pathog 1991; 10:183-98.
78. Driks A. The *Bacillus anthracis* spore. Mol Aspects Med 2009; 30:368-73.
79. Klietmann WF, Ruoff KL. Bioterrorism: implications for the clinical microbiologist. Clin Microbiol Rev 2001; 14:364-81.

80. Ross J. The pathogenesis of anthrax following the administration of spores by the respiratory route. J Pathol Bact 1957; 73:485–94.
81. Scobie HM, Rainey GJ*, et al.* Human capillary morphogenesis protein 2 functions as an anthrax toxin receptor. Proc Natl Acad Sci USA 2003; 100:5170-4.
82. Bradley KA, Mogridge J*, et al.* Identification of the cellular receptor for anthrax toxin. Nature 2001; 414:225-9.
83. Leppla SH, Friedlander AM*, et al.* Proteolytic activation of anthrax toxin bound to cellular receptors. In: Fehrenbach F, Alouf JE*, et al.*, eds. Bacterial protein toxins New York: Gustav Fischer Verlag, 1988:111-2.
84. Klimpel KR, Molloy SS*, et al.* Anthrax toxin protective antigen is activated by a cell surface protease with the sequence specificity and catalytic properties of furin. Proc Natl Acad Sci USA 1992; 89:10277-81.
85. Milne JC, Furlong D*, et al.* Anthrax protective antigen forms oligomers during intoxication of mammalian cells. J Biol Chem 1994; 269:20607-12.
86. Kintzer AF, Thoren KL*, et al.* The protective antigen component of anthrax toxin forms functional octameric complexes. J Mol Biol 2009; 392:614-29.
87. Mogridge J, Cunningham K*, et al.* The lethal and edema factors of anthrax toxin bind only to oligomeric forms of the protective antigen. Proc Natl Acad Sci USA 2002; 99:7045-8.
88. Abrami L, Bischofberger M*, et al.* Endocytosis of the anthrax toxin is mediated by clathrin, actin and unconventional adaptors. PLoS Pathog 2010; 6:e1000792.
89. Miller CJ, Elliott JL*, et al.* Anthrax protective antigen: prepore-to-pore conversion. Biochemistry 1999; 38:10432-41.
90. Abrami L, Lindsay M*, et al.* Membrane insertion of anthrax protective antigen and cytoplasmic delivery of lethal factor occur at different stages of the endocytic pathway. J Cell Biol 2004; 166:645-51.
91. Leppla SH. Anthrax toxin edema factor: a bacterial adenylate cyclase that increases cyclic AMP concentrations of eukaryotic cells. Proc Natl Acad Sci USA 1982; 79:3162-6.
92. Duesbery NS, Webb CP*, et al.* Proteolytic inactivation of MAP-kinase-kinase by anthrax lethal factor. Science 1998; 280:734-7.
93. Tournier JN, Quesnel-Hellmann A*, et al.* Anthrax edema toxin cooperates with lethal toxin to impair cytokine secretion during infection of dendritic cells. J Immunol 2005; 174:4934-41.
94. Park JM, Greten FR*, et al.* Macrophage apoptosis by anthrax lethal factor through p38 MAP kinase inhibition. Science 2002; 297:2048-51.
95. Zhang Y, Morar M*, et al.* Structural biology of the purine biosynthetic pathway. Cell Mol Life Sci 2008; 65:3699-724.
96. Read TD, Peterson SN*, et al.* The genome sequence of *Bacillus anthracis* Ames and comparison to closely related bacteria. Nature 2003; 423:81-6.
97. Blount KF, Breaker RR. Riboswitches as antibacterial drug targets. Nat Biotechnol 2006; 24:1558-64.
98. Ebbole DJ, Zalkin H. *Bacillus subtilis pur* operon expression and regulation. J Bacteriol 1989; 171:2136-41.
99. Price MN, Alm EJ*, et al.* Interruptions in gene expression drive highly expressed operons to the leading strand of DNA replication. Nucleic Acids Res 2005; 33:3224-34.
100. Price MN, Huang KH*, et al.* A novel method for accurate operon predictions in all sequenced prokaryotes. Nucleic Acids Res 2005; 33:880-92.
101. Kim A, Wolf NM*, et al.* Identification of *Bacillus anthracis* PurE inhibitors with antimicrobial activity. Bioorg Med Chem 2015; 23:1492-9.
102. Ames TD, Breaker RR. Bacterial riboswitch discovery and analysis. In: Mayer G, ed. The chemical biology of nucleic acids: John Wiley & Sons, Ltd, 2010:433-54.
103. Xu D, Evans KO*, et al.* Melting and premelting transitions of an oligomer measured by DNA base fluorescence and absorption. Biochemistry 1994; 33:9592-9.
104. Jean JM, Hall KB. 2-Aminopurine fluorescence quenching and lifetimes: role of base stacking. Proc Natl Acad Sci USA 2001; 98:37-41.
105. Lemay JF, Penedo JC*, et al.* Folding of the adenine riboswitch. Chem Biol 2006; 13:857-68.
106. Mulhbacher J, Lafontaine DA. Ligand recognition determinants of guanine riboswitches. Nucleic Acids Res 2007; 35:5568-80.

107. Soukup GA, Breaker RR. Relationship between internucleotide linkage geometry and the stability of RNA. RNA 1999; 5:1308-25.
108. Soukup GA, DeRose EC*, et al.* Generating new ligand-binding RNAs by affinity maturation and disintegration of allosteric ribozymes. RNA 2001; 7:524-36.
109. Merino EJ, Wilkinson KA*, et al.* RNA structure analysis at single nucleotide resolution by selective 2'-hydroxyl acylation and primer extension (SHAPE). J Am Chem Soc 2005; 127:4223-31.
110. Smith KD, Lipchock SV*, et al.* Structural basis of ligand binding by a c-di-GMP riboswitch. Nat Struct Mol Biol 2009; 16:1218-23.
111. Gusarov I, Nudler E. The mechanism of intrinsic transcription termination. Mol Cell 1999; 3:495-504.
112. Paige JS, Wu KY*, et al.* RNA mimics of green fluorescent protein. Science 2011; 333:642-6.
113. Kellenberger CA, Hammond MC. *In vitro* analysis of riboswitch-spinach aptamer fusions as metabolite-sensing fluorescent biosensors. Methods Enzymol 2015; 550:147-72.
114. Paige JS, Nguyen-Duc T*, et al.* Fluorescence imaging of cellular metabolites with RNA. Science 2012; 335:1194.
115. Fowler CC, Brown ED*, et al.* Using a riboswitch sensor to examine coenzyme B_{12} metabolism and transport in *E. coli*. Chem Biol 2010; 17:756-65.
116. Chen YY, Jensen MC*, et al.* Genetic control of mammalian T-cell proliferation with synthetic RNA regulatory systems. Proc Natl Acad Sci USA 2010; 107:8531-6.
117. Fowler CC, Brown ED*, et al.* A FACS-based approach to engineering artificial riboswitches. Chembiochem 2008; 9:1906-11.
118. Dixon N, Duncan JN*, et al.* Reengineering orthogonally selective riboswitches. Proc Natl Acad Sci USA 2010; 107:2830-5.
119. Ellington AD, Szostak JW. *In vitro* selection of RNA molecules that bind specific ligands. Nature 1990; 346:818-22.
120. Tuerk C, Gold L. Systematic evolution of ligands by exponential enrichment: RNA ligands to bacteriophage T4 DNA polymerase. Science 1990; 249:505-10.
121. Jenison RD, Gill SC*, et al.* High-resolution molecular discrimination by RNA. Science 1994; 263:1425-9.
122. Lynch SA, Desai SK*, et al.* A high-throughput screen for synthetic riboswitches reveals mechanistic insights into their function. Chem Biol 2007; 14:173-84.
123. Brodersen DE, Clemons WM, Jr.*, et al.* The structural basis for the action of the antibiotics tetracycline, pactamycin, and hygromycin B on the 30S ribosomal subunit. Cell 2000; 103:1143-54.
124. Azad RF, Brown-Driver V*, et al.* Antiviral activity of a phosphorothioate oligonucleotide complementary to human cytomegalovirus RNA when used in combination with antiviral nucleoside analogs. Antiviral Res 1995; 28:101-11.
125. Thomas JR, Hergenrother PJ. Targeting RNA with small molecules. Chem Rev 2008; 108:1171-224.
126. Kondo J, Westhof E. Base pairs and pseudo pairs observed in RNA-ligand complexes. J Mol Recognit 2010; 23:241-52.
127. Serganov A, Polonskaia A*, et al.* Structural basis for gene regulation by a thiamine pyrophosphate-sensing riboswitch. Nature 2006; 441:1167-71.
128. Daldrop P, Reyes FE*, et al.* Novel ligands for a purine riboswitch discovered by RNA-ligand docking. Chem Biol 2011; 18:324-35.
129. Kim JN, Blount KF*, et al.* Design and antimicrobial action of purine analogues that bind guanine riboswitches. ACS Chem Biol 2009; 4:915-27.
130. Blount K, Puskarz I*, et al.* Development and application of a high-throughput assay for *glmS* riboswitch activators. RNA Biol 2006; 3:77-81.
131. Howe JA, Wang H*, et al.* Selective small-molecule inhibition of an RNA structural element. Nature 2015; 526:672-7.
132. Mayer G, Famulok M. High-throughput-compatible assay for *glmS* riboswitch metabolite dependence. Chembiochem 2006; 7:602-4.
133. Nelson JW, Plummer MS*, et al.* Small molecule fluoride toxicity agonists. Chem Biol 2015; 22:527-34.

134. Lünse CE, Mayer G. Reporter gene-based screening for TPP riboswitch activators. Methods Mol Biol 2017; 1520:227-35.
135. Hughes JP, Rees S*, et al.* Principles of early drug discovery. Br J Pharmacol 2011; 162:1239-49.
136. Blount KF, Wang JX*, et al.* Antibacterial lysine analogs that target lysine riboswitches. Nat Chem Biol 2007; 3:44-9.
137. Ott E, Stolz J*, et al.* The RFN riboswitch of *Bacillus subtilis* is a target for the antibiotic roseoflavin produced by *Streptomyces davawensis*. RNA Biol 2009; 6:276-80.
138. Ster C, Allard M*, et al.* Experimental treatment of *Staphylococcus aureus* bovine intramammary infection using a guanine riboswitch ligand analog. J Dairy Sci 2013; 96:1000-8.
139. Patrick GL. Pharmacodynamics and pharmacokinetics. In: An introduction to medicinal chemistry. New York: Oxford University Press, 2009.
140. Lipinski CA, Lombardo F*, et al.* Experimental and computational approaches to estimate solubility and permeability in drug discovery and development settings. Adv Drug Deliv Rev 2001; 46:3-26.
141. Priest FG. Systematics and ecology of *Bacillus*. In: Sonenshein AL, Hoch JA*, et al.*, eds. *Bacillus subtilis* and other gram-positive bacteria: biochemistry, physiology, and molecular genetics. Washington: American Society for Microbiology, 1993.
142. FDA. Microorganisms & microbial-derived ingredients used in food. U.S. Food and Drug Administration, 2015.
143. Perego M. Integrational vectors for genetic manipulation in *Bacillus subtilis*. In: Sonenshein AL, Hoch JA*, et al.*, eds. *Bacillus subtilis* and other gram-positive bacteria: biochemistry, physiology, and molecular genetics. Washington: American Society for Microbiology, 1993.
144. Jannière L, Gruss A*, et al.* Plasmids. In: Sonenshein AL, Hoch JA*, et al.*, eds. *Bacillus subtilis* and other gram-positive bacteria: biochemistry, physiology, and molecular genetics. Washington: American Society for Microbiology, 1993.
145. Derré I, Rapoport G*, et al.* The CtsR regulator of stress response is active as a dimer and specifically degraded *in vivo* at 37 °C. Mol Microbiol 2000; 38:335-47.
146. Radeck J, Kraft K*, et al.* The *Bacillus* BioBrick Box: generation and evaluation of essential genetic building blocks for standardized work with *Bacillus subtilis*. J Biol Eng 2013; 7:29.
147. Kreuzer P, Gärtner D*, et al.* Identification and sequence analysis of the *Bacillus subtilis* W23 *xylR* gene and *xyl* operator. J Bacteriol 1989; 171:3840-5.
148. Grossman MJ, Curran IH*, et al.* Interaction of BlaI, the repressor for the beta-lactamase gene of *Bacillus licheniformis*, with the *blaP* and *blaI* promoters. FEBS Lett 1989; 246:83-8.
149. Duval V, Swinnen M*, et al.* The kinetic properties of the carboxy terminal domain of the *Bacillus licheniformis* 749/I BlaR penicillin-receptor shed a new light on the derepression of beta-lactamase synthesis. Mol Microbiol 2003; 48:1553-64.
150. Zhang HZ, Hackbarth CJ*, et al.* A proteolytic transmembrane signaling pathway and resistance to beta-lactams in *Staphylococci*. Science 2001; 291:1962-5.
151. Filée P, Benlafya K*, et al.* The fate of the BlaI repressor during the induction of the *Bacillus licheniformis* BlaP beta-lactamase. Mol Microbiol 2002; 44:685-94.
152. Brans A, Fileé P*, et al.* New integrative method to generate *Bacillus subtilis* recombinant strains free of selection markers. Appl Environ Microbiol 2004; 70:7241-50.
153. Yansura DG, Henner DJ. Use of the *Escherichia coli lac* repressor and operator to control gene expression in *Bacillus subtilis*. Proc Natl Acad Sci USA 1984; 81:439-43.
154. Nealson KH, Hastings JW. Bacterial bioluminescence: its control and ecological significance. Microbiol Rev 1979; 43:496-518.
155. Meighen EA. Molecular biology of bacterial bioluminescence. Microbiol Rev 1991; 55:123-42.
156. Boyle R. New experiments concerning the relation between light and air (in shining wood and fish). Phil Trans 1666; 2:581-600.
157. Ulitzur S, Hastings JW. Myristic acid stimulation of bacterial bioluminescence in "aldehyde" mutants. Proc Natl Acad Sci USA 1978; 75:266-9.

158. Strehler BL, Harvey EN*, et al.* The luminescent oxidation of reduced riboflavin or reduced riboflavin phosphate in the bacterial luciferin-luciferase reaction. Proc Natl Acad Sci USA 1954; 40:10-2.
159. Riendeau D, Rodriguez A*, et al.* Resolution of the fatty acid reductase from *Photobacterium phosphoreum* into acyl protein synthetase and acyl-CoA reductase activities. J Biol Chem 1982; 257:6908-15.
160. Rodriguez A, Riendeau D*, et al.* Purification of the acyl coenzyme A reductase component from a complex responsible for the reduction of fatty acids in bioluminescent bacteria. Properties and acyltransferase activity. J Biol Chem 1983; 258:5233-7.
161. Rodriguez A, Wall L*, et al.* Fatty acid acylation of proteins in bioluminescent bacteria. Biochemistry 1983; 22:5604-11.
162. Qazi SN, Counil E*, et al. agr* expression precedes escape of internalized *Staphylococcus aureus* from the host endosome. Infect Immun 2001; 69:7074-82.
163. Radeck J, Gebhard S*, et al.* Anatomy of the bacitracin resistance network in *Bacillus subtilis*. Mol Microbiol 2016; 100:607-20.
164. Cohn M, Monod J. Purification et propriétés de la β-galactosidase (lactase) d´*Escherichia coli*. Biochim Biophys Acta 1951; 7:153-74.
165. Schorpp K, Hadian K. Small molecule screening at Helmholtz Zentrum München - from biology to molecules. Comb Chem High Throughput Screen 2014; 17:266-71.
166. Commichau FM, Gunka K*, et al.* Glutamate metabolism in *Bacillus subtilis*: gene expression and enzyme activities evolved to avoid futile cycles and to allow rapid responses to perturbations of the system. J Bacteriol 2008; 190:3557-64.
167. Messing J. New M13 vectors for cloning. Methods Enzymol 1983; 101:20-78.
168. Toymentseva AA, Schrecke K*, et al.* The LIKE system, a novel protein expression toolbox for *Bacillus subtilis* based on the *liaI* promoter. Microb Cell Fact 2012; 11:143.
169. Kirchner M, Schneider S. Gene expression control by *Bacillus anthracis* purine riboswitches. RNA 2017; 23:762-9.
170. Kibbe WA. OligoCalc: an online oligonucleotide properties calculator. Nucleic Acids Res 2007; 35:W43-6.
171. Engler C, Kandzia R*, et al.* A one pot, one step, precision cloning method with high throughput capability. PLoS One 2008; 3:e3647.
172. Engler C, Gruetzner R*, et al.* Golden gate shuffling: a one-pot DNA shuffling method based on type IIs restriction enzymes. PLoS One 2009; 4:e5553.
173. Cutting S, Vander Horn P. Genetic analysis. In: Cutting S, Vander Horn P, eds. Molecular biological methods for *Bacillus*. Chichester, UK: John Wiley and Sons, Chichester, 1990:27–74.
174. Miller J. Experiments in molecular genetics. NY: Cold Spring Harbor Laboratory Press, 1972.
175. Wilson SC, Cohen DT*, et al.* A neutral pH thermal hydrolysis method for quantification of structured RNAs. RNA 2014; 20:1153-60.
176. Benson DA, Cavanaugh M*, et al.* GenBank. Nucleic Acids Res 2013; 41:D36-42.
177. McWilliam H, Li W*, et al.* Analysis tool web services from the EMBL-EBI. Nucleic Acids Res 2013; 41:597-600.
178. Li W, Cowley A*, et al.* The EMBL-EBI bioinformatics web and programmatic tools framework. Nucleic Acids Res 2015; 43:W580-4.
179. Dehal PS, Joachimiak MP*, et al.* MicrobesOnline: an integrated portal for comparative and functional genomics. Nucleic Acids Res 2010; 38:D396-400.
180. Gruber AR, Lorenz R*, et al.* The Vienna RNA websuite. Nucleic Acids Res 2008; 36:70-4.
181. Bernhart SH, Hofacker IL*, et al.* RNAalifold: improved consensus structure prediction for RNA alignments. BMC Bioinformatics 2008; 9:474.
182. Sievers F, Wilm A*, et al.* Fast, scalable generation of high-quality protein multiple sequence alignments using Clustal Omega. Mol Syst Biol 2011; 7:539.
183. Hall TA. BioEdit: a user-friendly biological sequence alignment editor and analysis program for Windows 95/98/NT. Nucleic Acids Symposium Series 1999; 41:95-8.
184. Hofacker IL. Vienna RNA secondary structure server. Nucleic Acids Res 2003; 31:3429-31.

185. Zuker M. Mfold web server for nucleic acid folding and hybridization prediction. Nucleic Acids Res 2003; 31:3406-15.
186. Waugh A, Gendron P*, et al.* RNAML: a standard syntax for exchanging RNA information. RNA 2002; 8:707-17.
187. Zuker M, Jacobson AB. Using reliability information to annotate RNA secondary structures. RNA 1998; 4:669-79.
188. Rice P, Longden I*, et al.* EMBOSS: the european molecular biology open software suite. Trends Genet 2000; 16:276-7.
189. Weinberg Z, Breaker RR. R2R--software to speed the depiction of aesthetic consensus RNA secondary structures. BMC Bioinformatics 2011; 12:3.
190. Zhang JH, Chung TD*, et al.* A simple statistical parameter for use in evaluation and validation of high throughput screening assays. J Biomol Screen 1999; 4:67-73.
191. Sittampalam GS, Iversen PW*, et al.* Design of signal windows in high throughput screening assays for drug discovery. J Biomol Screen 1997; 2:159-69.
192. Michna RH, Commichau FM*, et al.* SubtiWiki-a database for the model organism *Bacillus subtilis* that links pathway, interaction and expression information. Nucleic Acids Res 2014; 42:D692-8.
193. Weinberg Z, Barrick JE*, et al.* Identification of 22 candidate structured RNAs in bacteria using the CMfinder comparative genomics pipeline. Nucleic Acids Res 2007; 35:4809-19.
194. d'Aubenton Carafa Y, Brody E*, et al.* Prediction of rho-independent *Escherichia coli* transcription terminators. A statistical analysis of their RNA stem-loop structures. J Mol Biol 1990; 216:835-58.
195. Peters JM, Vangeloff AD*, et al.* Bacterial transcription terminators: the RNA 3'-end chronicles. J Mol Biol 2011; 412:793-813.
196. Weinberg Z, Breaker RR. R2R-software to speed the depiction of aesthetic consensus RNA secondary structures. BMC Bioinformatics 2011; 12:3.
197. Salerno AJ, Lampen JO. Transcriptional analysis of beta-lactamase regulation in *Bacillus licheniformis*. J Bacteriol 1986; 166:769-78.
198. de Hoon MJ, Makita Y*, et al.* Prediction of transcriptional terminators in *Bacillus subtilis* and related species. PLoS Comput Biol 2005; 1:e25.
199. de Saizieu A, Vankan P*, et al.* The *trp* RNA-binding attenuation protein (TRAP) regulates the steady-state levels of transcripts of the *Bacillus subtilis* folate operon. Microbiology 1997; 143 (Pt 3):979-89.
200. Vellanoweth RL, Rabinowitz JC. The influence of ribosome-binding-site elements on translational efficiency in *Bacillus subtilis* and *Escherichia coli in vivo*. Mol Microbiol 1992; 6:1105-14.
201. Kellenberger CA, Wilson SC*, et al.* RNA-based fluorescent biosensors for live cell imaging of second messengers cyclic di-GMP and cyclic AMP-GMP. J Am Chem Soc 2013; 135:4906-9.
202. Yakhnin AV, Babitzke P. NusA-stimulated RNA polymerase pausing and termination participates in the *Bacillus subtilis trp* operon attenuation mechanism *in vitro*. Proc Natl Acad Sci USA 2002; 99:11067-72.
203. Neff NF, Chamberlin MJ. Termination of transcription by *Escherichia coli* ribonucleic acid polymerase *in vitro*. Effect of altered reaction conditions and mutations in the enzyme protein on termination with T7 and T3 deoxyribonucleic acids. Biochemistry 1980; 19:3005-15.
204. Schorpp K, Rothenaigner I*, et al.* Identification of small-molecule frequent hitters from AlphaScreen high-throughput screens. J Biomol Screen 2013; 19:715-26.
205. Iversen PW, Eastwood BJ*, et al.* A comparison of assay performance measures in screening assays: signal window, Z' factor, and assay variability ratio. J Biomol Screen 2006; 11:247-52.
206. Iversen PW, Beck B*, et al.* HTS assay validation. In: Sittampalam GS, Coussens NP*, et al.*, eds. Assay Guidance Manual. Bethesda (MD), 2012.
207. Strauss JH, Jr., Kelly RB*, et al.* Denaturation of RNA with dimethyl sulfoxide. Biopolymers 1968; 6:793-807.
208. Lee J, Vogt CE*, et al.* Influence of dimethylsulfoxide on RNA structure and ligand binding. Anal Chem 2013; 85:9692-8.

209. DeLong DC, Hertel LW*, et al.* Antiviral activity of 2',2'-difluorodeoxycytidine. Meeting of American Society of Microbiology. Washington, DC, 1986.
210. Guchelaar HJ, Richel DJ*, et al.* Clinical, toxicological and pharmacological aspects of gemcitabine. Cancer Treat Rev 1996; 22:15-31.
211. Grunewald R, Kantarjian H*, et al.* Pharmacologically directed design of the dose rate and schedule of 2',2'-difluorodeoxycytidine (Gemcitabine) administration in leukemia. Cancer Res 1990; 50:6823-6.
212. Heinemann V, Hertel LW*, et al.* Comparison of the cellular pharmacokinetics and toxicity of 2',2'-difluorodeoxycytidine and 1-beta-D-arabinofuranosylcytosine. Cancer Res 1988; 48:4024-31.
213. Huang P, Chubb S*, et al.* Action of 2',2'-difluorodeoxycytidine on DNA synthesis. Cancer Res 1991; 51:6110-7.
214. Heinemann V, Xu YZ*, et al.* Inhibition of ribonucleotide reduction in CCRF-CEM cells by 2',2'-difluorodeoxycytidine. Mol Pharmacol 1990; 38:567-72.
215. Momparler RL, Onetto-Pothier N*, et al.* Cellular pharmacology of 1-beta-D-arabinofuranosylcytosine in human myeloid, B-lymphoid and T-lymphoid leukemic cells. Cancer Chemother Pharmacol 1990; 27:141-6.
216. Bouffard DY, Laliberté J*, et al.* Kinetic studies on 2',2'-difluorodeoxycytidine (Gemcitabine) with purified human deoxycytidine kinase and cytidine deaminase. Biochem Pharmacol 1993; 45:1857-61.
217. Rossi M, Momparler RL*, et al.* Studies on analogs of isosteric and allosteric ligands of deoxycytidylate aminohydrolase. Biochemistry 1970; 9:2539-43.
218. Heinemann V, Xu YZ*, et al.* Cellular elimination of 2',2'-difluorodeoxycytidine 5'-triphosphate: a mechanism of self-potentiation. Cancer Res 1992; 52:533-9.
219. Van Moorsel CJ, Smid K*, et al.* Effect of gemcitabine and cis-platinum combinations on ribonucleotide and deoxyribonucleotide pools in ovarian cancer cell lines. Int J Oncol 2003; 22:201-7.

8 Abbreviations

Table 14: Abbreviations used in this study.

AMP	adenosine monophosphate
B. anthracis (BA)	*Bacillus anthracis*
B. licheniformis	*Bacillus licheniformis*
B. subtilis (BS)	*Bacillus subtilis*
conc.	concentration
CRISPR	clustered regularly interspaced short palindromic repeats
CSE	C minimal medium with sodium succinate and potassium glutamate
dCMP	deoxycytidine monophosphate
dCTP	deoxycytidine triphosphate
°C	degree celsius
DFHBI	3,5-difluoro-4-hydroxybenzylidene imidazolinone
DMSO	dimethyl sulfoxide
DNA	deoxyribonucleic acid
dNTP	deoxynucleoside triphosphate
E. coli	*Escherichia coli*
EDTA	ethylenediaminetetraacetic acid
EF	endema factor
FDA	US Food and Drug administration
fl	full-length
FMN	flavin mononucleotide
FRET	fluorescence resonance energy transfer
1 g	9.81 m/s^2
GMP	guanosine monophosphate
GRAS	generally recognized as safe
GTP	guanosine triphosphate
gua	guanosine
h	hour(s)
HEPES	4-(2-hydroxyethyl)-1-piperazineethanesulfonic acid
IMP	inosine monophosphate
K_D	dissociation constant

kV	kilovolt
l	liter(s)
LB	Luria-Bertani
LF	lethal factor
m	meter(s)
M	mol/l
mA	milliampere
MCS	multiple cloning site
min.	minute(s)
MOPS	3-(*N*-morpholino)propanesulfonic acid
MU	Miller unit(s)
mRNA	messenger RNA
n	frequency of a nucleotide in the RNA sequence
neg	negative
NMR	nuclear magnetic resonance
NTP	nucleosidetriphosphate
OD	optical density (at 600 nm)
ONPG	*ortho*-nitrophenyl-β-galactoside
ORF	open reading frame
PA	protective antigen
PC1	2,5,6-triaminopyrimidin-4-one
PC2	2,6-diaminopyrimidin-4-one
PCR	polymerase chain reaction
piRNA	piwi-interacting RNA
PRPP	5-phosphoribosyl-α-1-pyrophosphate
RBS	ribosome binding site
RLU	relative luminescence units
RNA	ribonucleic acid
rpm	rounds per minute
RS	riboswitch
RT-qPCR	reverse-transcription quantitative PCR
sAMP	adenylosuccinate
S. aureus	*Staphylococcus aureus*

S/B	signal-to-background
SELEX	systematic evolution of ligands by exponential enrichment
SD	Shine-Dalgarno sequence
SHAPE	selective 2´-hydroxyl acylation and primer extension
siRNA	small interfering RNA
snoRNA	small nucleolar RNA
SOC	super optimal broth with catabolite repression
SW	signal window
TBE	Tris-Borate-EDTA
TE	Tris-EDTA
TPP	thiamine pyrophosphate
Tris	tris(hydroxymethyl)aminomethane
U	units
V	volt
vs.	versus
v/v	volume per volume
w/v	weight per volume
XMP	xanthosine monophosphate
xyl	xylose
ΔG	relative free energy
ε	molar extinction coefficient
σ	standard deviation
2AP	2-aminopurine